FEDERAL UNIVERSITY OF SÃO CARLOS
CENTER FOR EXACT SCIENCES AND TECHNOLOGY
GRADUATE PROGRAM IN ELECTRICAL ENGINEERING

CAÍQUE SANTOS LIMA

OxiTidy: motion artifact detection-reduction in photoplethysmographic signals using artificial neural networks

São Carlos - SP
2022

CAÍQUE SANTOS LIMA

OxiTidy: motion artifact detection-reduction in photoplethysmographic signals using artificial neural networks

Dissertation presented to the Graduate Program in Electrical Engineering at the Center for Exact Sciences and Technology at the Federal University of São Carlos, as part of the requirements for obtaining the title of Master in Electrical Engineering.

Concentration area: Electrical and Electronic Systems

Supervisor: Prof. Dr. André Carmona Hernandes

Co-supervisor: Prof. Dr. Rafael Vidal Aroca

São Carlos - SP

2022

Santos Lima, Caíque

OxiTidy: motion artifact detection-reduction in photoplethysmographic signals using artificial neural networks / Caíque Santos Lima -- 2022.
124f.

Dissertação (Mestrado) - Universidade Federal de São Carlos, campus São Carlos, São Carlos
Orientador (a): André Carmona Hernandes
Banca Examinadora: André Carmona Hernandes, Fernando José Von Zuben, Samuel Lourenço Nogueira
Bibliografia

1. Signal processing. 2. Machine learning. 3. Pulse oximetry. I. Santos Lima, Caíque. II. Título.

Ficha catalográfica desenvolvida pela Secretaria Geral de Informática (SIn)

DADOS FORNECIDOS PELO AUTOR

Bibliotecário responsável: Ronildo Santos Prado - CRB/8 7325

UNIVERSIDADE FEDERAL DE SÃO CARLOS

Centro de Ciências Exatas e de Tecnologia
Programa de Pós-Graduação em Engenharia Elétrica

Folha de Aprovação

Defesa de Dissertação de Mestrado do candidato Caíque Santos Lima, realizada em 22/07/2022.

Comissão Julgadora:

Prof. Dr. Andre Carmona Hernandes (UFSCar)

Prof. Dr. Samuel Lourenço Nogueira (UFSCar)

Prof. Dr. Fernando José Von Zuben (UNICAMP)

O Relatório de Defesa assinado pelos membros da Comissão Julgadora encontra-se arquivado junto ao Programa de Pós-Graduação em Engenharia Elétrica.

This work is dedicated to my family and to all the people who helped me get here.

Acknowledgements

First and foremost, I would like to thank all my family for encouraging my studies and for always rooting for my professional and personal success. I also would like to express my sincere gratitude to my supervisors Prof. Dr. André Carmona Hernandes and Prof. Dr. Rafael Vidal Aroca for the guidance, dedication, patience and trust placed in me.

I am also thankful to Prof. Dr. Fernando José Von Zuben, Prof. Dr. Samuel Lourenço Nogueira, Prof. Dr. Fernando Oscar Runstein and Prof. Dr. Ricardo José Ferrari for serving as members of my examination board.

Thanks should also go to the professors, colleagues and employees of the Department of Electrical Engineering and Computing Department of the Federal University of São Carlos where I studied the subjects essential to my research.

Words cannot express my gratitude to all the employees and volunteers of Instituto Crescer Cidadão in Ribeirão Preto, SP, who collaborated with the data for this work. This endeavor would not have been possible without the valuable help of Profa. Dra. Flávia Gomes Pileggi Gonçalves to whom I extend my special thanks.

Many thanks to Tayná Bertacine and Marcos Endo for helping me to develop the pulse oximeter prototype. I would like to extend my thanks to Diego Soler for his collaboration in the development of OxiCam.

Finally, I would like to thank Coordination for the Improvement of Higher Education Personnel (CAPES) for the financial support and granting of scholarships for most of the master's degree[1]. I also thank the Center for Exact Sciences and Technology of the Federal University of São Carlos (CCET-UFSCar) for making the MATLAB software available through Process nº 2015/25146-3, São Paulo Research Foundation (FAPESP).

[1] This study was financed in part by the Coordenação de Aperfeiçoamento de Pessoal de Nível Superior - Brasil (CAPES) - Finance Code 001

"A cabeça pensa onde os pés pisam."

(Frei Betto)

Abstract

LIMA, Caíque Santos. **OxiTidy**: motion artifact detection-reduction in photoplethysmographic signals using artificial neural networks. 2022. 123 p. Dissertation (Master's in Electrical Engineering) – Department of Electrical Engineering, Federal University of São Carlos, São Carlos, 2022.

Nowadays, technological evolution has allowed advances in several areas, especially in healthcare. Digital transformation in health has brought benefits to both professionals and patients. What was possible to do only with high-cost and unwieldy biomedical equipment, has been popularized with the emergence of wearable devices. This technology allows clinical monitoring beyond medical offices, being able to be incorporated into the daily life of patients and working as another tool for prevention and promotion of health and well-being. Among the various features present in wearables is pulse oximetry. Through this non-invasive technique, it is possible to measure physiological parameters, such as oxygen saturation (SpO_2) and heart rate (HR). However, the way pulse oximeters are developed and used directly influences the quality of the information provided to the user. Photoplethysmographic (PPG) signals from pulse oximeters are susceptible to noise, which is largely caused by user movement during monitoring. These motion artifacts can cause measurement errors and false alarms. In order to mitigate these issues, this work proposes an algorithm based on artificial neural networks (ANNs) capable of detecting and reducing the undesirable effects produced by noise in PPG signals. The performance of this algorithm, called OxiTidy, was compared with three other approaches — *raw*, discrete Fourier transform (DFT) and simple moving average (SMA) —, using data from 17 healthy volunteers. OxiTidy identified the intervals where the measurements were incorrect and estimate new SpO_2 values with a good approximation to the readings performed by a pulse oximeter certified by the Brazilian Health Regulatory Agency (Anvisa).

Keywords: Photoplethysmography. Signal processing. Motion artifact. Machine learning. Multilayer perceptron. Oxygen saturation. Heart rate. Pulse oximeter. Wearables.

Resumo

LIMA, Caíque Santos. **OxiTidy**: detecção e redução de artefato de movimento em sinais fotopletismográficos usando redes neurais artificiais. 2022. 123 págs. Dissertação (Mestrado em Engenharia Elétrica) – Departamento de Engenharia Elétrica, Universidade Federal de São Carlos, São Carlos, 2022.

A evolução tecnológica tem permitido o avanço em diversas áreas do conhecimento nos últimos anos, especialmente na assistência médica. Essa transformação digital na saúde trouxe benefícios para os profissionais da saúde e pacientes. O que era possível fazer apenas com equipamentos biomédicos de alto custo e de difícil manuseio, foi popularizado com o surgimento dos dispositivos vestíveis (*wearables*). Essa tecnologia permite o acompanhamento clínico para além dos consultórios, podendo ser incorporada ao dia a dia dos pacientes e sendo mais uma ferramenta para prevenção e promoção de saúde e bem-estar. Entre as diversas funcionalidades presentes nos *wearables* está a oximetria de pulso. Através desta técnica não invasiva é possível medir parâmetros fisiológicos, como a saturação de oxigênio (SpO_2) e a frequência cardíaca (HR). No entanto, a forma como esses dispositivos são construídos e usados influencia diretamente a qualidade das informações fornecidas ao usuário. Os sinais fotopletismográficos (PPG) dos oxímetros de pulso são suscetíveis a ruídos que, em grande parte, são provocados pela movimentação do usuário durante o monitoramento. Esses artefatos de movimento podem provocar erros nas leituras e causar alarmes falsos. Visando mitigar esses problemas, este trabalho propõe um algoritmo baseado em redes neurais artificiais (RNAs) capaz de detectar e reduzir os efeitos indesejáveis produzidos pelo ruído nos sinais PPG. O desempenho deste algoritmo, denominado OxiTidy, foi comparado com outras três abordagens — *raw*, transformada discreta de Fourier (DFT) e a média móvel simples (SMA) —, usando dados de 17 voluntários saudáveis. O OxiTidy foi capaz de identificar os intervalos em que as medidas estavam incorretas e estimar novos valores de SpO_2 com uma boa aproximação às leituras realizadas por um oxímetro de pulso certificado pela Agência Nacional de Vigilância Sanitária (Anvisa).

Palavras-chaves: Fotopletismografia. Processamento de sinal. Artefato de movimento. Aprendizado de máquina. Perceptron multicamadas. Saturação de oxigênio. Frequência cardíaca. Oxímetro de pulso. Dispositivos vestíveis.

List of Figures

List of algorithms

List of Tables

List of abbreviations and acronyms

ABG	Arterial blood gas
ABNT	Associação Brasileira de Normas Técnicas (Brazilian Association of Technical Standards)
ANFIS	Adaptive neuro-fuzzy inference system
ANN	Artificial neural network
Anvisa	Agência Nacional de Vigilância Sanitária (Brazilian Health Regulatory Agency)
ATP	Adenosine triphosphate
BIDMC	Beth Israel Deaconess Medical Center
BPF	Bandpass filter
bpm	Beats per minute
$C_6H_{12}O_6$	Glucose
CEP	Comitê de Ética em Pesquisa em Seres Humanos (Research Ethics Committee)
CO_2	Carbon dioxide
DFT	Discrete Fourier transform
DOF	Degrees of freedom
e.g.	*Exempli gratia* (for the sake of example, for example)
ECG	Electrocardiogram
EDA	Exploratory data analysis
FDA	Food and Drug Administration
FFT	Fast Fourier transform

fs	Sampling frequency or sampling rate
FT	Fourier transform
H_2O	Water
Hb	Hemoglobin
HbCO	Carboxyhemoglobin
HbMet	Methemoglobin
HbO_2	Oxyhemoglobin
HR	Heart rate
i.e.	*Id est* (that is)
ICU	Intensive care unit
IIR	Infinite impulse response
IMU	Inertial measurement unit
IoT	Internet of Things
ISO	International Organization for Standardization
LED	Light-emitting diode
LPF	Low-pass filter
MA	Motion artifact
MAE	Mean absolute error
MLP	Multilayer perceptron
NBR	Norma Brasileira (Brazilian Standard)
NEVS	Núcleo Executivo de Vigilância em Saúde (Executive Center for Health Surveillance)
NICU	Neonatal intensive care unit

no.	Number
NTP	Network Time Protocol
O_2	Oxygen
OCR	Optical character recognition
PCB	Printed circuit board
PI	Perfusion index
PICU	Pediatric intensive care unit
PO_2	Partial pressures of oxygen
PPG	Photoplethysmography
RBF	Radial basis function
RHb	Reduced hemoglobin
SaO_2	Arterial oxygen saturation
SD	Standard deviation
SMA	Simple moving average
SpO_2	Peripheral oxyhemoglobin saturation
SPWVD	Smoothed pseudo Wigner-Ville distribution
SSA	Singular spectrum analysis
TCLE	Termo de Consentimento Livre e Esclarecido (Free and Informed Consent Form)
UFSCar	Universidade Federal de São Carlos (Federal University of São Carlos)
VFCDM	Variable frequency complex demodulation
WHO	World Health Organization
WMA	Weighted moving average

Contents

1 Introduction

The first chapter of this work endeavours to discuss how modern medicine has evolved in recent years and how technology has contributed to this unprecedented advance. This chapter also introduces fundamental concepts about oximetry and factors that interfere in its measurement. Section 1.1 describes how a tech-driven concept has transformed the traditional healthcare industry. Sections 1.2 and 1.3 explain the importance of blood oxygenation in the human body and what is oxygen saturation, respectively. Section 1.4 presents the heart rate (HR). In section 1.5, different types of oximeters are presented as well as their functioning. Finally, external factors that interfere with pulse oximeters will be discussed in section 1.6.

1.1 Health 4.0: the heart of healthcare in 21st century

The significant increase in life expectancy is one of the factors that indicate the improvement in people's quality of life over the years. In 1950, the world life expectancy was only 47 years. Half a century has passed, and that number has approached 66 years (UNITED NATIONS, 2019). This expressive fact is partly explained by advances in modern medicine (MISHRA, 2016).

According to Kocheva (2021), COVID-19 altered the way we obtain health care and accelerated the need to find a way to offer healthcare services remotely. These types of services have been enhanced by the use of cloud computing, big data analytics, smart algorithms, Internet of Things (IoT), various forms of wireless Internet and 5G technologies, telemonitoring, machine learning, cryptography, blockchain, among other technologies that form the Health 4.0 digital ecosystem.

In addition to innovations in medicines and treatments, technological evolution in medicine has contributed to the efficiency of health services offered to the world's population, including the poorest countries. The emergence of new forms of electronic communication has facilitated the transmission of information, especially in the area of health care (MISHRA, 2016). An example that has gained prominence lately is telemedicine (AZIZ; ABOCHAR, 2015).

This term was coined in the 1970s by the World Health Organization (WHO) and refers to the provision of clinical care through electronic means of communication.

Telemedicine applications and services include tools such as: e-mail, videoconferencing, smartphones, wireless biomedical devices, among other technologies (AZIZ; ABOCHAR, 2015).

Among the possibilities, biomedical vital signs sensors have gained space in domestic use, which were exclusive to large hospitals and clinics. They can be used from diagnosis and prevention, as well as during the disease treatment phase (RODRIGUES et al., 2017)(CHACON et al., 2019).

Among several electronic devices that have helped health professionals to detect and treat the effects produced by infectious agents, the pulse oximeter stands out. This non-invasive instrument is of great relevance for monitoring blood oxygenation (JUBRAN, 2015), and has been an important tool for detecting cases of hypoxemia in people affected by COVID-19 (TOBIN; LAGHI; JUBRAN, 2020), for example.

1.2 The importance of blood oxygenation

The functioning of every cell in the human body depends on the presence of oxygen (O_2). This important substrate is associated with the process of cellular respiration, also known as cellular metabolism. Through this process, ingested food molecules, such as $C_6H_{12}O_6$ (glucose), are broken down into simpler molecules of CO_2 (carbon dioxide) and H_2O (water) to obtain energy in the form of adenosine triphosphate (ATP). The lack of oxygen in cellular metabolism inhibits the production of ATP, from which cellular processes begin to shut down. Therefore, one of the main functions of the respiratory system is to supply oxygen to cells so that they can produce ATP and perform their functions (WHITTEMORE, 2004).

According to Whittemore (2004), some cells are more resistant to oxygen deprivation than others, however, prolonged lack of oxygen results in cell collapse. For example, after a lack of oxygen supply to the brain, irreversible damage can occur within minutes. The adult brain represents about 2% of the body weight, but uses approximately 20% of the oxygen consumed by the body (ROUX; ODDO, 2013), i.e., the great demand of the brain makes oxygenation tracking essential. Another important point is the immune system itself, since cells that are well supplied with oxygen are able to exert a better defense against viruses and bacteria (ZENEWICZ, 2017).

Some abnormalities can also lead to a drop in oxygen supply, such as anemia. Anemia is a disorder caused by a decrease in the amount of hemoglobin in the blood. Therefore, as they are responsible for transporting oxygen, there is a reduction in their supply to the tissues. Although anemia is the most common blood disorder, other comorbidities can also affect the availability of oxygen in the blood, e.g. respiratory failure, lung diseases and circulatory problems that reduce blood flow directly affecting oxygen delivery (TORTORA; DERRICKSON, 2014).

In technical terms, when the demand for oxygen in the tissue is greater than the amount supplied, it is named hypoxia. Symptoms resulting from this condition vary depending on its severity and can include headaches, nausea, cyanosis (blue or gray color of the skin, nails, lips or around the eyes), hyperventilation, fatigue, seizures, and in severe cases, result in coma and death (WEBSTER, 1997).

According to Tortora e Derrickson (2014), hypoxia can be classified according to its cause into four groups: hypoxic, anemic, ischemic or histotoxic. In hypoxic hypoxia, the oxygen concentration in arterial blood is low due to low PO_2 (partial pressures of oxygen) in the blood caused by high altitude, airway obstruction or fluid in the lungs. In anemic hypoxia, the amount of hemoglobin is reduced, which reduces the transport of oxygen to the cells, among its causes are hemorrhage and anemia. In ischemic hypoxia, although PO_2 and HbO_2 (oxyhemoglobin) level are normal, blood flow to a tissue is so reduced that very little oxygen is delivered to it. In histotoxic hypoxia, the blood delivers adequate oxygen to the tissues, but the tissues are unable to use it properly due to the action of some toxic agent. One cause is cyanide poisoning, in which cyanide blocks an enzyme needed to use oxygen during the synthesis of ATP.

The SARS-CoV-2 virus, which causes COVID-19, primarily affects the respiratory system, although other organ systems are also involved. This causes concern since, in severe cases of the disease, blood oxygenation can be compromised due to respiratory complications caused by the new coronavirus (YUKI; FUJIOGI; KOUTSOGIANNAKI, 2020). Due to the COVID-19 pandemic, the blood oxygen level has become a parameter of great concern, as the person with COVID-19 does not always have symptoms such as shortness of breath, for example (TOBIN; LAGHI; JUBRAN, 2020).

Many patients infected with SARS-CoV-2, despite not complaining of shortness of breath, have a dangerous drop in blood oxygen level (TOBIN; LAGHI; JUBRAN, 2020)(COUZIN-FRANKEL, 2020). This condition became known as silent hypoxia, where

although patients had mild symptoms and felt apparently fine, they were unaware that their oxygen saturation was dangerously low (TOBIN; LAGHI; JUBRAN, 2020). In this context, the pulse oximeter has become a widely used instrument to monitor the level of oxygen in the blood, especially in less symptomatic cases, where patients can be affected by silent hypoxia (COUZIN-FRANKEL, 2020).

1.3 Oxygen saturation

One of the ways to know the level of oxygen essential for the body's vital functions is to measure the percentage of oxygen available in hemoglobin, with SaO_2 (arterial oxygen saturation) being one of the variables that can indicate whether tissues are being adequately oxygenated. This occurs because, if there is low SaO_2, there will be hypoxia (low oxygen concentration in the tissues), one of the factors being hypoxemia, which is low oxygenation in the blood (WEBSTER, 1997).

SaO_2 can be measured using a procedure named arterial blood gas (ABG) test, while SpO_2 (peripheral oxyhemoglobin saturation) refers to SaO_2 measured by pulse oximeter. ABG test is an invasive procedure that requires a blood sample from the person to determine the arterial oxygen level. On the other hand, SpO_2 can be obtained using a pulse oximeter in a non-invasive and painless way (MOYLE, 2002).

In specific analysis, hemoglobin (Hb) is present in the blood in mainly two forms, in HbO_2, when it is bound to the oxygen molecule, and in reduced hemoglobin (RHb), when it is not (URPALAINEN, 2011). Thus, it is possible to define the *functional* SaO_2, in percentage, as follows:

$$functional\ SaO_2 = 100 \times \frac{c_{HbO_2}}{c_{HbO_2} + c_{RHb}}, \tag{1}$$

where c_{HbO_2} and c_{RHb} are the concentrations of HbO_2 and RHb, respectively.

On the other hand, there is also the *fractional* SaO_2 which includes the four types of hemoglobin: HbO_2, RHb, HbCO (when the person is exposed to carbon monoxide gas) and HbMet (hemoglobin with Fe^{+3}, which does not bind oxygen) (URPALAINEN, 2011). The *fractional* SaO_2 is defined according to the equation:

$$fractional\ SaO_2 = 100 \times \frac{c_{HbO_2}}{c_{HbO_2} + c_{RHb} + c_{HbCO} + c_{HbMet}}, \tag{2}$$

where c_{HbO_2}, c_{RHb}, c_{HbCO} and c_{HbMet} are the concentrations of HbO_2, RHb, HbCO and HbMet, respectively.

According to World Health Organization (2011), oxygen saturation in healthy people of any age should be 95% or higher. If a person's SpO_2 is 94% or less, they should be evaluated quickly to identify and treat the cause. Levels below 90% are considered a clinical emergency and should be treated urgently. As mentioned, pulse oximetry is a non-invasive technique that is capable of performing this measurement effectively.

1.4 Heart rate

HR is the number of times the heart beats per minute (bpm). The normal pulse for healthy adults ranges from 60 to 100 bpm. But athletes, who do a lot of cardiovascular conditioning, may have heart rates near 40 bpm (JOHNS HOPKINS MEDICINE, 2022). The maximum human HR is about 220 minus the subject's age (AMERICAN HEART ASSOCIATION, 2021). The Table 1 shows target heart rate zones for different ages during physical activity. According to American Heart Association (2021), "[...] target heart rate during moderate intensity activities is about 50 – 70% of maximum heart rate, while during vigorous physical activity it's about 70 – 85% of maximum."

Table 1 – Maximum and target heart rate (HR) during physical activity by age.

Age (years)	Target HR zone, 50 – 85% (bpm)	Average max. HR, 100% (bpm)
20	100 – 170	200
30	95 – 162	190
35	93 – 157	185
40	90 – 153	180
45	88 – 149	175
50	85 – 145	170
55	83 – 140	165
60	80 – 136	160
65	78 – 132	155
70	75 – 128	150

Source – American Heart Association (2021).

In addition to the HR varying with physical activity, other factors can influence the pulse rate, such as: illness, injuries and emotions (JOHNS HOPKINS MEDICINE, 2022). Like SpO_2, HR is a vital measurement during hospital assessments and has become increasingly popular with the emergence of wearable devices initially designed to track physical activity, now evolving into applications in medicine, sports, studies of people's

habits, risk assessment of injuries during physical exercise, monitoring of the elderly and monitoring of physiological signs (HAGHI; THUROW; STOLL, 2017).

1.5 Pulse oximeter

Since the pulse oximeter was invented in the 1970s by the Japanese electrical engineer Takuo Aoyagi (AOYAGI, 2003), invasive methods for oximetry detection are only necessary when the percentage of oxygen in the blood cannot be obtained using a pulse oximeter (SINCHAI et al., 2018) and for device calibration process. Pulse oximeters, frequently used by health professionals, in addition to indirectly measuring SpO_2, also measure other physiological parameters, such as heart rate (SALEHIZADEH et al., 2014). The SpO_2 obtained through pulse oximetry is important to evaluate cases of hypoxemia, pulmonary embolism, congenital heart disease, acute heart failure and chronic obstructive pulmonary disease (SINCHAI et al., 2018).

Figure 1 shows the different models of pulse oximeters. These devices can be used in hospitals or at home. Generally, the oximeters present in medical centers are larger, expensive and unwieldy. On the other hand, oximeters used at home are portable, wireless, compact and relatively cheaper devices.

Figure 1 – Pulse oximeters models: (A) wireless oximeter, (B) ICU oximeter, (C) NICU oximeter, and (D) wearable oximeter (smartwatch).

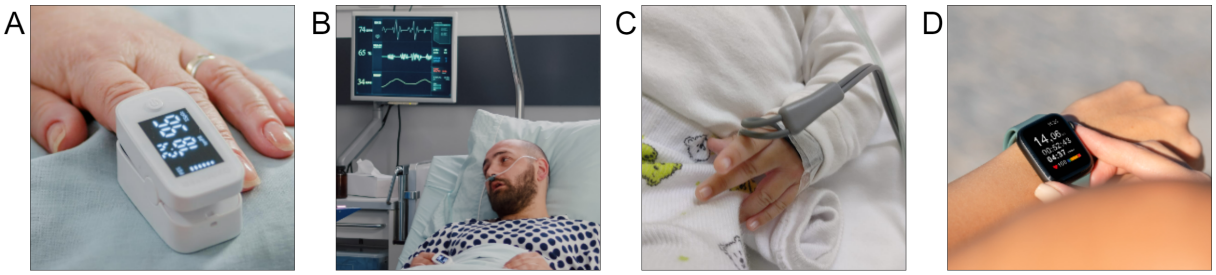

Source – (A) DCStudio (2022b), (B) DCStudio (2022a), (C) Flávia Gomes Pileggi Gonçalves (2022), (D) Freepik (2022).

Conventional pulse oximeters show PPG signal, SpO_2 and HR values. Some of them may also display the perfusion index (PI), which is an indication of the pulse strength at the sensor site. Basically, the PI provides instant and continuous feedback on peripheral perfusion, and if it drops below the minimums required for monitoring (low perfusion),

the PI alerts the user to consider adjusting the monitoring site (MASIMO, 2007). Figure 2 below depicts a typical view of pulse oximeter screen.

Figure 2 – A typical view of pulse oximeter display. In addition to SpO_2 value, PPG signal, pulse rate and perfusion index are shown.

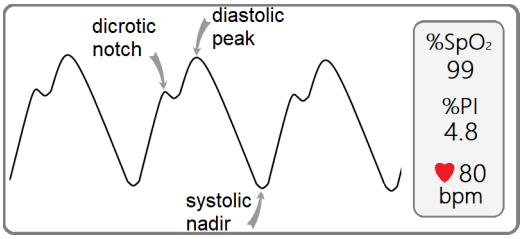

Source – adapted from Urpalainen (2011, p. 9).

1.5.1 Photoplethysmography

The measurements performed by pulse oximeters are obtained through the photoplethysmography (PPG). This phenomenon was described in the 1930s by Alrick Hertzman. According to Alian e Shelley (2014), Hertzman chose the term *plethysmos*, derived from the Greek word for fullness, based on his belief that his first observations were related to changes in blood volume. His theories were derived from the Beer-Lambert law, whose main premises were that the absorption of light is directly proportional to the path length, the concentration of substances and the absorption of light by each of these substances (ALIAN; SHELLEY, 2014). Figure 3 illustrates the Beer-Lambert law that describes light attenuation through a sample of homogenous non-scattering media.

Figure 3 – Beer–Lambert law.

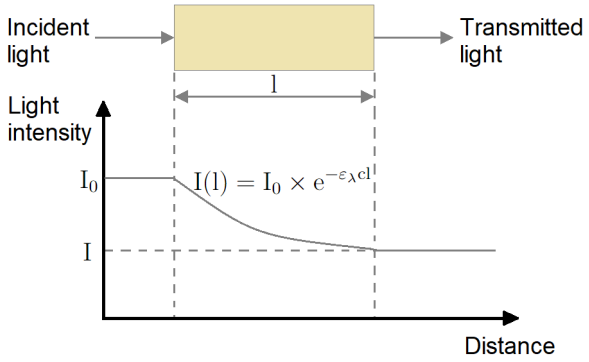

Source – adapted from Urpalainen (2011, p. 10).

The equation that expresses the Beer-Lambert law is presented as:

$$I = I_o \times e^{-\varepsilon_\lambda cl}, \tag{3}$$

where I indicates the intensity of the transmitted light, i.e., the light that has passed through the media, I_0 is the intensity of the incident light, ε_λ is the extinction coefficient of the substance at a given wavelength λ, c is the concentration of the substance, and l the optical path-length of the sample.

Through the photoplethysmographic technique, optical properties of body tissue and blood can be characterized using light sources (red and infrared) and a photodetector. The intensity of the reflected light changes when the volume of the arterial vessel changes during the systolic phase, which is the ejection phase of blood during the cardiac cycle. This light intensity variation is converted into an electrical signal by the oximeter (CHACON et al., 2019).

Pulsatile arterial blood absorbs and modulates the light emitted by the oximeter that passes through body tissue and forms the PPG signal. The AC component of this signal, represented by the light absorbed by pulsatile arterial blood, is the only variable term. While the DC component, represented by the light absorbed by non-pulsatile arterial blood, venous blood and tissues such as skin, nerves and bones, remains static (MAXIM INTEGRATED, 2014)(CHACON et al., 2019). Figure 4 shows the components of the signal PPG described above.

Figure 4 – Light reflection during plethysmographic measurement.

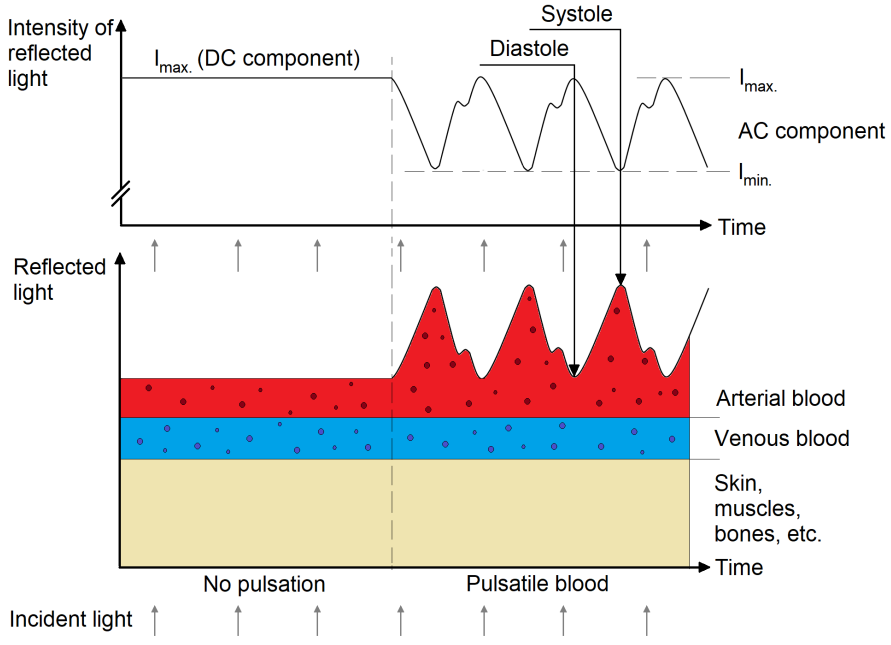

Source – adapted from Urpalainen (2011, p. 13).

It should be noted that the DC and AC components of the generated PPG signals are different for each LED. This is due to the distinct absorption characteristics of Hb,

HbO_2 and other body tissue components for different wavelengths. From this difference it is possible to calculate the blood oxygen saturation (MAXIM INTEGRATED, 2014)(CHACON et al., 2019). The graph in Figure 5 shows the light absorption coefficients for Hb and HbO_2 at red (660 nm) and infrared (940 nm) wavelengths. The vertical axis indicates the molar extinction coefficient, i.e., the ability of a mole of substance to attenuate light falling at a given wavelength.

Figure 5 – Molar extinction coefficient for Hb and HbO_2 in the range from 570 to 1000 nm.

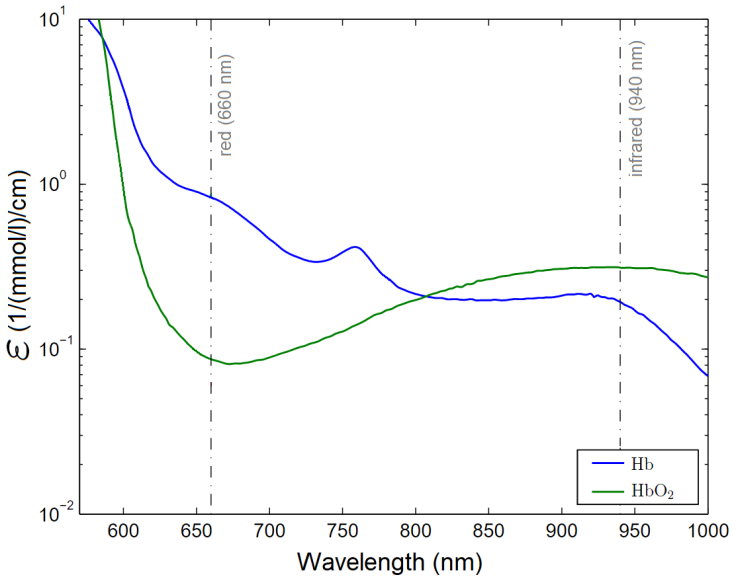

Source – adapted from Urpalainen (2011, p. 11).

1.5.2 Working principle

Pulse oximeters can be of the transmission or reflectance type. In transmission pulse oximeters (Figure 6A), the LEDs and the photodetector are positioned oppositely and the measurement surface is between them. Reflection-type pulse oximeters (Figure 6B) contain the LEDs and the photodetector on the same side, and the light reflected by the measurement surface is used to determine the SpO_2. According to Elgendi (2021), in addition to their constructive differences, these two types of oximeters have some peculiarities: although the reflectance pulse oximeter is wider in terms of the places where it is possible to measure SpO_2 (in addition to the fingers, they can be worn on the wrist or forehead), they are more susceptible to noise caused by movements and pressure of the clip.

Figure 6 – Pulse oximeters types: (A) transmission-type and (B) reflection-type.

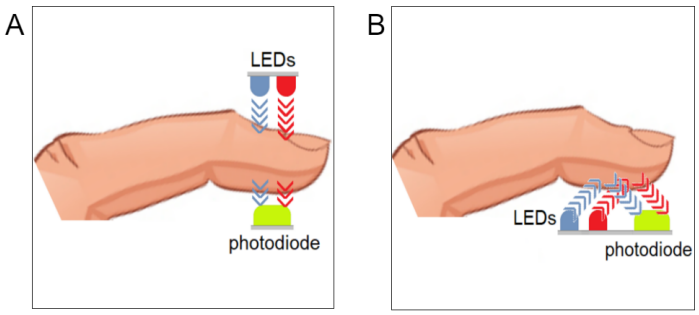

Source – Caíque Santos Lima, 2022.

These devices are usually placed on peripheral parts of the patient, such as the index fingertip, through a clip that secures the oximeter during measurement. Pulse oximeters are basically made up of a photodetector and two light sources: a red (660 nm) and an infrared (940 nm), where the idea is to use the absorption difference shown in Figure 5 to estimate oxygen saturation. The light is captured by a photodetector (photodiode), which produces a signal similar to Figure 4.

The measurement and signal processing algorithms are implemented in a microcontroller that also has the function of controlling the activation of the LEDs and the photodiode. As they are portable wireless devices, these oximeters have batteries and the monitored data is displayed through their own display. Figure 7 illustrates how a reflection-type pulse oximeter works. Part of the light reflected by Hb and HbO_2 is absorbed by the photoreceptor which modulates the lights to form the PPG signals.

Figure 7 – Operation diagram of a reflection-type pulse oximeter.

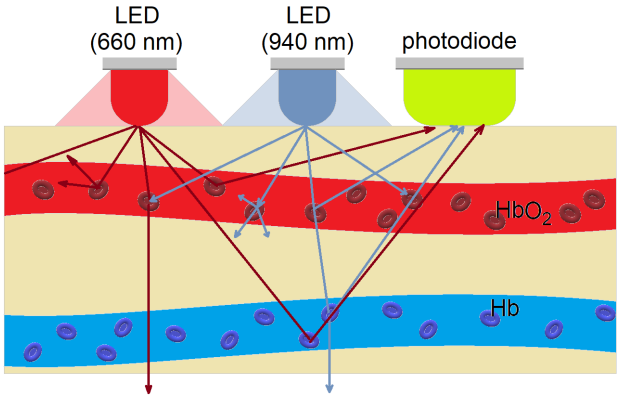

Source – adapted from Chacon et al. (2019, p. 1506).

1.6 External interference on pulse oximeters

Pulse oximeters may favor faster treatment of severe cases of hypoxemia, where the level of oxygen in the blood drops to levels that can have serious consequences for the human body (JUBRAN, 2015). However, it should be considered that the result of the oximetric reading is influenced by the way the device is used and, especially, by the quality of the device (GIULIANO; LIU, 2006). The accuracy of pulse oximeters tends to decrease as external factors interfere with the PPG signal, for example, external lights and device movements resulting from patient breathing and/or movement, such as: walking, finger tremors, hand movement, etc (LEE; JUNG; KANG, 2003).

According to Hayes e Smith (2001) and Yousefi et al. (2014), motion in oximeters is the most common problem of noise in the PPG signal, which can compromise and even corrupt it to the point that it is impossible to use it in monitoring SpO_2. This problem is frequent in ambulatory, pediatric and trauma settings, where uncontrolled patient movements are unavoidable (HAYES; SMITH, 2001). According to Ram et al. (2012), the pulsatile component of the signal PPG represents about 0.1% of the total amplitude of the signal, i.e., any small movement of the patient will result in an inaccurate estimation of the SpO_2.

According to Hayes e Smith (2001) and Lee, Jung e Kang (2003), removing noise caused by patient movement from the PPG signal may not be a simple task, when using only signal processing techniques, such as a filter that has a fixed cutoff frequency. Typically, the respiration frequency band is 0.04–1.6 Hz; of the oximeter pulse wave is 0.5–4 Hz; and the frequency band of noise caused by patient movement is 0.1 Hz or more. Therefore, it is complex to remove the noise since the frequency band of this noise is superimposed on the patient's pulse wave measured by the oximeter (LEE; JUNG; KANG, 2003).

In Figure 8, it is possible to observe that in the range where the oximeter is moving (from 18 to 54 seconds), both PPG signals are affected. This causes changes in the *raw* SpO_2 estimation (red line), which drastically reduces the oxygen saturation value displayed in the range where the user's hand is moving. In this interval, readings from static reference oximeter showed SpO_2 remained constant (see SpO_2 *ref.*). Comparing the normal value of the reference with the *raw* estimation of SpO_2, it is possible to observe the false alarm the movement caused.

Figure 8 – PPG signals with motion interference and oximeter acceleration plot. Herein, it is possible to see that SpO_2 is affected by motion artifacts.

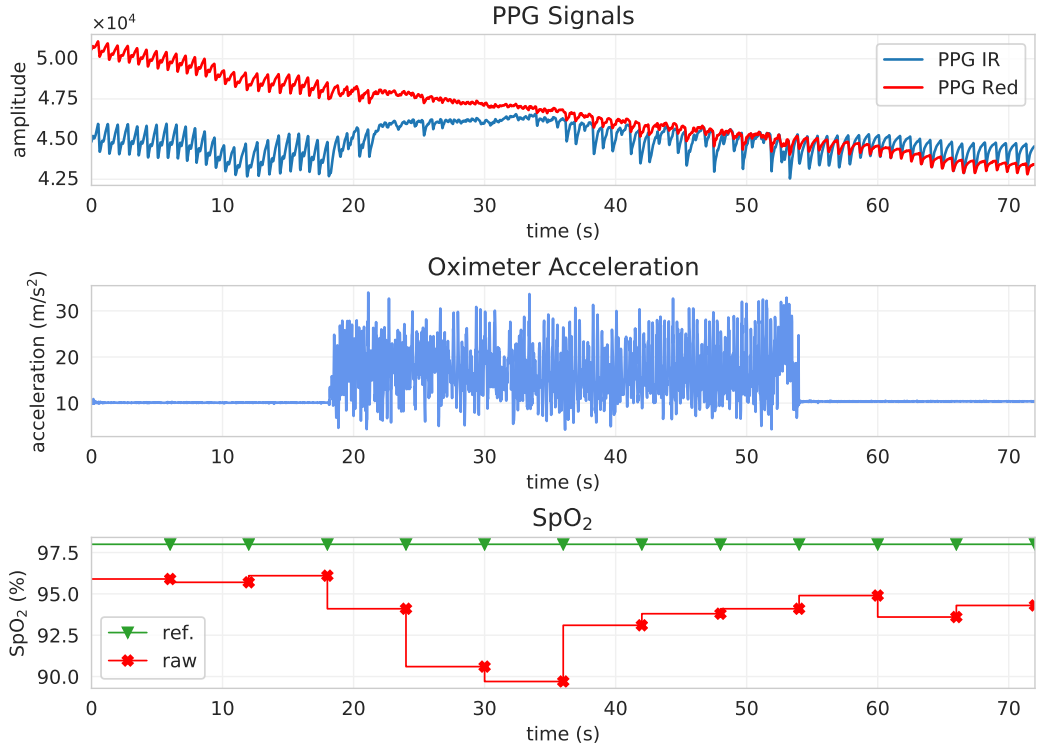

Source – Caíque Santos Lima, 2022.

2 Theoretical reference

The theoretical reference of this work lays the foundation for obtaining the oximetric parameters and introduces some techniques presented in the literature about the PPG signals. Sections 2.1 and 2.2 describe how to use different methods to get SpO_2 and HR from PPG signals, respectively. Section 2.3 discusses the calibration process for pulse oximeters and in section 2.4 the "gold standard" for the calibration of these oximeters is described. Section 2.5 presents PPG signal correction techniques found in the literature. Last but not least, the objectives of this research are listed in section 2.6.

2.1 Obtaining SpO_2 from photoplethysmographic signals

As seen in subsection 1.5.1, SpO_2 can be estimated from the red and infrared PPG signals. Three methods are presented below to obtain SpO_2 estimations, namely: *SpO_2 classical method*, *SpO_2 PPG differentials* and *SpO_2 spectral analysis*.

2.1.1 SpO_2 classical method

Oxygen saturation can be obtained by calculating the ratio between the light of the red and the infrared LEDs. The AC and DC components of the signals PPG are normalized (calculating the ratio of AC to DC) to obtain the R ratio (equation 4), which is given by the ratio of red light normalized by infrared light normalized. Finally, a linear approximation is applied to calculate SpO_2 (MAXIM INTEGRATED, 2018b)(STROGONOVS, 2017).

In Figure 9, the DC component of the infrared light (DC_{IR}) is obtained from the points P_1, P_2 and P_3. DC_{IR} is obtained by drawing a line between the points P_1 and P_3 (systolic nadir), and then a line parallel to the y-axis from the point P_2 (diastolic peak) to the line connecting P_1 and P_3. The y-coordinate of the intersection point P_a of the two lines is the DC_{IR} value. Conversely, the DC component of red light (DC_{red}) is obtained from the points P_4, P_5 and P_6. DC_{red} is obtained by drawing a line between the points P_4 and P_6, and then a line parallel to the y-axis from the point P_5 to the line connecting P_4 and P_6. The y-coordinate of the point P_b of intersection of these two lines is the DC_{red} value.

The AC component of infrared light (AC_{IR}) is obtained by subtracting the y-coordinate of the point P_2 from the y-coordinate of the point P_a. And the AC component of red light (AC_{red}) is obtained by subtracting the y-coordinate of the point P_5 by the y-coordinate of the point P_b.

Figure 9 shows PPG signals obtained from a MAX30102 sensor (MAXIM INTEGRATED, 2018a). In this example, it is demonstrated how SpO_2 is obtained from infrared and red lights. The first plot presents the PPG signal generated by the infrared LED, and the second plot the PPG signal generated by the red LED. The vertical axes indicate the light detected by the photodiode and the horizontal axes indicate the time in seconds.

Figure 9 – Classic method to obtain AC and DC values from PPG signals.

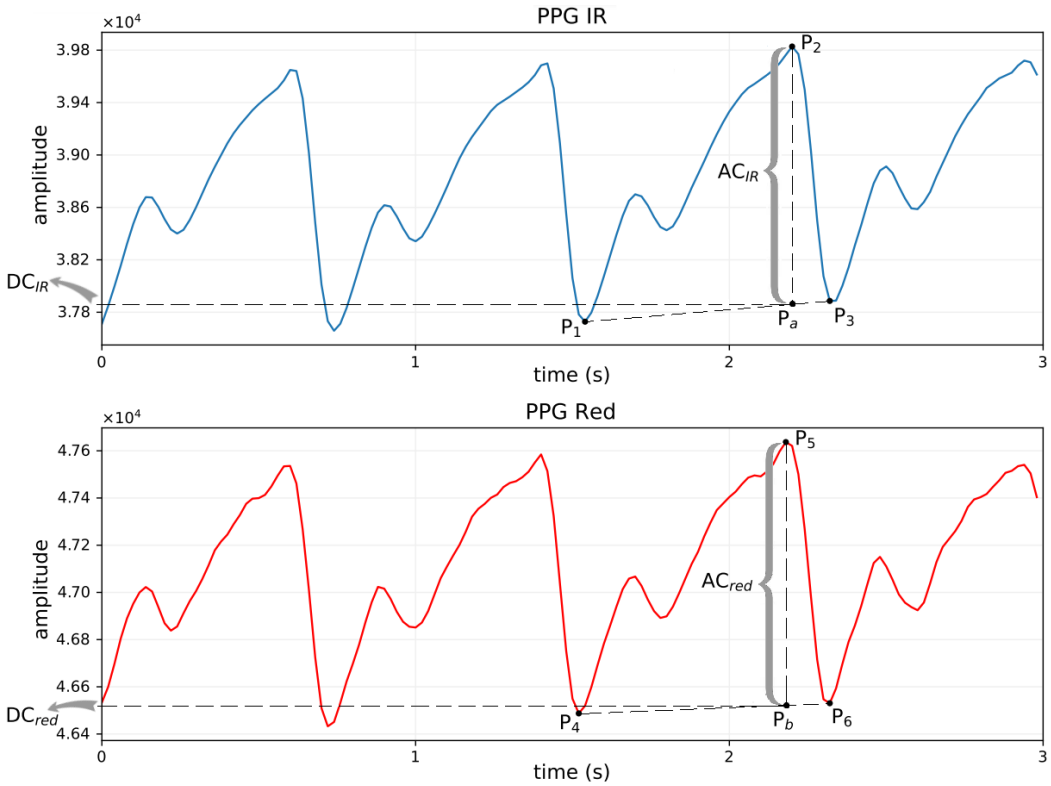

Source – Caíque Santos Lima, 2022.

After obtaining the values of the AC and DC components of each signal, the value of R (equation 4) is calculated. Then, SpO_2 is obtained from a linear approximation (MAXIM INTEGRATED, 2018b) determined by the sensor manufacturer (equation 5).

$$R = \frac{\frac{AC_{red}}{DC_{red}}}{\frac{AC_{IR}}{DC_{IR}}} \tag{4}$$

$$SpO_2 = 104 - 17 \times R \tag{5}$$

For the example shown in Figure 9, SpO_2 can be obtained using the equations 4 and 5 as follows:

$$R = \frac{\frac{47637 - 46519}{46519}}{\frac{39828 - 37866}{37866}} \approx 0.46383$$

$$SpO_2 = 104 - 17 \times 0.46383 \approx 96.1\%$$

2.1.2 SpO_2 PPG differentials

As discussed in subsection 2.1.1, to get SpO_2 from the PPG signals it is necessary to obtain the AC and DC components first. In addition to the classical method (Figure 10A), the AC components can be obtained through the mean amplitude difference between consecutive sample points in a PPG signal, as depicted in Figure 10B. According to Mendelson (1992 apud JOHNSTON, 2006), the advantages of this method are its high processing speeds and the minimal resources needed to implement the algorithms. However, the average should be used to smooth out the final results, as there are usually small variations between consecutive measurements. Another advantage lies in the fact that in the *SpO_2 PPG differentials* method it is not necessary to have a complete waveform of the PPG signal which depends on the person's heart rate.

Figure 10 – AC component estimation based on (A) peak-nadir differences and (B) point-to-point differentials.

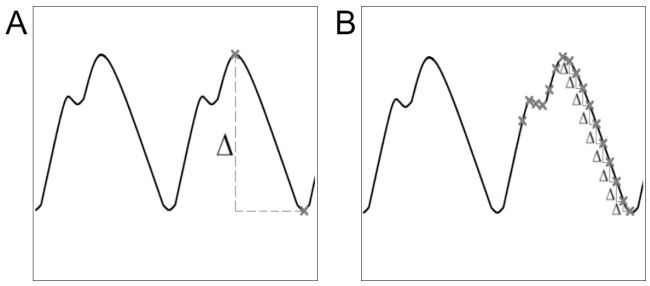

Source – adapted from Johnston (2006, p. 19).

The DC components in this approach can be obtained from the average value of a samples section of the PPG signal (JOHNSTON, 2006). In a 6-second section, as shown in Figure 11, the absolute derivative is averaged to produce the AC component. After calculating these components, the equations 4 and 5 are applied to obtain the SpO_2.

Figure 11 – PPG signal with corresponding derivative and absolute derivative. The red dotted lines are used to obtain DC and AC values.

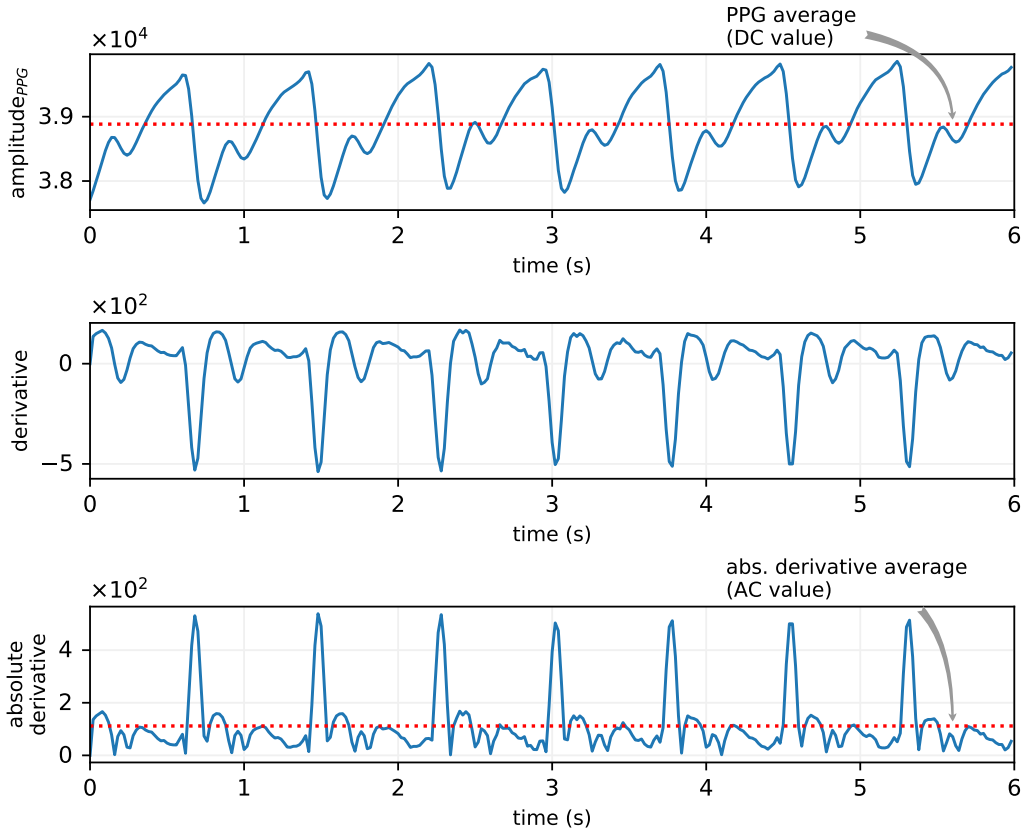

Source – Caíque Santos Lima, 2022.

2.1.3 SpO_2 spectral analysis

Finally, an alternative method to obtain the AC and DC components, through the frequency domain, is the *SpO_2 spectral analysis* (JOHNSTON, 2006). The DC and AC components can be estimated based on the heights of the 0 Hz and cardiac spectral peaks, respectively, as shown in Figure 12. Then, the equations 4 and 5 are applied to obtain the SpO_2. According to Johnston (2006, p. 20), "[...] spectral analysis boasts potential improvements over time-based computations, including greater measurement accuracy, insensitivity to high frequency noise, and better stability in the presence of light motion artifacts."

Figure 12 – Fourier transform of a PPG signal. The x-markers are used to obtain DC and AC values.

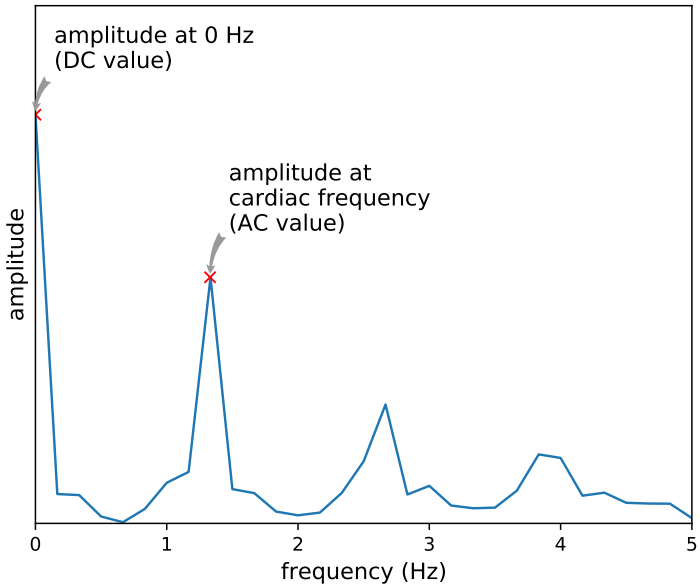

Source – Caíque Santos Lima, 2022.

2.2 Obtaining HR from photoplethysmographic signal

HR measurements can be estimated based on the PPG signal as there is a strong influence of cardiac activity on the pulsatile nature of arterial blood flow (JOHNSTON, 2006). Next, two different methods will be presented to obtain HR from the PPG signal. It is worth noting that for this, conventionally, only the infrared PPG signal is used, although it is also possible to obtain HR through the red PPG signal.

2.2.1 HR PPG differentials

In the *HR PPG differentials* method, the absolute derivative of PPG signal is used to identify pulse peaks and estimate HR, it determines the number of times the heart beats. These peaks are generated in the systolic phase and the interval at which they occur determines the duration of a cardiac cycle. In Figure 13, it is possible to observe that the x-markers in the absolute derivative of the PPG signal determine the beginning of the cardiac cycle.

Figure 13 – Use of absolute derivatives to identify pulse peaks.

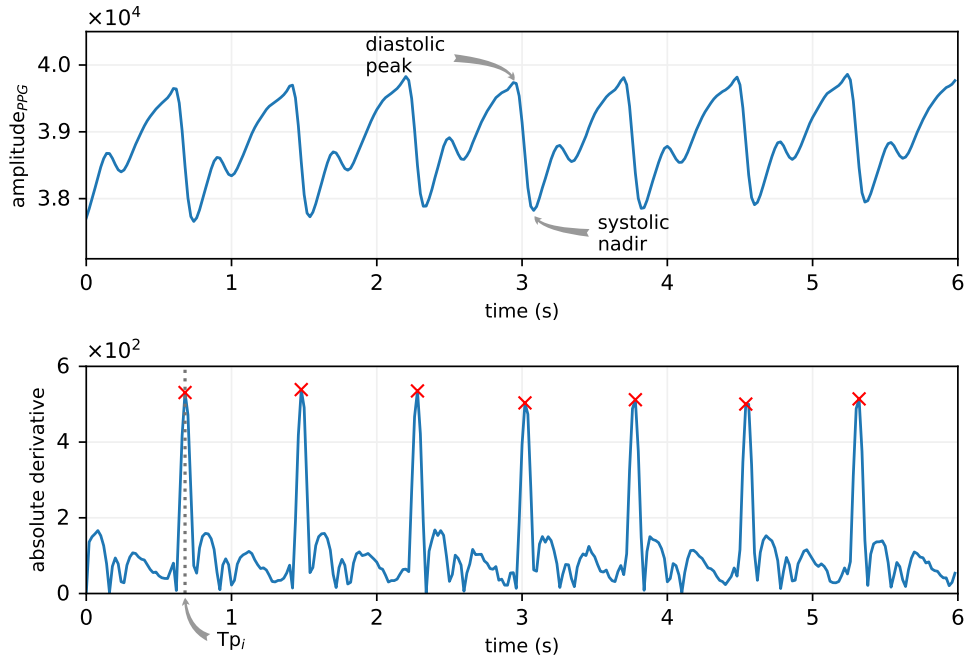

Source – Caíque Santos Lima, 2022.

The number of pulse peaks that occur in a 60-second period determines the HR in bpm. In the example illustrated in Figure 13, the HR can be obtained as follows:

$$HR = \frac{60}{\frac{1}{n-1} \times \sum_{i=2}^{n} (Tp_i - Tp_{i-1})}, \tag{6}$$

where Tp_i is the time at which the pulse peak occur of the i-th sample and n is the number of pulse peaks counted in a given window.

In this work, HR measurements were estimated in a 6-second window, i.e., at each 6-second section a new measurement was computed from the samples corresponding to that section. To guarantee that at least two positive and two negative pulse peaks were present in any given window, the window width was set to 6 seconds (JOHNSTON, 2006).

2.2.2 HR spectral analysis

According to Reuss e Bahr (2002 apud JOHNSTON, 2006), HR measurements can also be obtained using spectral analysis. The DFT of the PPG signal, as illustrated in Figure 14, normally contain a high-amplitude peak located at the cardiac frequency.

Figure 14 – Fourier transform of a PPG signal. The x-marker is used to obtain cardiac frequency and then HR.

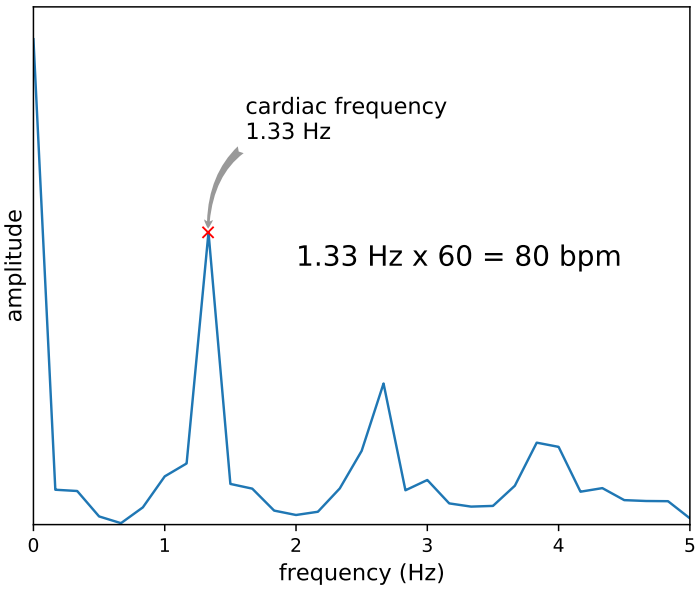

Source – Caíque Santos Lima, 2022.

In the example shown in Figure 14, the HR, in bpm, can be obtained using the cardiac frequency (fc) by applying equation 7.

$$HR = 60 \times fc. \tag{7}$$

2.3 Calibration process

As shown earlier, SpO_2 is obtained through the R ratio. A large set of data obtained from clinical studies is collected containing information about the R ratio calculated by the pulse oximeter and the actual SaO_2 measured by a very accurate method such as the CO-oximeter (WEBSTER, 1997). The Beer–Lambert law does not apply to pulse oximeters due to the scattering effects of the blood stream (MOYLE, 2002)(WEBSTER, 1997). According to Moyle (2002), all pulse oximeter manufacturers no longer use the method of obtaining SpO_2 by the Beer–Lambert law, for that, empirical data are used for calibration.

During the *in vivo* calibration process, the SpO_2 of test participants is controlled via a gas mask. During data collection, the amount of oxygen in the blood is gradually reduced, leaving the volunteer's respiratory gas mixtures with low oxygen content. Blood samples are collected at each level when the pulse oximeter shows a stable reading and

they are analyzed with the CO-oximeter. These samples are collected in the saturation range of 70% to 100%. Due to ethical issues, saturation levels below 60% can only be achieved through the *in vitro* method of calibration, i.e., with systems that artificially simulate the SpO_2 of a person (WEBSTER, 1997).

In the pulse oximeter calibration curve, SaO_2, obtained by CO-oximetry, is plotted against the R ratio, measured by the pulse oximeter. Through the recorded data, the curve is fitted using regression methods. These tests are performed to determine the pulse oximeter calibration equation coefficients. An example of a calibration graph is shown in Figure 15. The vertical axis indicates SaO_2 in percentage and the horizontal axis the values of R measured by the pulse oximeter in calibration.

Figure 15 – Example of a calibration dataset and a best fit SpO_2 calibration curve.

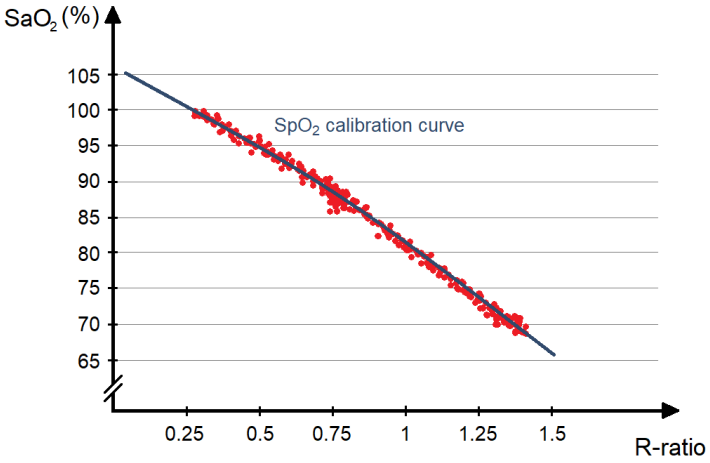

Source – adapted from Urpalainen (2011, p. 15).

Before being made available on the market, pulse oximeters are evaluated according to technical criteria to attest to their good performance. For example, FDA (Food and Drug Administration) recommends using the ISO 9919 standard which has been revised with the ISO 80601-2-61 standard (ISO, 2017). It requires manufacturers to report the calibration range, reference, accuracy, calibration methods and range of displayed SpO_2 levels. In addition, FDA recommends that at least 200 data points evenly spaced in a saturation range of 70 to 100% be collected in the calibration process and the accuracy to be at least 3 to 5% (URPALAINEN, 2011).

In Brazil, the standard that regulates pulse oximetry is ABNT NBR ISO 80601-2-61:2015 (ABNT, 2015). It establishes that SpO_2 measured by pulse oximeters must have an error lower than or equal to 4% over the range from 70 to 100% of SaO_2. This standard

recommends that the calibration study include a sufficient number of volunteers to reach the statistical significance necessary to demonstrate such accuracy.

2.4 CO-oximeter

The CO-oximeter is considered the gold standard for the calibration of pulse oximeters, i.e., it refers to the most accurate way in which it is possible to determine the level of oxygen in the blood. The term CO-oximeter was coined by Instrumentation Laboratories Inc. who launched the first product on the market in 1966 (MOYLE, 2002). They are spectrophotometers designed to analyze the concentrations of different types of hemoglobin, including RHb, HbO_2, HbCO and HbMet. Each of these forms of hemoglobin has its own molar extinction coefficient curve (Figure 16). From four wavelengths of light, the amount of each of these forms of hemoglobin can be determined from a blood sample (WEBSTER, 1997).

Figure 16 – Molar extinction coefficient for RHb, HbO_2, HbCO and HbMet in the range from 570 to 1000 nm.

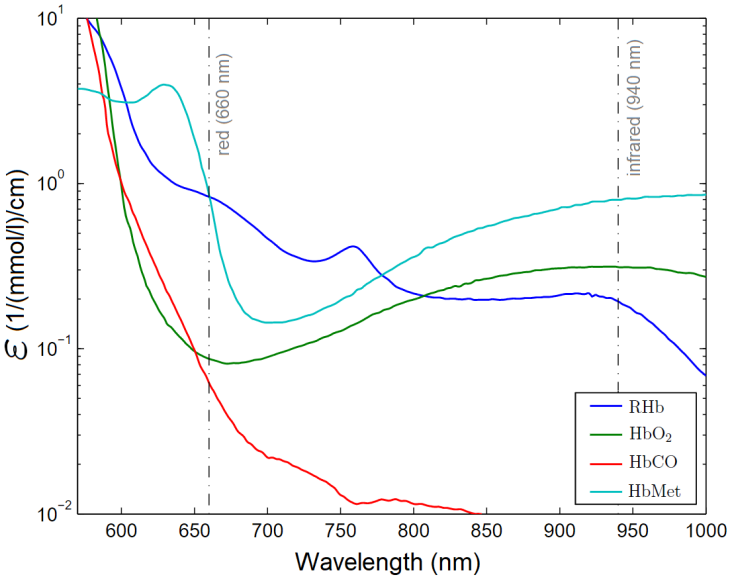

Source – adapted from Urpalainen (2011, p. 11).

The CO-oximeter measures SaO_2 through a technique of quantitative analysis of the absorption of light from a sample of the individual's blood, therefore, it is possible to determine the oxygen level only at the moment when the blood was collected. CO-oximeters measure oxygen saturation by a spectrophotometric technique such as pulse oximetry, but these devices do not use the same wavelengths as pulse oximeters. While most pulse

oximeters use red (660 nm) and infrared (940 nm), most CO-oximeters operate in the visible range (400–660 nm) as they only work with hemoglobin solution in plasma, whereas unlike pulse oximeters that operate through skin, muscle and bone (MOYLE, 2002).

Unlike pulse oximeters, which are portable and wieldy devices, CO-oximeters are unwieldy equipments and have their application mainly as a standard for pulse oximeter calibration. Although the CO-oximeter has the most accurate method for measuring hemoglobin, pulse oximeters are the most suitable devices for monitoring SpO_2 over time (WEBSTER, 1997). Figure 17 presents a model of CO-oximeter.

Figure 17 – CO-oximeter Avoximeter™ 4000.

Source – Kinoshita et al. (2017).

2.5 Photoplethysmographic signal correction techniques

Since movement noise is a problem, several techniques have been used to detect and remove it (SALEHIZADEH et al., 2014). Among them, the moving average is a method that can be used to eliminate noise, although for cases where the patient has continuous chills and recurrent tremors, the error of SpO_2 can be considerably large (LEE; JUNG; KANG, 2003). Another means used to deal with noise are adaptive filters, in addition to being easy to implement, they can also be used in real-time applications, but their main disadvantage is that to provide the input signals it is necessary to install additional sensors (SALEHIZADEH et al., 2014).

Other signal processing techniques can be applied in order to mitigate noise caused by movement. Among them are: the fast Fourier transform (FFT) and the smoothed pseudo Wigner-Ville distribution (SPWVD) (CHO; KIM; YOON, 2014). According to Yan, Poon e Zhang (2005 apud CHO; KIM; YOON, 2014), these techniques have some disadvantages: SpO_2 values take a long time to be updated and they demand high computing power, which makes it difficult to implement them in compact and cheap commercial products.

In the 1990s, several signal processing techniques were incorporated into pulse oximeters. Among them, the mathematical manipulation of red and infrared lights signals to measure and subtract noise components associated with motion and low perfusion (DUMAS; WAHR; TREMPER, 1996). An example of this technique is the Masimo Signal Extraction Technology (SET®). The proprietary code of this company contains, in its first stage, a filtering and normalization of the LEDs signals, which feed 4 parallel algorithms, all registered and with a combinatorial logic capable of separating the noisy data from the oxygenation (MASIMO, 2020).

In addition to the signal processing techniques applied for decades, other mechanisms can also be applied with the same objective of improving the performance of pulse oximeters, for example, algorithms based on artificial intelligence for photoplethysmographic wave correction (BARKER, 2002)(TARVIRDIZADEH et al., 2020). Among the clever techniques that are able to detect noise from motion and reconstruct, in real time, the corrupted parts of the PPG signal, the following stand out: the modeling based on the multilayer perceptron (MLP), radial basis function (RBF) and adaptive neuro-fuzzy inference system (ANFIS).

Table 2 presents a summary of the literature found about the techniques for correction of the PPG signal. In work [1] the SPWVD approach is compared with the weighted moving average (WMA) and the FFT approaches. In [2] the performance of algorithms based on MLP, RBF and ANFIS was compared to detect movements and reconstruct the corrupted parts of the PPG signal. Through the singular spectrum analysis (SSA) technique, the authors of [3] proposed an algorithm for motion detection and reconstruction of PPG signal. In [4], through an low-pass filter (LPF) and an infinite impulse response (IIR) filter, a real-time monitoring algorithm was presented to remove data affected by motion. The authors of [5] created an algorithm named OxiMA, based on variable frequency complex demodulation (VFCDM) to analyze the frequencies that make up the PPG signals and reconstruct them. In [6], using an accelerometer and signal filtering

techniques, an algorithm capable of detecting and discarding PPG signals corrupted by motion was proposed.

Table 2 – Different PPG signal correction techniques.

Ref.	Techniques used	Additional sensors?	Reconstruction of the signal?	Experimental protocol	Performance
[1]	SPWVD, WMA and FFT	×	×	6 healthy subjects	SpO_2: SPWVD, WMA and FFT approaches differed from the reference by -1.07 ±2.42%, -1.31 ±3.58% and -1.42 ±3.18%, respectively. HR: MAE of 5.62, 16.4 and 11.2 bpm, respectively.
[2]	MLP, RBF and ANFIS	×	✓	23 healthy volunteers with an average age of 26.6 years (±1.3)	ANFIS: PCC = 0.8 ICC = 0.77
[3]	SSA	×	✓	11 healthy volunteers	–
[4]	LPF, 2nd order IIR filter and decision algorithm to remove data affected by motion	×	×	5 newborns with normal breathing in a NICU with an average age of 44.8 days (±44.1)	Detection of 20.6% of movements in the range of 93% to 100% of SpO_2
[5]	VFCDM	×	✓	10 volunteers in induced hypoxia with an average age of 27 years	Improvement of 8.75% and 5.82% in HR and SpO_2 estimations, respectively
[6]	LPF for the PPG signals and BPF for the accelerometer	✓	×	4 volunteers aged between 20 and 54 years old	Std. deviation of SpO_2<1.2 and valid estimations of SpO_2 in 90% of frames

Source – [1] Yan, Poon e Zhang (2005); [2] Tarvirdizadeh et al. (2020); [3] Salehizadeh et al. (2014); [4] Cho, Kim e Yoon (2014); [5] Harvey et al. (2019) and [6] Williamson et al. (2018).

2.6 Research objectives

From the problems previously reported, this research sought to develop an algorithm to give robustness to the measurement of SpO_2 and HR in the presence of motion in the pulse oximeter. The use of artificial intelligence techniques and additional sensors to attenuate undesirable effects on the oximetry signal was evaluated. This smart system improved a pulse oximeter developed at the Federal University of São Carlos (UFSCar).

The specific objectives of this research were:

1. study and understand the PPG signal from the factors that interfere with the photoplethysmographic wave;

2. through machine learning techniques, classify whether the data was affected by motion in the oximeter;
3. create a dataset from oximetry signals collected from volunteers;
4. propose an algorithm that combines the classification of the affected PPG signal with the estimations of SpO_2 and HR;
5. compare the performance of the proposed algorithm with other techniques:
    a) simple moving average (SMA);
    b) FFT (YAN; POON; ZHANG, 2005).

3 Materials and methods

This chapter gives a detailed account of the procedures as well as the materials, techniques and metrics used in this work. Section 3.1 presents the datasets used. The pulse oximeter prototype is described in section 3.2. The artificial neural network (ANN) and the digital filters used in the algorithms proposed here are introduced in sections 3.3 and 3.4, respectively. Finally, the metrics used to assess these algorithms are presented in sections 3.5 and 3.6.

3.1 Datasets

To assess how external factors could affect PPG signals, the first step was to analyze data from previous works. For this, two independent and public datasets available on the Internet were used: *BIDMC PPG and Respiration Dataset* (GOLDBERGER et al., 2000), and the *PPG Diary Dataset* (CHARLTON, 2021). In addition to these datasets found on the Internet, a dataset was also created, named *Personal PPG Dataset*, from PPG signals collected from the author of this work. Another dataset called *Vols PPG Dataset* collected from 20 healthy volunteers was also a result of this work. Each of these datasets are described below.

3.1.1 BIDMC PPG and Respiration Dataset

The data contained in the BIDMC PPG and Respiration Dataset were collected from critically ill patients during hospital care in Boston, USA, at Beth Israel Deaconess Medical Center (BIDMC). The recorded data includes physiological signals, physiological parameters, fixed parameters (age and sex) and manual notes of each patient's breathing (GOLDBERGER et al., 2000). Physiological signals were sampled at fs = 125 Hz, from 53 adult patients with an average age of 64.81 years, ranging from 19 to 90+ years, 32 women and 21 men (PIMENTEL et al., 2017). In total, 53 records were made, each one lasting 8 minutes and the data were identified by numbers (from 01 to 53) in order to preserve the confidentiality of each patient.

Figure 18 shows part of the data that make up the BIDMC PPG and Respiration Dataset. The illustration on the left shows some data collected from the first patient,

classified as *bidmc_01*. The graph on the right shows the PPG signal, in which it is possible to observe that, after 91 seconds, the PLETH signal does not present the PPG pattern observed in the previous moments. From the information contained in this dataset, it is not possible to identify the cause of this inconsistency. There is no information about possible motion on the oximeter during monitoring and it is unclear whether the PLETH signal refers to raw red or infrared light data from the sensor.

Figure 18 – BIDMC PPG and Respiration Dataset.

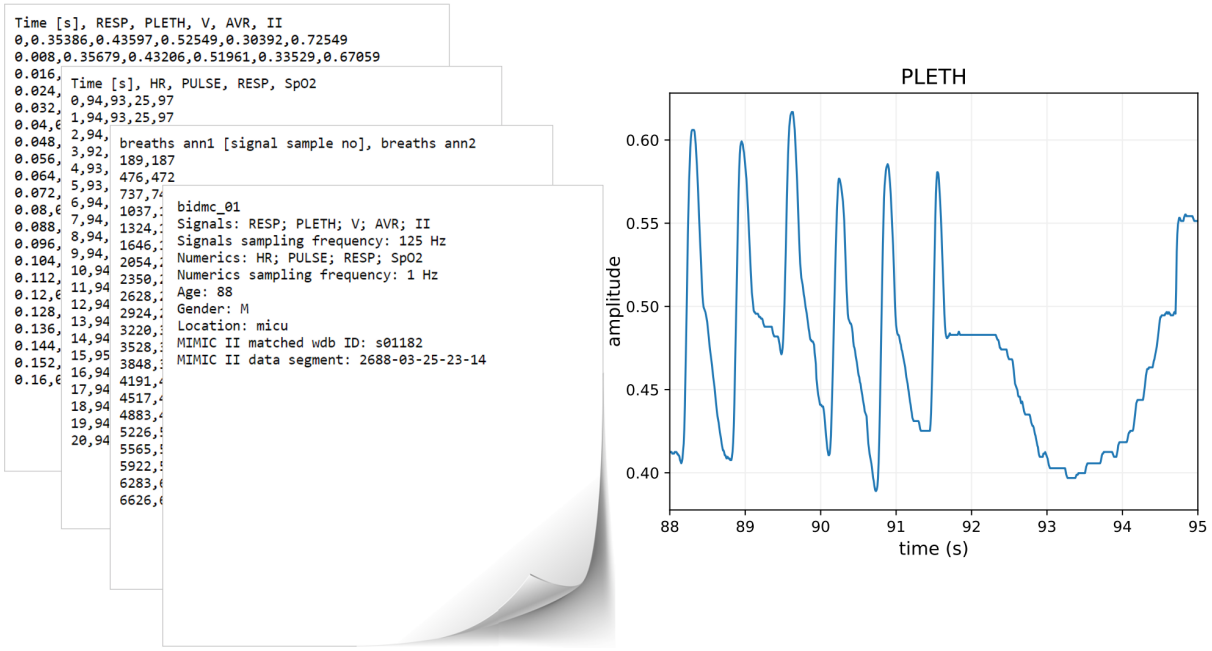

Source – Caíque Santos Lima, 2022.

In the illustration on the left in Figure 18 it is possible to observe the physiological signals, such as PPG (PLETH), respiratory impedance signal (RESP) and electrocardiogram (ECG). Physiological parameters such as HR, respiratory rate and the level of SpO_2 are also noted. These parameters were sampled at 1 Hz. Additionally, manual breathing notes made by two researchers (*ann1* and *ann2*) were included. Finally, the personal parameters of each patient were recorded: identification, age and sex, named fixed parameters.

3.1.2 PPG Diary Dataset

The PPG Diary Project aims to assess the feasibility of acquiring data PPG during people's daily lives, thus, new solutions for health monitoring can be developed, according

to the authors. On the project's webpage, some subsets of preliminary data have already been made available and the authors report that they intend to make all data from the study available in due course (CHARLTON, 2021). The data available include the simultaneous recording of PPG signals (red and infrared), sampled at fs = 100 Hz, during one hour of sleep by a volunteer.

Figure 19 presents part of the data that compose the PPG Diary Dataset. The illustration on the left shows some data that were recorded during the one-hour period in which the volunteer slept. The graphs on the right show that both PPG signals (infrared and red), just before 30 seconds, no longer show the pattern PPG observed in the previous moments. As there is no additional information about this pattern change, it is not possible to determine the cause of this inconsistency.

Figure 19 – PPG Diary Dataset.

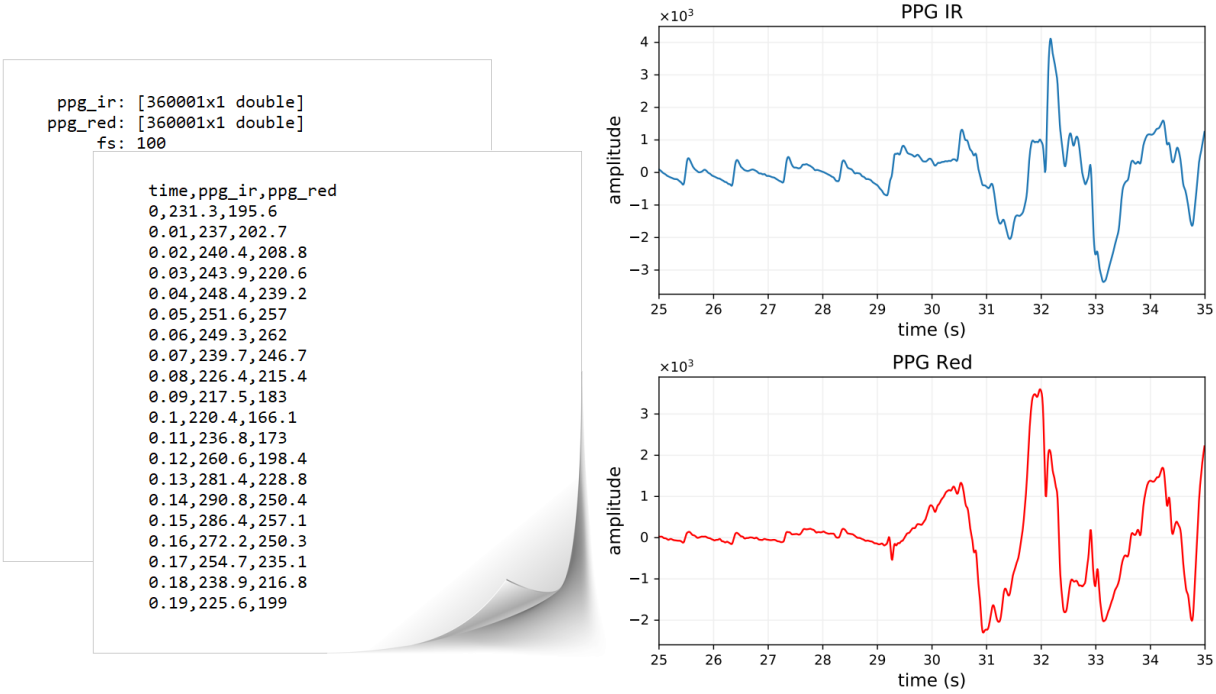

Source – Caíque Santos Lima, 2022.

In the illustration on the left in Figure 19 it is possible to visualize the time in seconds, the strength of the infrared PPG signal and the red PPG signal, in the 1st, 2nd and 3rd columns, respectively. This dataset does not provide additional data about interference factors in PPG signals, nor information about the volunteer.

3.1.3 Personal PPG Dataset

From the datasets shown in the 3.1.1 and 3.1.2 subsections, it was not possible to quantitatively assess how the PPG signals were affected by the motion, since both datasets obtained, did not bring information about interference factors in PPG signals. In these datasets, the signals at certain times seemed to be affected, however, there was no additional information to determine the cause of these inconsistencies.

Aiming to investigate the interference in the PPG signals caused by the movement of the oximeter, the Personal PPG Dataset was created using a MAX30102 photoplethysmographic sensor. To record the magnitude of the movements applied to the sensor, an MPU-9250 accelerometer was used. Later these sensors will be presented in detail. The data that make up the "Personal" dataset were sampled at a frequency fs = 50 Hz. Logged information includes NTP (Network Time Protocol); the time in seconds; the strength of the infrared and red PPG signals; the acceleration on the x, y and z axes; SpO_2 and HR measured by a reference oximeter (this procedure will be presented in section 4.2); and, finally, a column that identifies the samples affected by motion artifact (MA). In all, 40 records were collected from the author himself (27 years old), each one lasting 72 seconds, totaling 48 minutes of oximetric recordings.

These records were collected over three consecutive days, in the three periods of the day: during the morning, in the afternoon and at night. During each collection, movements were produced in order to affect the PPG signals for half of the total time of 72 seconds, i.e., during the initial 18 seconds, the oximeter was kept at rest, then it was moved for 36 seconds and, for end, returned to be held at rest in the final 18 seconds. This approach was adopted so that there was a balance between the amount of affected and normal samples.

Figure 20 presents part of the data that compose the Personal PPG Dataset. The illustration on the left shows some data that were recorded in one of the tests, in which movements were applied to the sensor to observe the behavior of the PPG signals while recording the sensor's acceleration. The graphs on the right show that from the moment the sensor started moving (around 18 seconds), the PPG signals were affected. In the illustration on the left in Figure 20 it is possible to see all the logged parameters.

Figure 20 – Personal PPG Dataset.

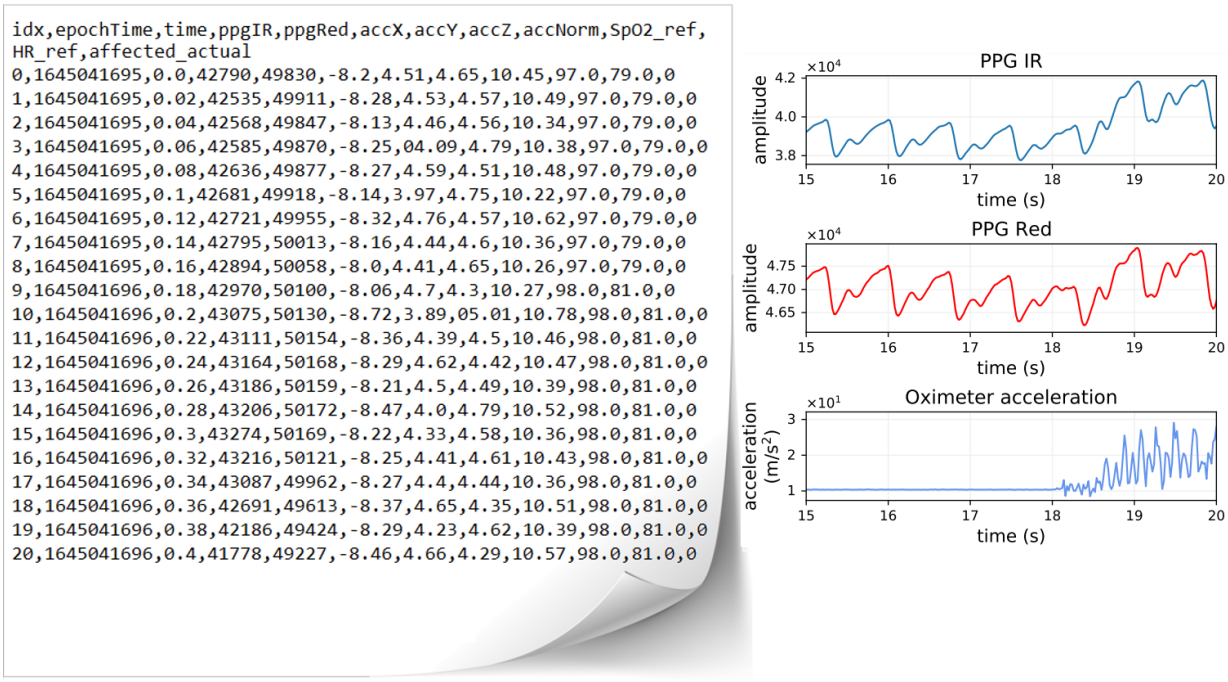

Source – Caíque Santos Lima, 2022.

3.1.4 Vols PPG Dataset

As explained above, the Personal PPG Dataset was useful to assess the interferences in the PPG signals caused by the movement of the oximeter. However, this dataset is restricted to single subject data. In order to increase the variability of oximetric data, the Vols PPG Dataset was created.

The "Vols" dataset features data from 20 healthy volunteers. Logged information acquired at fs = 50 Hz in this dataset includes the same parameters recorded in the "Personal" dataset. As it is an initial exploratory study, the Vols PPG Dataset contains health information of 2 men and 18 women with a average age of 36.15 years, ranging from 24 to 57 years. In all, 100 records were collected from these volunteers (5 records of each), each one lasting 72 seconds, totaling 2 hours of oximetric recordings.

These records were collected over one day, without distinction of periods of the day for each volunteer. Each recording was collected immediately after the previous one. As in the "Personal" dataset, during each collection, movements were produced in order to affect the PPG signals that make up the Vols PPG Dataset.

Figure 21 shows part of the data that compose the Vols PPG Dataset. The illustration on the left shows some data that were recorded as well as the personal information of each volunteer, including the questions asked to each of them. The graphs on the right show the parameters of interest in this dataset.

Figure 21 – Vols PPG Dataset.

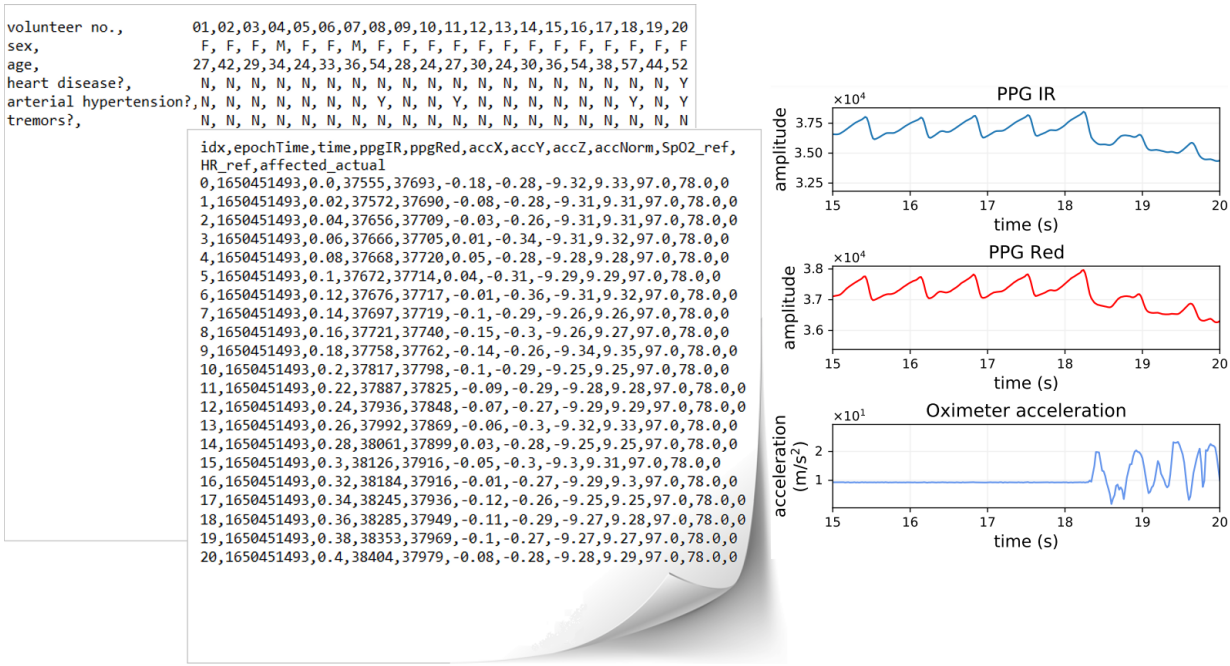

Source – Caíque Santos Lima, 2022.

In order to protect the identity of each volunteer and facilitate the organization of data, each record was named according to the logic presented in Figure 22. With *volunteer no.* ranging from 01 to 20 and *record no.* ranging from 01 to 05. The way in which these data were subdivided and used in this work can be consulted in the Appendix D.

Figure 22 – File naming of the Vols PPG Dataset.

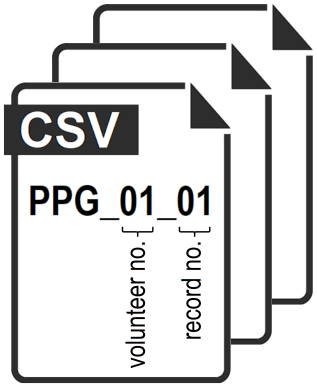

Source – Caíque Santos Lima, 2022.

3.2 Pulse oximeter prototype

This work focuses on studying the interference caused in the oximetry signal in a reflection-type pulse oximeter that is being developed at UFSCar. This prototype features a Wemos D1 Mini microcontroller, a 3.7 V – 1 Ah battery and a module with the MAX30102 sensor manufactured by Maxim Integrated. This sensor combines two LEDs (red and infrared) and a photodiode, being able to measure oxygen saturation and heart rate (MAXIM INTEGRATED, 2018a).

The sensor MAX30102 includes low-noise electronics with ambient light rejection. It is a tiny optical module to ease the design-in process for mobile and wearable devices. According to Maxim Integrated (2018a), this PPG sensor is a device that is robust to motion artifacts. Table 3 presents the main specifications of the module that contains the MAX30102 sensor.

Table 3 – Main features of the reflection-type PPG sensor.

Module with MAX30102 sensor
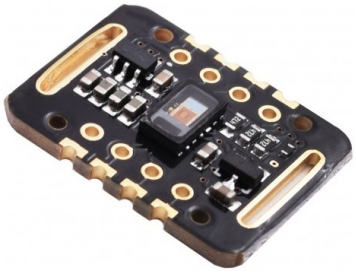
✓ Tiny 20.3×15.2 mm optical module, weight: 1.1 g
✓ Ultra-low power operation for mobile devices
✓ Fast data output capability
✓ -40°C to +85°C operating temperature range
✓ 3.3–5 V supply voltage
✓ I^2C communication
✓ Ultra-low shutdown current (0.7 µA typ., sensor)
✓ Approximate price: US$ 2.90

Source – Smart Prototyping (2022b) and Maxim Integrated (2018a).

To evaluate the influence of motion on PPG signals, an inertial measurement unit (IMU) sensor was applied to the prototype. The device used to measure the acceleration caused by the movement of the person's hand is a module with a MPU-9250 sensor manufactured by InvenSense Inc. This sensor combines a 3-axis gyroscope, a 3-axis

accelerometer and a 3-axis magnetometer (INVENSENSE INC., 2014). Table 4 presents the main specifications of the module that contains the MPU-9250 sensor.

Table 4 – Main features of the IMU sensor.

MPU-9250 6DOF sensor breakout board
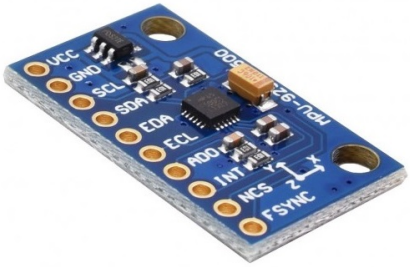
✓ Small 15×25 mm package, weight: 2 g
✓ Gyroscope range: ±250, ±500, ±1000 and ±2000°/s
✓ Accelerometer range: ±2, ±4, ±8 and ±16 g
✓ Magnetometer range: ±4800 µT
✓ 3.3–5 V supply voltage
✓ I^2C/SPI communication
✓ Operating current: 3.5 mA
✓ Approximate price: US$ 2.90

Source – Smart Prototyping (2022a) and InvenSense Inc. (2014).

The algorithms proposed in this work were tested in the prototype of a Wi-Fi pulse oximeter developed at UFSCar[1]. Figure 23 presents the main components of this device.

Figure 23 – Pulse oximeter prototype: (A) case attached to the forearm, (B) case with the battery and microcontroller, (C) fingertip-clip that houses the sensor and (D) case attachment strap.

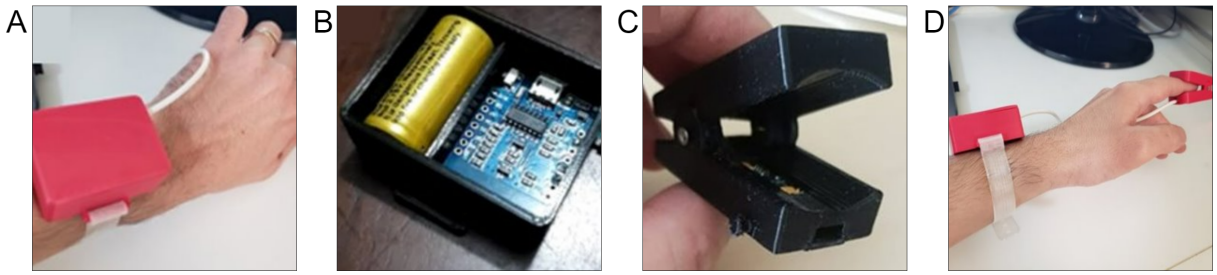

Source – Rafael Vidal Aroca, 2020.

[1] According to Agência de Inovação da UFSCar (2020), this is an open project to assist in remote monitoring of patients by measuring heart rate, blood oxygenation and temperature. The system automatically collects data and sends it to a cloud server, which enables remote monitoring of patients. More information can be accessed on the project website: ⟨https://bipes.net.br/UFSCar/oximetro/⟩

3.3 Artificial neural network

According to Reis (2016), artificial neural networks (ANNs) are computational models capable of performing pattern recognition and machine learning, being inspired by the central nervous system of an animal, in particular the brain. The ANN are basically presented as a system of interconnected neurons that process input values to generate values at the network output.

The ANN are applied in areas of classification and prediction, i.e., areas where regression models and other related statistical techniques are traditionally used. They have been widely used in many areas, including health and medicine. Neural networks are powerful computational models that resulted from work in the field of neurophysiology and are increasingly being applied to medical problems. In clinical medicine, these computational models are used to aid in the diagnosis, detection and classification of diseases (PALIWAL; KUMAR, 2009). It is already possible to find examples where medical artificial intelligence can outperform physicians: heart disease diagnosis better than cardiologists, algorithms identify eye diseases and skin cancer as well as specialized physicians (LONGONI; MOREWEDGE, 2019).

As presented in section 2.5, neural networks are also applied in problems related to interference in the photoplethysmographic signal of pulse oximeters. Another area of health in which ANN is applied and which has gained prominence lately due to the COVID-19 pandemic is epidemiology. Neural networks have been used in the development of prediction models in epidemiological research (ROCHA et al., 2020).

3.3.1 Multilayer perceptron

The multilayer perceptron (MLP) is a model of ANN similar to another simpler model named *perceptron*. Unlike *perceptron* which has only one node, MLP has at least three layers: an input layer, one (or more) hidden layer(s) and an output layer. The layers are interconnected by weighted synapses. Each network node (except input nodes) is a neuron. The activation function $\phi(.)$ is responsible for activating the output of each neuron. Optionally, a *bias* can be applied to each neuron, which has the function of increasing or decreasing the input of the activation function (HAYKIN, 1998).

Figure 24 presents the graphical architecture of a MLP with 2 input nodes (x_1 and x_2), 3 neurons in the hidden layer and 2 neurons in the output layer. A bias (represented by the red lines) was applied to each neuron. The signal flow through the network progresses in a direct direction layer by layer, from left to right (HAYKIN, 2008).

Figure 24 – Topology of a multilayer perceptron (2-3-2).

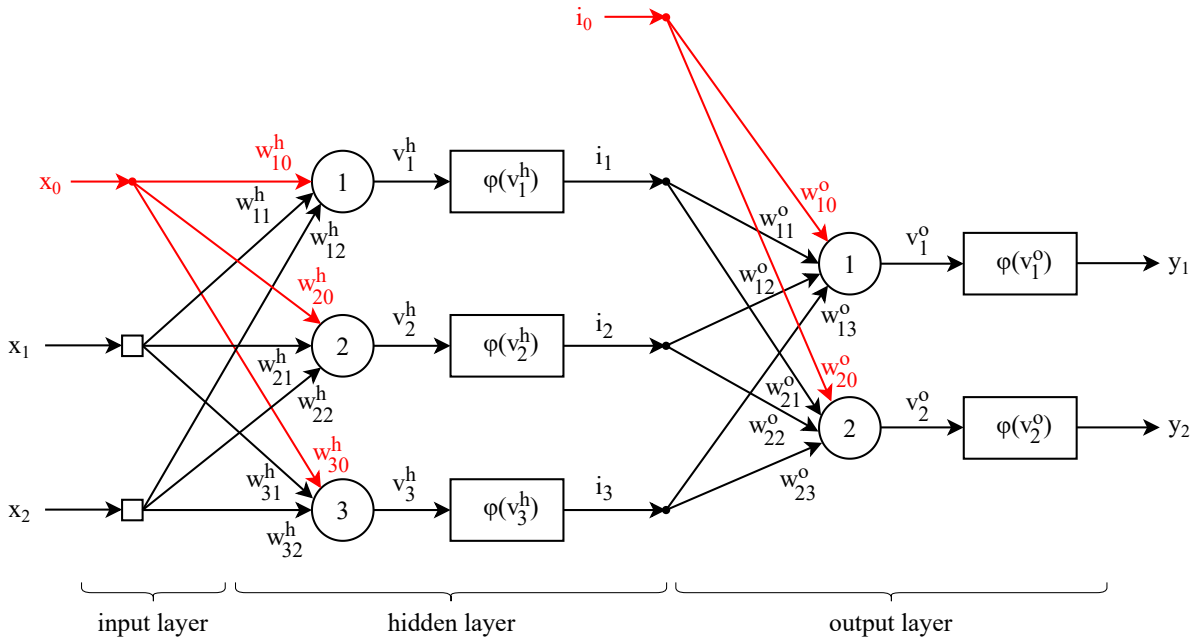

Source – Caíque Santos Lima, 2022.

Backpropagation is a widely used algorithm to train neural networks in a supervised way. This technique consists of two phases of passing the signal through the network to update the weights (w). In the progressive phase, the synaptic weights of the network are fixed and the input signal is propagated through the network, layer by layer, until reaching the output. In reverse phase, an error signal is produced by comparing the network output with a desired response. The resulting error signal is propagated through the network, again layer by layer, but this time propagation is carried out in the reverse direction, from right to left. Thus, successive adjustments are made to the synaptic weights of the network (HAYKIN, 2008).

3.4 Digital filters

Digital filters play an important role in signal processing. They are used to extract parts that may be useful or to reduce undesirable aspects of the digital signal

(OPPENHEIM; SCHAFER, 2014). The digital filters used in this work will be defined below.

3.4.1 Simple moving average

As discussed in section 2.5, a very simple way to deal with noise in the PPG signal is to calculate the average of a selected range. As Yan, Poon e Zhang (2005) showed in their work, typical averaging methods can be used to stabilize the SpO_2 and HR readings. The *simple moving average* (SMA) is an arithmetic moving average calculated by adding the measurements and dividing this value by the number of measurements in the corresponding period. The SMA is calculate as the following equation:

$$SMA = \frac{1}{n} \times \sum_{i=1}^{n} x_i, \tag{8}$$

where x_i is the i-th sample and n is the number of measurements in a given period.

3.4.2 Savitzky-Golay filter

An issue when working with digital data that can be affected by high frequency noise is finding a digital filter that increases the precision of the data without distorting the signal tendency. For this case, one of the most commonly used and frequently cited solution is the digital filter presented by Savitzky e Golay (1964), popularly named: Savitzky-Golay filter, or *savgol*. It is often used as a preprocessing in spectroscopy and signal processing to reduce high frequency noise in a signal due to its smoothing properties. Savgol also can be used to reduce low frequency signal (due to offsets and slopes) using differentiation (GALLAGHER, 2020).

Savgol is a type of low-pass filter that derive directly from the time-domain problem of data smoothing, moreover, it has highly desirable properties for this application (PRESS; TEUKOLSKY, 1990). As demonstrated by Gallagher (2020, p. 1), "[...] for a given signal measured at **N** points and a filter of width **w**, savgol calculates a polynomial fit of order **o** in each filter window as the filter is moved across the signal."

Savgol filter can be easily implemented using a free and open source Python library named SciPy. The Algorithm 1 present an example of a 1 dimensional filter. It is worth

mentioning that if the data to be filtered has dimension greater than 1, through this library, it is also possible to define the axis along which the filter is applied.

Algorithm 1 Savitzky-Golay filter with a window length of 5 and a degree 2 polynomial.

```
1: import numpy as np
2: from scipy.signal import savgol_filter
3:
4: x = np.array([2, 2, 5, 2, 1, 0, 1, 4, 9])     # example array
5:
6: savgol_filter(x, 5, 2)     # window_length = 5, polyorder = 2
```

Source – Virtanen et al. (2020).

3.4.3 Discrete Fourier transform

As shown in section 2.5, the Fourier transform (FT) is a tool that can be used to analyze the characteristics of a PPG wave. For this, it decomposes any signal into a sum of simple sine and cosine waves where it is possible to measure frequency, amplitude and phase (KONG; SIAUW; BAYEN, 2020). Using the discrete Fourier transform (DFT), it is possible to represent the PPG signal as a series of sinusoids and each of them will have a different frequency, as illustrated in Figure 25.

Figure 25 – Discrete Fourier transform scheme.

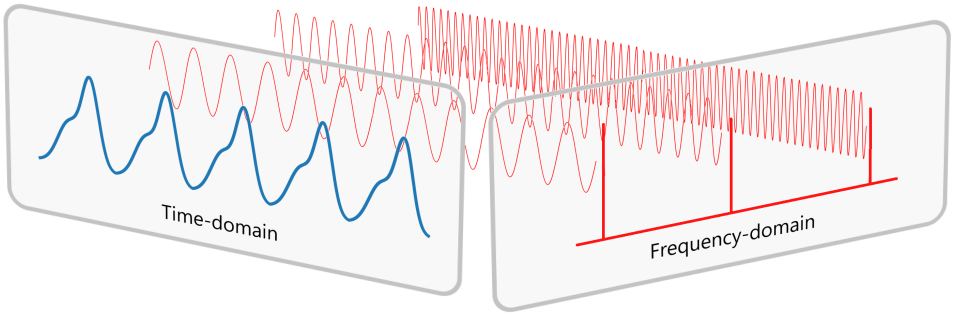

Source – Caíque Santos Lima, 2022.

Mathematically, the forward DFT is defined as follows:

$$X_k = \sum_{n=0}^{N-1} x_n \cdot \left[cos\left(\frac{2\pi}{N} kn\right) - i \cdot sin\left(\frac{2\pi}{N} kn\right) \right] = \sum_{n=0}^{N-1} x_n \cdot e^{-\frac{i2\pi}{N} kn}, \tag{9}$$

where N is the number of samples; n is the current sample, where each value of n provides a sample of the signal in the time-domain; k is the current frequency, where $k \in [0, N-1]$; x_n is the sine value at sample n; and X_k is the DFT which include information of both

amplitude and phase. The sum of the time-samples multiplied (scalar product) by the complex function gives a discrete Fourier component for each value of k.

Each X_k is a complex number with both amplitude and phase of a complex sinusoidal component $e^{i2\pi kn/N}$ of function x_n. The *amplitude* and *phase* of the signal can be calculated using equation 10 and 11, respectively, as follows:

$$amplitude = \frac{|X_k|}{N} = \frac{\sqrt{Re(X_k)^2 + Im(X_k)^2}}{N}, \tag{10}$$

$$phase = atan2[Im(X_k), Re(X_k)], \tag{11}$$

where $Im(X_k)$ and $Re(X_k)$ are the imagery and real part of the complex number, $atan2$ is the two-argument form of the *arctangent* function.

The Algorithm 2 present a function to calculate the DFT of a 1 dimensional real-valued signal x using Python.

Algorithm 2 Discrete Fourier Transform of a 1D real-valued signal x.

```
1: import numpy as np
2:
3: def DFT(x):
4:       N = len(x)
5:       n = np.arange(N)
6:       k = n.reshape((N, 1))
7:       e = np.exp(-2j*np.pi*k*n/N)
8:
9:       X = np.dot(e, x)
10:
11:       return X
```

Source – Kong, Siauw e Bayen (2020).

The main issue with the DFT implementation presented above is that it is not efficient for a signal with many samples, thus, it may take a long time to compute the DFT. To solve this problem, Cooley e Tukey (1965) proposed an efficient solution named fast Fourier transform (FFT). Its basic ideas were popularized in 1965, but some preliminary algorithms had been introduced as early as 1805 (KONG; SIAUW; BAYEN, 2020).

According to Kong, Siauw e Bayen (2020), to reduce DFT computing time, FFT uses a *divide-and-conquer algorithm* that, basically, recursively breaks the DFT into smaller DFTs to bring down the computation. For an input vector of length N, this solution reduces the complexity of the DFT from $\mathcal{O}(N^2)$ to $\mathcal{O}(N\log_2 N)$. This means that for N=10^6 elements, the FFT is expected to complete in something around 50 ms, while the DFT would take almost 20 hours, as demonstrated by VanderPlas (2013).

As shown in the following analytical demonstration, the symmetry approach can be applied to split the DFT computation into two smaller parts. From the definition of the forward DFT presented in equation 9, it is calculated:

$$\begin{aligned} X_{k+N} &= \sum_{n=0}^{N-1} x_n \cdot e^{-i2\pi(k+N)n/N} \\ &= \sum_{n=0}^{N-1} x_n \cdot e^{-i2\pi n} \cdot e^{-i2\pi kn/N}. \end{aligned} \tag{12}$$

Since $e^{-i2\pi n} = 1$, then the symmetry property of the DFT can be shown:

$$X_{k+N} = \sum_{n=0}^{N-1} x_n \cdot e^{-i2\pi kn/N} = X_k. \tag{13}$$

Likewise:

$$X_{k+i\cdot N} = X_k, \tag{14}$$

for any integer i. Using this symmetry, it is possible to reduce the computation, since to calculate both X_k and X_{k+N}, it is only necessary to do this once. This is the idea behind the FFT (COOLEY; TUKEY, 1965).

From the definition of the DFT, it is possible to divide the whole series into two parts, i.e., the even-numbered values and odd-numbered values, as follows:

$$\begin{aligned} X_k &= \sum_{n=0}^{N-1} x_n \cdot e^{-i2\pi kn/N} \\ &= \sum_{m=0}^{N/2-1} x_{2m} \cdot e^{-i2\pi k(2m)/N} + \sum_{m=0}^{N/2-1} x_{2m+1} \cdot e^{-i2\pi k(2m+1)/N} \\ &= \sum_{m=0}^{N/2-1} x_{2m} \cdot e^{-i2\pi km/(N/2)} + e^{-i2\pi k/N} \sum_{m=0}^{N/2-1} x_{2m+1} \cdot e^{-i2\pi km/(N/2)}, \end{aligned} \tag{15}$$

herein, the two smaller terms which only have half of the size $(N/2)$ are two smaller DFTs. According to the symmetry properties described above, it is necessary only to perform half the computations for each sub-problem, because $k \in [0, N)$, while $n \in [0, M)$, where $M \equiv N/2$.

Now, the $\mathcal{O}(N^2)$ computation has become $\mathcal{O}(M^2)$, with M half the size of N. As long as smaller Fourier transforms have an even-valued M, it is possible to reapply this divide-and-conquer approach, halving the computational cost each time, until the arrays are small enough so that the strategy is no longer beneficial. In the asymptotic limit, this recursive approach is $\mathcal{O}(N\log_2 N)$ (VANDERPLAS, 2013).

The Algorithm 3, produced in Python, shows a function to calculate the FFT using the 1 dimensional Cooley-Tukey approach.

Algorithm 3 A recursive implementation of the 1D Cooley-Tukey FFT.

```
import numpy as np

def FFT(x):
      N = len(x)

      if N == 1:
           return x
      else:
           X_even = FFT(x[::2])
           X_odd = FFT(x[1::2])
           factor = np.exp(-2j*np.pi*np.arange(N)/N)

           X = np.concatenate([X_even+factor[:int(N/2)]*X_odd,
                               X_even+factor[int(N/2):]*X_odd])
      return X
```

Source – Kong, Siauw e Bayen (2020).

3.5 Classification metrics

In the field of machine learning, a tool used to evaluate the performance of a model is the confusion matrix. It consists of a table that allows to calculate the model accuracy and visualize the performance of a classification algorithm.

For example, let's take a dataset with 10 samples of a signal, where 4 samples were affected (1) and 6 samples were not affected (0), thus producing:

$$\text{actual values} = [1, 0, 1, 0, 0, 0, 1, 0, 1, 0],$$

now suppose the model predicted the following set:

$$\text{predicted values} = [1, 0, 0, 1, 0, 0, 1, 1, 1, 0].$$

From these two sets, a confusion matrix can be created that will summarize the results of this model. Table 5 illustrates this example and then the results are discussed.

Table 5 – Example of a confusion matrix.

		Predicted	
		Yes (1)	No (0)
Actual	Yes (1)	**3** (*TP*)	1 (*FN*)
	No (0)	2 (*FP*)	**4** (*TN*)

Source – Caíque Santos Lima, 2022.

In this example, the model correctly classified 3 samples of the signal that were affected and 4 samples that were not affected. On the other hand, the model incorrectly classified 2 samples of the signal as affected and 1 sample as unaffected. Therefore, the confusion matrix presents the frequency of:

true positive (TP) – the sample belongs to the affected signal class (1) and the model correctly predicted this;

true negative (TN) – the sample belongs to the unaffected signal class (0) and the model correctly predicted this;

false positive (FP) – the sample belongs to the class of unaffected signal (0) and the model predicted that the sample belongs to the class of affected signal (1);

false negative (FN) – the sample belongs to the affected signal class (1) and the model predicted that the sample belongs to the unaffected signal class (0).

From the confusion matrix it is possible to obtain the following classification metrics:

$$accuracy = \frac{correct\ predictions}{total\ of\ predictions} = \frac{TP + TN}{TP + TN + FP + FN}, \tag{16}$$

$$precision = \frac{correct\ positive\ predictions}{positive\ predictions} = \frac{TP}{TP + FP}, \tag{17}$$

$$recall = \frac{correct\ actual\ positives}{actual\ positives} = \frac{TP}{TP + FN}, \tag{18}$$

$$F1\text{-}score = 2 \times \frac{precision \times recall}{precision + recall}. \tag{19}$$

Therefore, in the example above, the model achieved an *accuracy* of 70%, as it correctly classified 7 out of 10 samples. The *precision* of the classifier was 60%, i.e., of the 5 samples said to be positive by the classifier, only 3 were truly positive. The *recall* was 75%, i.e., of the 4 truly positive samples, the classifier identified only 3. Finally, the *F*1-*score* was 66.67%, this metric represents the harmonic mean of the *precision* and *recall*.

3.6 Regression metrics

In this work, two metrics were used to assess the performance of oximetry algorithms, namely: *bias* and *precision* (BARKER, 2002 apud YAN; POON; ZHANG, 2005). Both metrics were used to assess SpO_2 and HR readings. In subsections 3.6.1 and 3.6.2 the bias and precision are described, respectively.

3.6.1 Bias

Herein, *bias* is defined as the mean of the differences between reference and estimated values, in this case, SpO_2 and HR estimations. Where the reference value is a measurement obtained by a reliable equipment, such as a certified oximeter. Mathematically, it is represented as:

$$bias = \frac{1}{n} \times \sum_{i=1}^{n} (y_i - \hat{y}_i), \tag{20}$$

where y_i is the corresponding reference value, $\hat{y}_i$ is the estimated value of the i-th sample and n is the number of samples.

3.6.2 Precision

In this work, *precision* (referring to regression metrics) is the standard deviation (SD) of the differences between reference (certified oximeter) and estimated values, SpO_2 and HR estimations as well. The following equation 21 expresses this metric.

$$precision = \sqrt{\frac{1}{n} \times \sum_{i=1}^{n} [(y_i - \hat{y}_i) - bias]^2}, \tag{21}$$

where y_i is the corresponding reference value, $\hat{y}_i$ is the estimated value of the i-th sample and n is the number of samples.

4 Experimental setups

Chapter 4 describes how the experiment was done and the procedure followed to collect the data that make up the "Personal" and "Vols" datasets. Section 4.1 argues about the ethical aspects of research involving human beings. The methods used to obtain the oximetry are presented in section 4.2. Finally, the solution developed to acquire oximetry data is presented in section 4.3 and the experimental protocol for collecting data from volunteers is described in section 4.4.

4.1 Human data collection

As explained in detail in subsection 3.1.4, the Vols PPG Dataset was created to assess the OxiTidy algorithms in a widely set of oximetric data. In order to build a database with PPG signals from several people, thus allowing a diversity in the study data, a human research project was submitted to the Research Ethics Committee (CEP). More details about this project can be found in the Appendix B.

After the approval of this project by the CEP, an observational study was carried out on April 20, 2022, with 20 volunteers at the Instituto Crescer Cidadão in Ribeirão Preto, SP. This study was supervised by the physician Flávia Gomes Pileggi Gonçalves. The participation of Dra. Flávia was fundamental for the success of the research and also to clarify some volunteers' questions on the day of the observational study.

The volunteers who participated in this observational study, in addition to contributing to the development of this work, had access to their physiological parameters, e.g. oximetry, heart rate and body temperature. The risks and benefits of this research were explained to the volunteers, as well as their rights. And the author of this work made himself available to the volunteers during and after the observational study to answer any questions about the research.

4.2 Methods for obtaining oximetry

The fidelity of the results generated by the prototype oximeter presented in this work was determined by comparing the estimated SpO_2 and HR with a reference value

measured by a pulse oximeter certified by the Brazilian Health Regulatory Agency (Anvisa). More details about this oximeter used as a standard can be found in Annex A.

In order to synchronize the samples of SpO_2 and HR obtained by the two oximeters, a computer vision solution was developed in partnership with researcher Diego Pavan Soler to identify and record the values measured by the standard oximeter. A camera was used to capture the standard-parameters (left hand) so that it was possible to synchronize them with the samples obtained by the oximeter under development (right hand). Thus, it was possible to compare the measurements performed at each moment by each oximeter on the computer.

The measurements captured by the computer vision solution (left hand) were synchronized with the measurements taken by the prototype oximeter (right hand) from the timestamp recorded on each device. Thus, it was possible to merge the data from the two files generated with reference to the timestamp with a delay of less than 1 s, a delay certainly smaller than that caused if the measurements were performed manually.

In both datasets created, the standard oximeter was placed on the left hand fingertip and kept at rest throughout. While the developing oximeter was placed on the fingertip of the right hand and during half of the collection time random movements were applied in order to affect the PPG signals. Figure 26 illustrates how the data were recorded.

Figure 26 – Methods used to obtain the oximetric parameters. (A) With both hands at rest. (B) With the left hand at rest and the right hand applying movements. (C) Pulse oximeter Model L5. (D) Fingertip-clip of pulse oximeter under development.

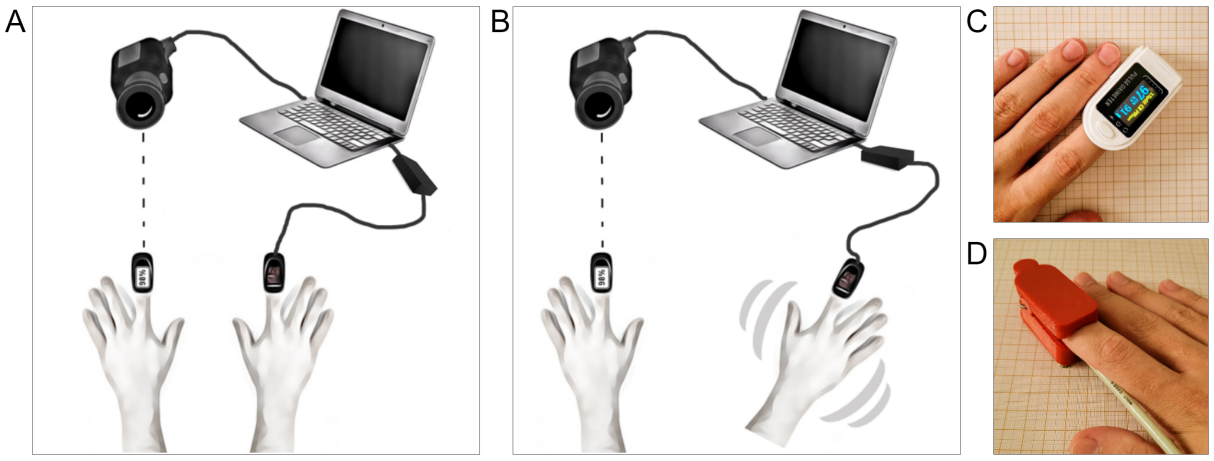

Source – Caíque Santos Lima, 2022.

The idea behind the method presented above was to automate the process of reading and recording SpO_2 and HR by the oximeters without having to manually take notes, avoiding the loss of information and difficulty in synchronizing the data. Additional details related to this method will be presented in section 4.3.

4.3 OxiCam: computer vision to oximetry data acquisition

The computer vision-based method used to acquire the oximetry data in this work is called *OxiCam*. It used the recorded videos of each volunteer's left hand during the data collection process to identify the SpO_2 and HR values that were measured by the standard oximeter and later synchronize them with the measurements performed by the prototype.

Using each video, OxiCam virtually converted characters that displayed SpO_2 and HR into machine-readable versions. This was done through a technique popularly known as optical character recognition (OCR). Through the video and its metadata, OxiCam identified the time and values of the recognized measurements, and later these values were merged with the data obtained by the prototype oximeter.

For this, a free and open-source software library for machine learning called TensorFlow was used. Keras was also used as an interface for the TensorFlow library. The algorithm was implemented through Google Collaboratory which is a free Jupyter notebook environment that requires no setup and runs entirely in the cloud and stores its notebooks on Google Drive, where the videos were also stored. Figure 27 below depicts the steps that OxiCam recognizes and merges the data to generate a file with the volunteers' measurements.

Figure 27 – OxiCam diagram.

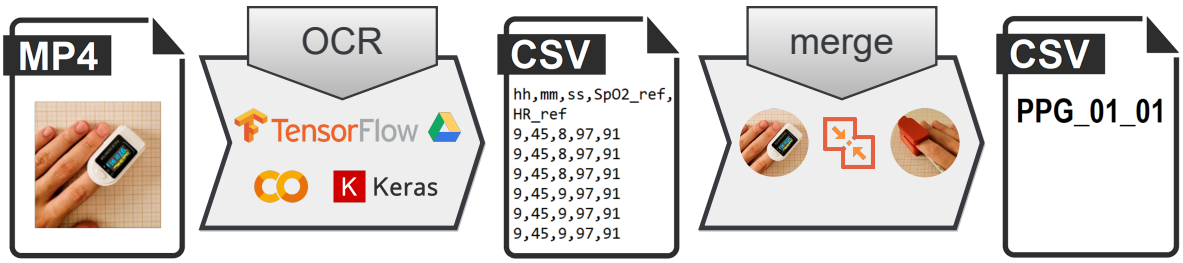

Source – Caíque Santos Lima, 2022.

4.4 Experimental protocol

The purpose of the experiment carried out in this work was to compare the performance of five methods (raw, DFT, SMA, OxiTidy v.1 and OxiTidy v.2) in estimating SpO_2 and HR on subjects when they were (i.) in a resting position and (ii.) in motion.

For this, 20 volunteers participated in the study in addition to the author of this work. Subjects were asked to sit in a chair and place their hands on a table so that their fingers did not move. In each subject, five consecutive oximetric collections were performed with a duration of 72 seconds each. For the first 18 seconds, both hands remained at rest. After these 18 seconds, a beep signaled the volunteer to start moving his right hand (oximeter prototype) for a magnitude of 20–50 cm at a frequency of 0.5–3 Hz, while keeping their left hand stationary. After 36 seconds of hand motion (x and y axes), another beep warned the volunteer to return to the resting position, remaining so until the end of the collection. Figure 28 depicts this process to obtain the data.

Figure 28 – Procedure adopted for data acquisition.

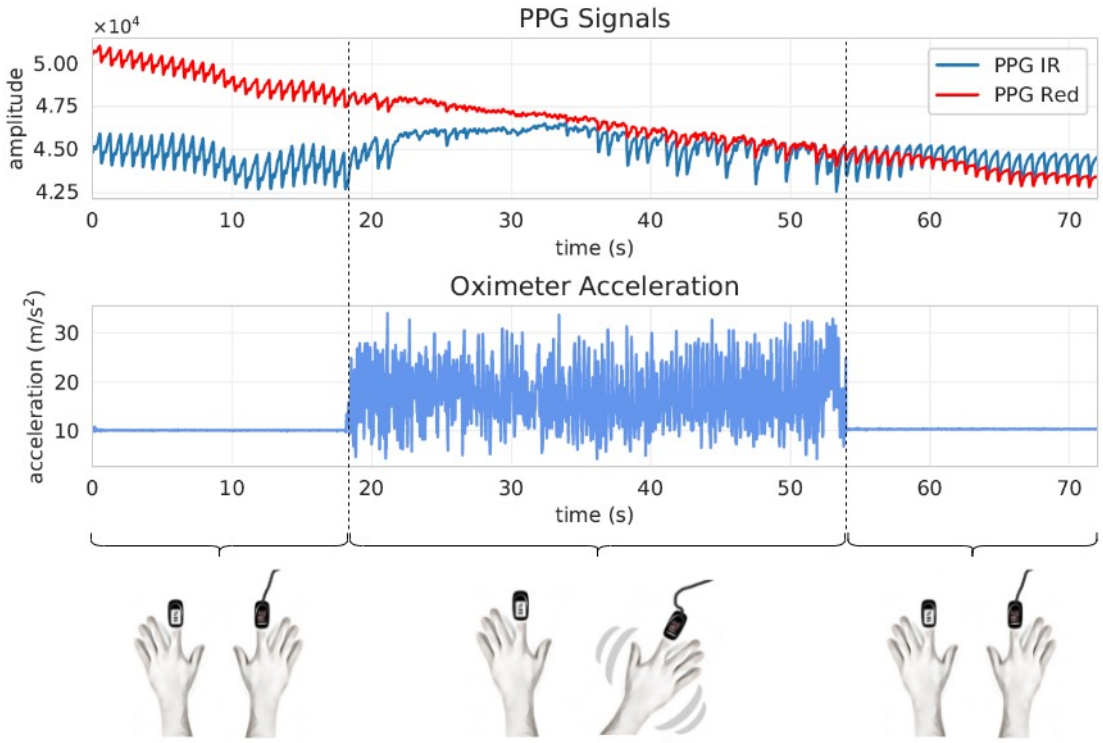

Source – Caíque Santos Lima, 2022.

Before starting each collection, the body temperature of each volunteer was measured, all of them were afebrile. Each volunteer was asked some personal information listed

in Table 6 below. Where “M” stands for *male* and “F” stands for *female*. The “Y” stands for *yes* and the “N” is *no*.

Table 6 – Volunteers’ information in “Vols” dataset.

Volunteer no.	01	02	03	04	05	06	07	08	09	10	11	12	13	14	15	16	17	18	19	20
Sex	F	F	F	M	F	F	M	F	F	F	F	F	F	F	F	F	F	F	F	F
Age	27	42	29	34	24	33	36	54	28	24	27	30	24	30	36	54	38	57	44	52
Heart disease?	N	N	N	N	N	N	N	N	N	N	N	N	N	N	N	N	N	N	N	Y
Arterial hypertension?	N	N	N	N	N	N	N	Y	N	N	Y	N	N	N	N	N	N	Y	N	Y
Tremors?	N	N	N	N	N	N	N	N	N	N	N	N	N	N	N	N	N	N	N	N

Source – Caíque Santos Lima, 2022.

5 Exploratory data analysis

According to Faceli et al. (2021), exploratory data analysis (EDA) in a dataset allows for the discovery of patterns and trends that can provide valuable insights that help to understand the process that generated this data. These insights can be obtained through the application of statistical formulas and can also be observed through the use of visualization techniques.

Visualization techniques are very useful to show, in a summarized way, important characteristics of the data. This step was essential to understand the problem and seek the most appropriate technique to deal with motion artifact (MA). To analyze the relationship between the variables of the created datasets, scatter plots were created to analyze the influence of movement on PPG signals. On the other hand, boxplots were also created to facilitate the visualization of the distribution of each attribute, as well as to analyze the presence of outliers.

The EDAs applied to each dataset created in this work will be presented below in sections 5.1 and 5.2, as well as the insights obtained from these analyzes. Furthermore, the main findings of the EDAs applied to each of these datasets are discussed in section 5.3.

5.1 EDA in Personal PPG Dataset

The Personal PPG Dataset was used for a pre-processing of the oximetric data in order to understand how the data were distributed, facilitating its visualization and interpretation. This step was also fundamental to understand the process of generating these data and planning the design of the experiment (which was discussed in the chapter 4) to create the Vols PPG Dataset.

In Figure 29, it is possible to observe that the amplitude of the movement (observed by the amplitude of the acceleration dispersion) is the major factor for the sample to be classified as affected, as expected. The points in this figure represent all the samples that make up the “Personal” dataset. In orange are all samples that were manually classified as affected and in blue the samples that were not affected. The labeling process of these samples was done in each 72 s record analyzing the waveform of the PPGs signals. In the

same figure it is possible to notice that the bulk of the samples belonging to the *normal* class remain intact throughout steady state, around 10 m/s^2.

Figure 29 – Oximeter norm acceleration and PPG infrared in Personal PPG Dataset.

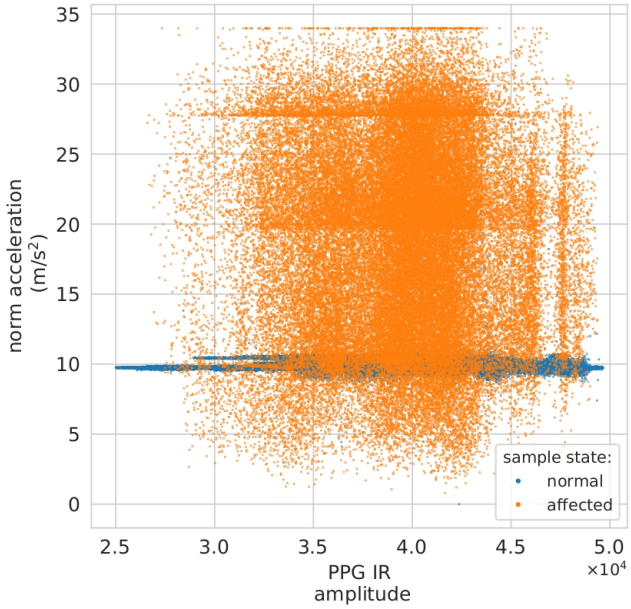

Source – Caíque Santos Lima, 2022.

Figure 30 presents the boxplots for each class of the problem, i.e., for the samples that remained normal and for those that were affected and, consequently, produced erroneous SpO_2 and HR estimations. The boxplots in this figure are formed from all the samples that make up the "Personal" dataset, they present the three-axis acceleration (Acc_x, Acc_y and Acc_z), norm acceleration, infrared and red PPG, and reference SpO_2 and HR.

As expected, the samples belonging to the *affected* class presented a greater degree of dispersion in the data of each attribute. Except for the *PPG IR* and *PPG Red* attributes which maintained a more similar interquartile range in both rest and motion states. This once again confirms that acceleration is the preponderant factor to characterize the sample as *affected* or *normal*.

During the manual process of labeling the data, i.e., identifying the class of each sample, certain samples were classified as *normal* although they belonged to the class of *affected* and therefore it is possible to see the presence of these outliers in the acceleration boxplots during rest. This issue did not affect the ANN training, as there were few samples and no problems were observed in the debugging process.

Figure 30 – Boxplots for the samples that remained normal and those that were affected by motion artifact in Personal PPG Dataset.

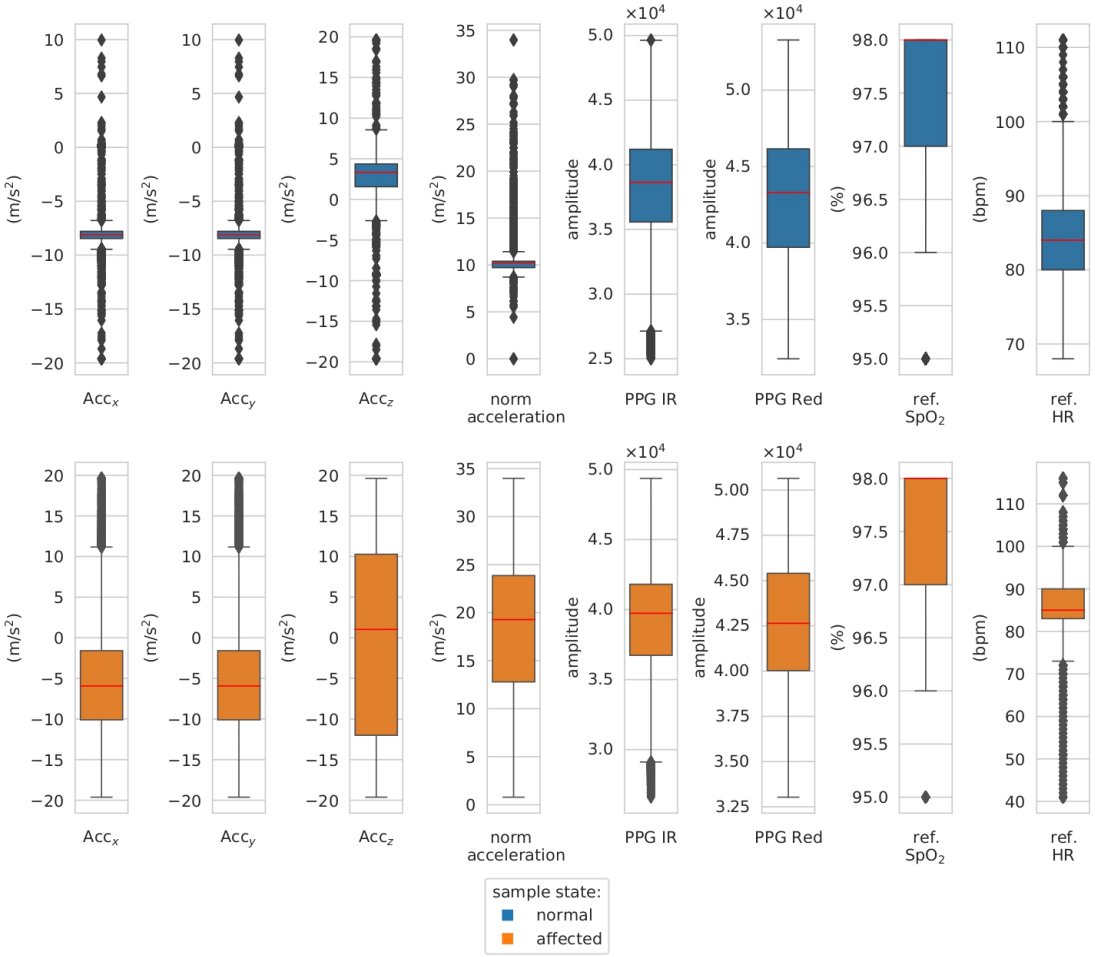

Source – Caíque Santos Lima, 2022.

5.2 EDA in Vols PPG Dataset

As explained earlier, the creation of the Vols PPG Dataset was important for analyzing oximetric data on a larger set of people. Thus, confirming some findings previously obtained in the Personal PPG Dataset and to explore how oximetric and acceleration parameters occur in different subjects.

As noted in the "Personal" dataset scatter plot, the oximeter acceleration is the major factor for the sample to be classified as affected. This can be observed once again in Figure 31, where the concentration of unaffected samples around 10 m/s^2 can be seen.

Figure 32 presents the boxplots for each class of the samples normal and affected in the "Vols" dataset. As previously noted, acceleration is the preponderant factor to characterize the sample state also in a set with data from different subjects.

Figure 31 – Oximeter norm acceleration and PPG infrared in Vols PPG Dataset.

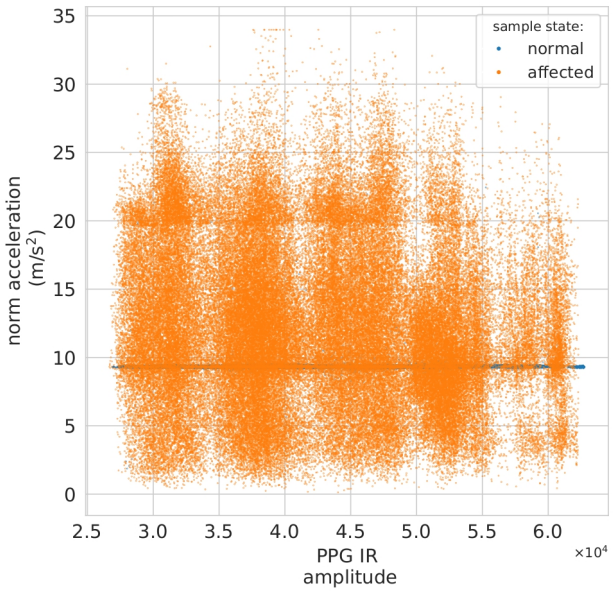

Source – Caíque Santos Lima, 2022.

Figure 32 – Boxplots for the samples that remained normal and those that were affected by motion artifact in Vols PPG Dataset.

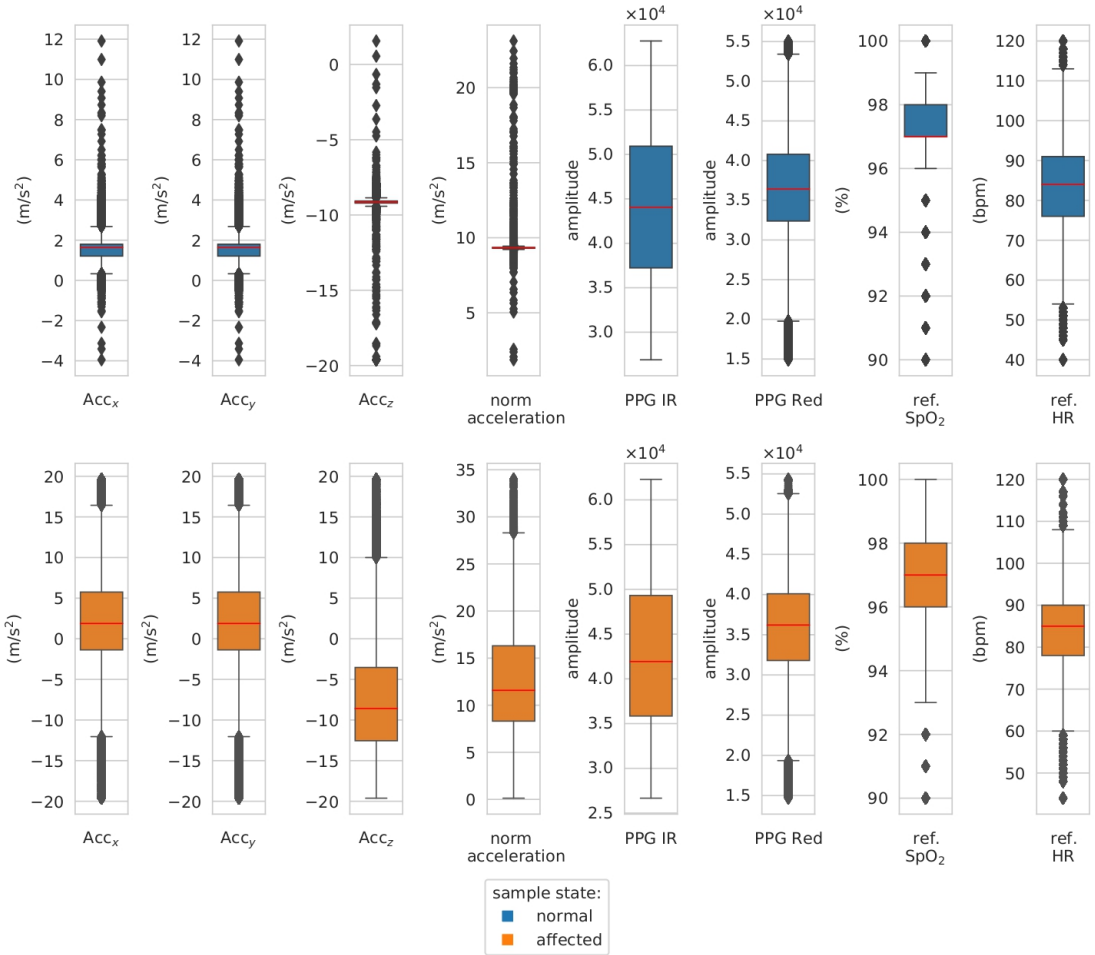

Source – Caíque Santos Lima, 2022.

5.3 Personal PPG Dataset versus Vols PPG Dataset

The advantage of working with data from different people is the possibility of dividing them into ANN training and ANN testing sets, i.e., data that were used to train the ANN and others that were used to validate the model, respectively. After training the ANN, it is expected that the designed network will be able to generalize. A network is said to generalize well when the input-output mapping computed by the network is correct (or approximately correct) for the sample set not used in the network training process.

This approach was validated by separating each volunteer's data from the Vols PPG Dataset for training and testing the network, so that the data used for training would not be the same data used for testing (validation) and vice versa. And as will be detailed in chapter 7, the proposed ANN was able to provide a good generalization and work well even with a sample set not used in the network training process.

However, when the Personal PPG Dataset was used to train the ANN and the Vols PPG Dataset to validate it (and vice versa), the network found was not able to generalize. Through the EDA, it was possible to confirm the hypothesis that the change in the type of movement performed in each dataset influenced the ANN's capacity to generalize.

In the "Personal" dataset, the movement performed by the subject was of the "bending" type, i.e., the right-hand (oximeter under development) was resting on the table and only the index finger moved as illustrated in Figure 33A. Conversely, in the "Vols" dataset, the movements performed by the volunteers' hands were in the x and z directions (see Figure 33B).

Figure 33 – Different types of motions performed in each dataset: (A) Personal PPG Dataset and (B) Vols PPG Dataset.

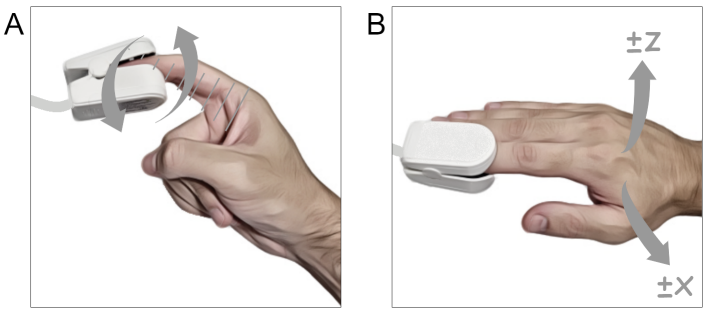

Source – Caíque Santos Lima, 2022.

Comparing the distribution of attributes in each dataset in the boxplots presented in Figure 34, there is a difference in the interquartile ranges, since the movements performed

in each dataset were also different. In other words, the type of movement produced by the subject is an important factor to be considered in the ANN training process. The boxplots in Figure 34 show the variation of the acceleration attributes of all the samples that make up each of the datasets.

Figure 34 – Boxplots for the acceleration attributes in the Personal PPG Dataset and Vols PPG Dataset.

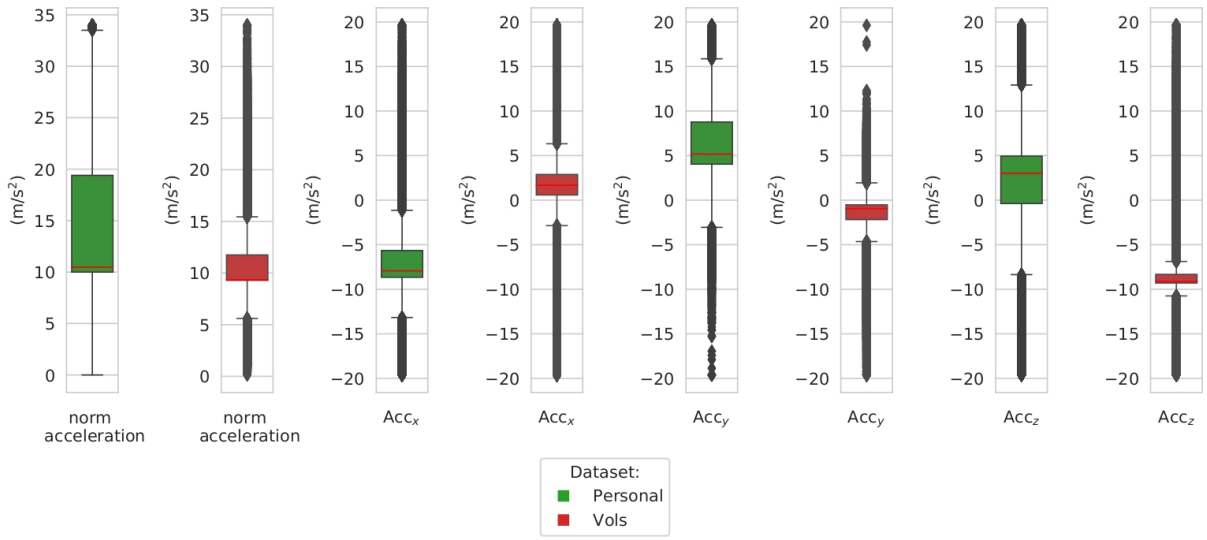

Source – Caíque Santos Lima, 2022.

6 Compared approaches

This chapter endeavours to explain in a summarized way the different approaches compared in this work. Sections 6.1, 6.2 and 6.3 present the *raw*, *simple moving average (SMA)* and *DFT* techniques, respectively. Finally, the two versions of the algorithm proposed here are presented in sections 6.4 and 6.5.

6.1 Raw

In this work, the simplest technique to obtain SpO_2 and HR measurements is called the *raw* technique. This approach does not use any digital filter or other more complex processing and works only with raw PPG signals. The stages used to obtain the measurements through this technique are described in Table 7.

Table 7 – Raw approach: SpO_2 and HR estimations.

Stage 1	**Raw data acquisition**
1.1	Gets IR and red PPG signals.
Stage 2	**Calculation of AC and DC components every 6 seconds**
2.1	Uses all samples collected within a 6-second period to calculate AC for PPG IR and PPG red signals using the SpO_2 PPG differentials method.
2.2	Uses all samples collected within a 6-second period to calculate DC for PPG IR and PPG red signals using the SpO_2 PPG differentials method.
Stage 3	**SpO_2 estimations**
3.1	Computes R ratio using values of stage 2.
3.2	Estimates SpO_2 (equation 5) using value of substage 3.1.
Stage 4	**HR estimations**
4.1	Uses PPG IR signal to calculate 1st derivative (within a 6-second period).
4.2	Gets the absolute values of substage 4.1.
4.3	Finds the peaks referring to the cardiac cycle.
4.4	Computes the number of peaks found in substage 4.3 using the HR PPG differentials method to estimate HR in bpm.

Source – Caíque Santos Lima, 2022.

6.2 DFT

In the *DFT* method, spectral analysis was used to obtain the measurements of SpO_2 and HR. The details of how this technique works can be reviewed in the subsections 2.1.3 and 2.2.2. In order to have the frequency band of interest, in this work, the cardiac frequency band was predetermined as 0.6–2 Hz, corresponding to 36–120 bpm. The procedure for the DFT approach is presented in Table 8.

Table 8 – DFT approach: SpO_2 and HR estimations.

Stage 1	**Raw data acquisition**
1.1	Gets IR and red PPG signals.
Stage 2	**Calculation of AC and DC components every 6 seconds**
2.1	Uses all samples collected within a 6-second period to calculate AC for PPG IR and PPG red signals using the SpO_2 spectral analysis method.
2.2	Uses all samples collected within a 6-second period to calculate DC for PPG IR and PPG red signals using the SpO_2 spectral analysis method.
Stage 3	**SpO_2 estimations**
3.1	Computes R ratio using values of stage 2.
3.2	Estimates SpO_2 (equation 5) using value of substage 3.1.
Stage 4	**HR estimations**
4.1	Uses PPG IR signal to calculate HR (within a 6-second period) using the HR spectral analysis method.

Source – Caíque Santos Lima, 2022.

6.3 SMA

In this work, the mesurements obtained by the *SMA* approach was the unweighted mean of SpO_2 and HR mesurements in a 6-second period. A measurement was calculated every 2 seconds and at the end of a 6-second section, the average of these three measurements was calculated. Table 9 below describes in detail the stages used to obtain the SpO_2 and HR using this method.

Table 9 – SMA approach: SpO_2 and HR estimations.

Stage 1	**Raw data acquisition**
1.1	Gets IR and red PPG signals.
Stage 2	**SpO_2 estimations**
2.1	Uses all samples collected within a 2-second period to calculate AC and DC for PPG IR and PPG red signals using the SpO_2 PPG differentials method.
2.2	Computes R ratio using values of substage 2.1.
2.3	Estimates SpO_2 (equation 5) using value of substage 2.2.
2.4	Computes the SMA of the values obtained in substage 2.3 to result the SpO_2 in a 6-second section.
Stage 3	**HR estimations**
3.1	Uses PPG IR signal to calculate 1st derivative (within a 2-second period).
3.2	Gets the absolute values of substage 3.1.
3.3	Finds the peaks referring to the cardiac cycle.
3.4	Computes the number of peaks found in substage 3.3 using the HR PPG differentials method to estimate HR in bpm.
3.5	Computes the SMA of the values obtained in substage 3.4 to result the HR in a 6-second section.

Source – Caíque Santos Lima, 2022.

6.4 OxiTidy v.1: motion artifact detection in PPG signals using ANN

User motion may result in loss of SpO_2 and HR measurements, and it can also cause false alarms, displaying warnings of desaturation (hypoxemia) even though the patient is fine. This issue is often observed during oximetrics readings, a study in the pediatric intensive care unit (PICU) found that 71% of all pulse oximeter alarms were false (BARKER, 2002). This can be very risky, according to Barker (2002, p. 967), "[...] This frequent false-positive rate encourages nurses and other care providers to manually disable alarms, thereby risking failure to detect actual sudden hypoxemia."

Given the importance of correctly obtaining these measurements, the algorithm called *OxiTidy v.1*, was proposed as a new approach based on ANN and IMU used to detect affected samples of PPG signals and prevent SpO_2 and HR measurements from being displayed incorrectly to the user. In this approach, these affected samples were not used to the measurements computation, instead a linear interpolation between two normal measurements of SpO_2 or HR was performed. It worked mainly in cases where the PPG signals were affected by noise caused by the users movements. For this, a 3-axis accelerometer and a savgol-filter of polynomial order equal to 3 and window width of 7 (samples) were applied.

According to Yan, Poon e Zhang (2005), the rate of change of oximetry measurements is relatively slow, i.e., SpO_2 that changes by more than 2% per second can be considered to be physiologically impossible, which could indicate a false alarm. Based on this premise, OxiTidy v.1 detects samples affected by MA and disregards these measurements, which are replaced by interpolated values from two known normal measurements. In other words, instead of displaying the incorrect value, it shows a more accurate value, given the established range.

As it was found, and it was expected, the ANN prediction process performed by OxiTidy v.1 presented a small error where samples that belonged to the *affected* class were classified as *normal* and vice versa. For this, in this algorithm, a threshold was implemented precisely to make this distinction between the two classes. During the tests with the data predicted by the ANN, the threshold of 1% of samples affected was reached, i.e., if the number of samples affected in a section was greater than 1%, these measurements were rejected and, in this referred section, SpO_2 and HR estimations were linearly interpolated

from two measurements obtained with samples from a section with a threshold less than or equal to 1%. The procedure of the OxiTidy v.1 algorithm and its respective computation steps are presented in Table 10.

Table 10 – OxiTidy v.1 algorithm: SpO_2 and HR estimations.

Stage 1	**Raw data acquisition**
1.1	Gets IR and red PPG signals, and 3-axis acceleration (xyz).
Stage 2	**Sample state prediction – Classifier ANN (MLP 3-3-1)**
2.1	Gets 3-axis acceleration to predict sample state (affected or normal).
Stage 3	**Savitzky-Golay filter**
3.1	Apply savgol-filter on PPG IR and PPG red signals.
Stage 4	**Calculation of AC and DC components every 6 seconds**
4.1	Uses all samples collected within a 6-second period to calculate AC for PPG IR and PPG red signals using the SpO_2 PPG differentials method.
4.2	Uses all samples collected within a 6-second period to calculate DC for PPG IR and PPG red signals using the SpO_2 PPG differentials method.
Stage 5	**SpO_2 estimation**
5.1	Computes R ratio using values of stage 4.
5.2	Estimates SpO_2 (equation 5) using value of substage 5.1.
Stage 6	**HR estimation**
6.1	Uses PPG IR signal to calculate 1st derivative (within a 6-second period).
6.2	Gets the absolute values of substage 6.1.
6.3	Finds the peaks referring to the cardiac cycle.
6.4	Computes the number of peaks found in substage 6.3 using the HR PPG differentials method to estimate HR in bpm.
Stage 7	**Removal of affected samples**
7.1	If the number of affected samples is greater than 1% (within a 6-second period), the calculated SpO_2 is rejected (NaN).
7.2	If the number of affected samples is greater than 1% (within a 6-second period), the calculated HR is rejected (NaN).
Stage 8	**Correction of NaN[1] values – linear interpolation**
8.1	For each standard 6-second period, interpolates the NaN values using two regular SpO_2 measurements.
8.2	For each standard 6-second period, interpolates the NaN values using two regular HR measurements.

[1] NaN standing for *Not a Number*, is a symbol used to represent an undefined numeric value.

Source – Caíque Santos Lima, 2022.

In this approach, an MLP with 3 input nodes, 3 neurons in the hidden layer and 1 neuron in the output layer was used. This topology (3-3-1) was chosen aiming at a good performance, as will be detailed in section 7.1. A bias was applied to each neuron. The classifier created from this network uses as input the acceleration measured by the IMU on the x, y and z axes. And its output classifies the state of the sample: affected (1) or normal (0). Figure 35 presents the graphical architecture of this classifier.

Figure 35 – OxiTidy classifier topology.

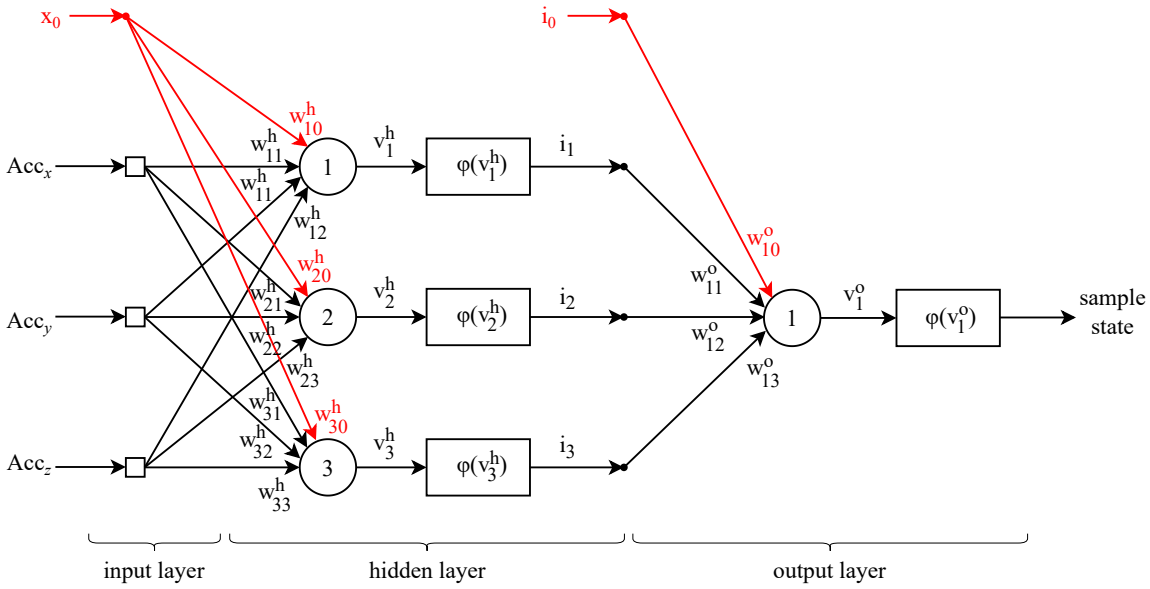

Source – Caíque Santos Lima, 2022.

Figure 36 depicts the samples of PPG signals that were affected (1) and those that remained normal (0) during the acquisition.

Figure 36 – Samples predicted by the ANN as affected by motion artifact in one of the records.

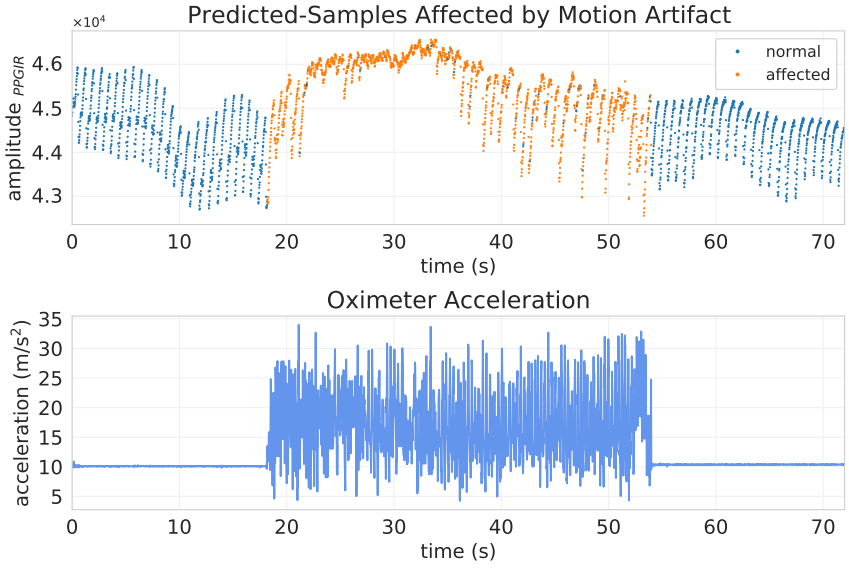

Source – Caíque Santos Lima, 2022.

6.5 OxiTidy v.2: motion artifact reduction in PPG signals using ANN

Considering that OxiTidy v.1 does not use the affected signals to estimate SpO_2 and HR values in the presence of MAs, version no. 2 of the algorithm proposed in this

work, named *OxiTidy v.2*, is an effort to improve the performance of measurements using also the affected signals.

The OxiTidy v.2 algorithm is identical to its first version up to the step of removing affected samples, i.e., the steps presented in Table 10 are the same up to stage 7. The difference from the previous version is in stage 8, where a regression ANN was used to predict the measurements from the affected samples. The stages used to obtain the measurements through OxiTidy v.2 algorithm are described in Table 11.

Table 11 – OxiTidy v.2 algorithm: SpO_2 and HR estimations.

Stage 1	**Raw data acquisition**
1.1	Gets IR and red PPG signals, and 3-axis acceleration (xyz).
Stage 2	**Sample state prediction – Classifier ANN (MLP 3-3-1)**
2.1	Gets 3-axis acceleration to predict sample state (affected or normal).
Stage 3	**Savitzky-Golay filter**
3.1	Apply savgol-filter on PPG IR and PPG red signals.
Stage 4	**Calculation of AC and DC components every 6 seconds**
4.1	Uses all samples collected within a 6-second period to calculate AC for PPG IR and PPG red signals using the SpO_2 PPG differentials method.
4.2	Uses all samples collected within a 6-second period to calculate DC for PPG IR and PPG red signals using the SpO_2 PPG differentials method.
Stage 5	**SpO_2 estimation**
5.1	Computes R ratio using values of stage 4.
5.2	Estimates SpO_2 (equation 5) using value of substage 5.1.
Stage 6	**HR estimation**
6.1	Uses PPG IR signal to calculate 1st derivative (within a 6-second period).
6.2	Gets the absolute values of substage 6.1.
6.3	Finds the peaks referring to the cardiac cycle.
6.4	Computes the number of peaks found in substage 6.3 using the HR PPG differentials method to estimate HR in bpm.
Stage 7	**Removal of affected samples**
7.1	If the number of affected samples is greater than 1% (within a 6-second period), the calculated SpO_2 is rejected (NaN).
7.2	If the number of affected samples is greater than 1% (within a 6-second period), the calculated HR is rejected (NaN).
Stage 8	**Correction of NaN values – Regression ANN (MLP 5-5-1)**
8.1	For each standard 6-second period, replaces the NaN values using the SpO_2 measurements obtained through the regression ANN.
8.2	For each standard 6-second period, replaces the NaN values using the HR measurements obtained through the regression ANN.

Source – Caíque Santos Lima, 2022.

The classifier (3-3-1) used in this approach is the same as described in section 6.4. To predict the SpO_2 and HR measurements, two MLP with 5 input nodes, 5 neurons in the hidden layer and 1 neuron in the output layer (5-5-1) was used. As with the classifier, each

neuron has a bias. These regression ANNs use 3-axis acceleration and both PPG signals as input. And the outputs of these networks predict the SpO_2 and HR values, respectively. Figure 37 depicts the graphic architecture of these ANNs.

Figure 37 – OxiTidy v.2 regression ANN topology.

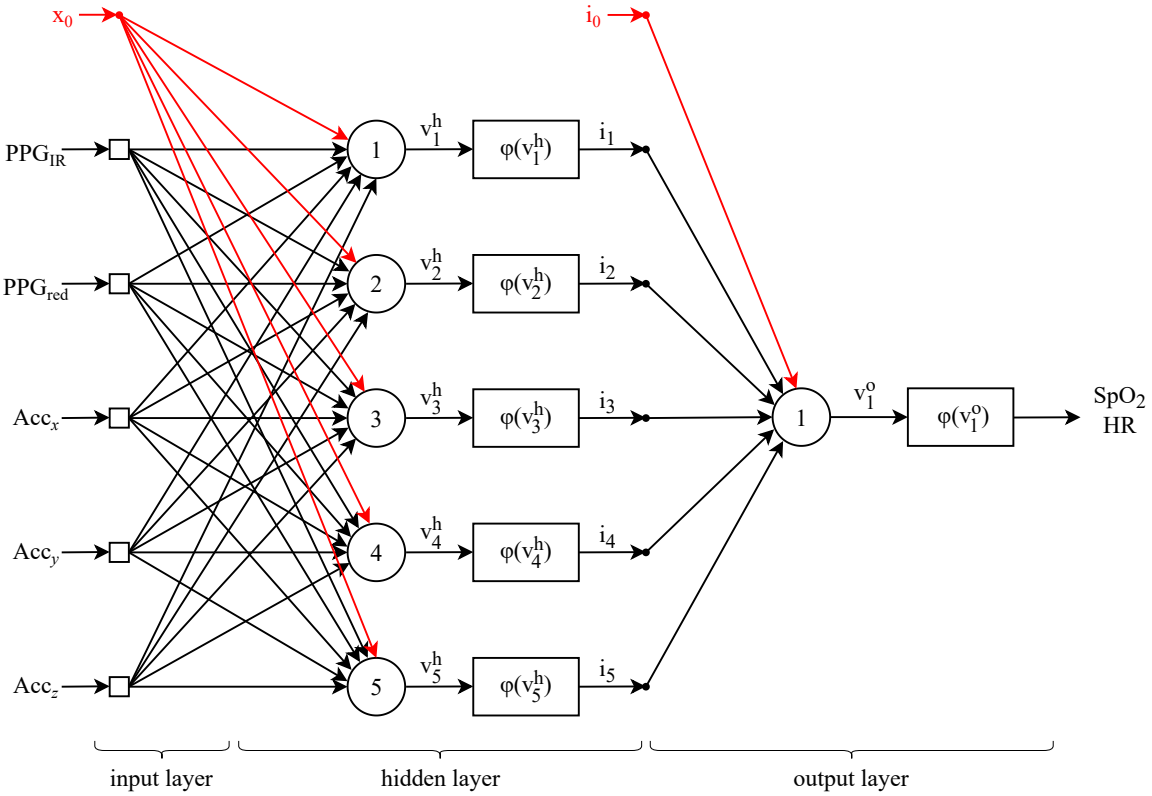

Source – Caíque Santos Lima, 2022.

Table 12 shows the details of the ANNs used in both versions of OxiTidy previously illustrated in Figures 35 and 37. To implement these networks, open source machine learning libraries such as scikit-learn and Keras were used.

Table 12 – ANN parameters.

Parameter/method	Value/description	
	classifier	regression ANN
No. of hidden layers	1	1
No. of hidden neurons	3	5
No. of output neurons	1	1
Learning algorithm	Backpropagation	Backpropagation
Activation function of hidden neurons	Hyperbolic tangent	ReLU
Activation function of output neurons	Sigmoid	Linear
Learning epochs	20	EarlyStopping (Keras)
Input data preprocessing	StandardScaler (sklearn)	StandardScaler (sklearn)

Source – Caíque Santos Lima, 2022.

7 Results and discussion

This chapter discusses the results obtained during the process of creating the classifier that is part of OxiTidy and the performance of each approach compared in this work using the Vols PPG Dataset. Then, in section 7.1, the different ANN topologies evaluated to create the classifier are presented. Section 7.2 describes the evaluation process of this classifier. And finally, the final performance of each approach is discussed in section 7.3.

7.1 Classifier ANN topology

The first step, based on exploratory data analysis, was to define an appropriate technique capable of classifying samples affected by MA. In order to identify the intervals where the PPG signals were affected by the MA, different topologies of ANNs based on the MLP were evaluated using the "Personal" dataset. 75% of the records that make up this dataset were used to train the eleven evaluated topologies and the remaining 25% were used to validate them.

The *average performance* and *standard deviation* of each record predict by each topology of ANN were calculated. In other words, the classification metrics presented in section 3.5 were used to evaluate each topology. It is possible to observe that the acceleration was the major factor to determine the state of the sample, and the use of an accelerometer was fundamental since the information coming only from the PPG signals were not enough for the ANNs to achieve a good performance. This can be seen in the fourth and fifth lines of Figure 38[1], where the acceleration data were not applied and, in this case, the ANNs presented the worst performance among the evaluated topologies.

Aiming at a good performance in the face of the four evaluated metrics and a simplified ANN topology, the 3-3-1 model was chosen, applying the acceleration attributes in the xyz-axes to the ANN input. This topology (3-3-1) was applied in both classifiers of the OxiTidy v.1 and v.2 approaches (see Figure 35).

[1] Herein, the green color was used to indicate the best performance, i.e., the greener the cell, the better the performance. This also applies to Figure 39.

Figure 38 – Performance of the ANNs evaluated using the Personal PPG Dataset.

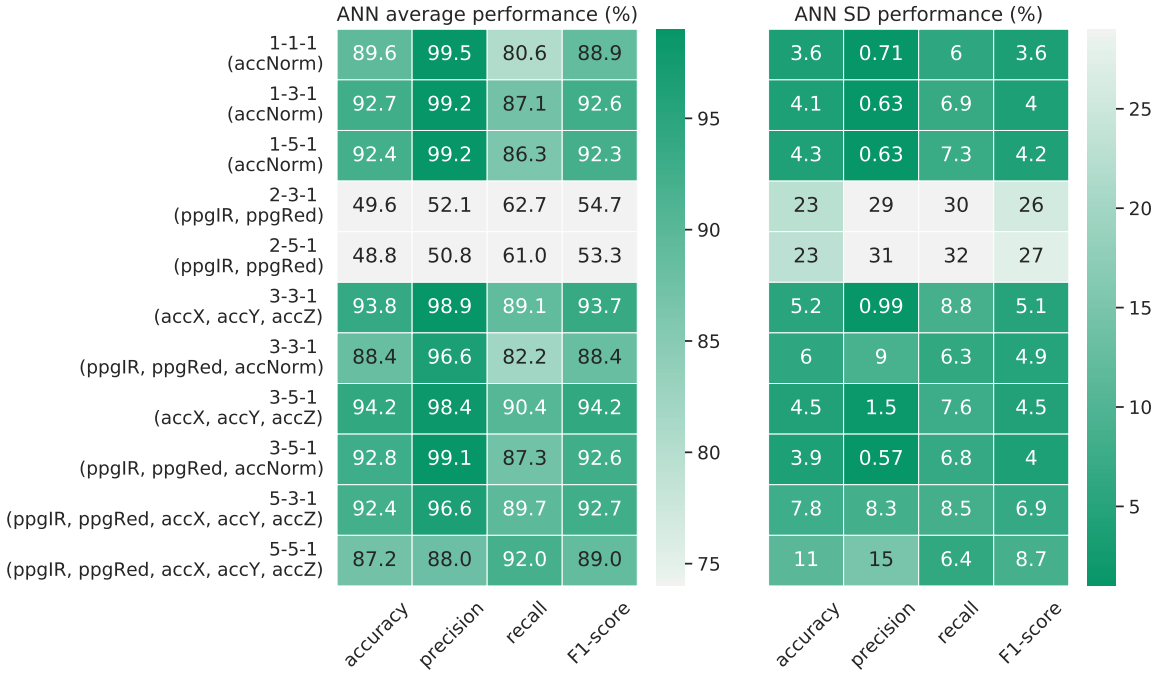

Source – Caíque Santos Lima, 2022.

7.2 Classifier ANN performance

According to Faceli et al. (2021), to obtain a more reliable predictive performance of an ANN, alternative sampling methods must be used, defining subsets for training and testing. In other words, the training data are used in the network learning process, while the test data simulate the parsing of new objects to the ANN, which were not seen in the learning process.

Among the main existing sampling methods is *k-fold cross-validation*. In this method, the dataset is divided into k subsets of approximately equal sizes. Where the objects from $k-1$ partitions are used in training a classifier, which is then tested on the remaining partition. This process is repeated k times, each cycle using a different partition to test (FACELI et al., 2021).

In this work, the records that make up the "Vols" dataset were randomly divided into 10 folds ($k = 10$), as shown in Appendix D. Then, the cross-validation process was performed and the performance in each fold of the ANN is given by the mean and standard deviation shown in Figure 39. It is possible to see that in each iteration the average

performance of the classifier was above 91%, which represents a good network forecasting capacity.

Figure 39 – Classifier ANN performance using the Vols PPG Dataset.

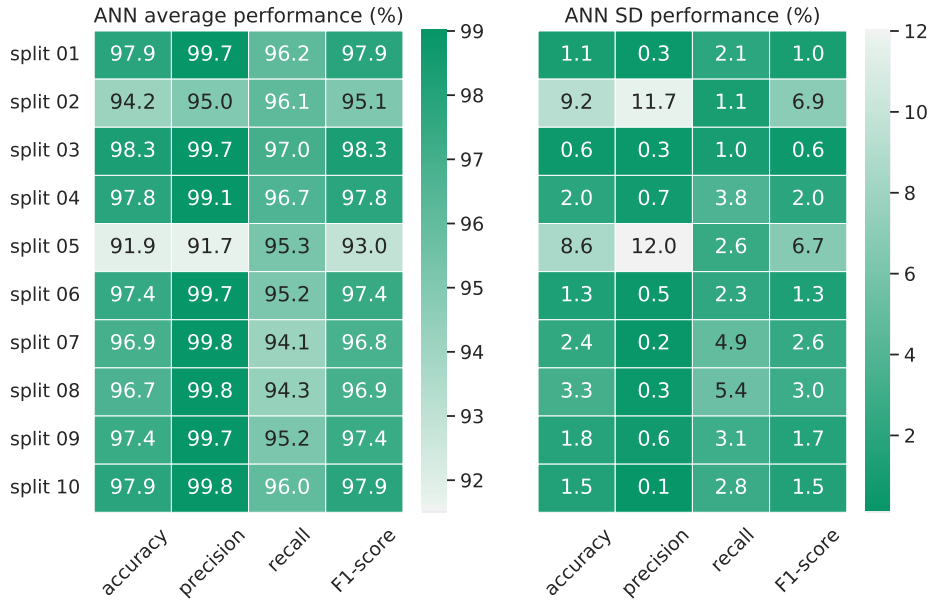

Source – Caíque Santos Lima, 2022.

7.3 Performance of compared approaches

The purpose of the experiment performed with "Vols" dataset was to compare the performance of five different approaches in estimating SpO_2 and HR on subjects when they were (i.) in a resting position and (ii.) in motion, as detailed in section 4.4. For this, the *bias* and *precision* for SpO_2 and HR were calculated. As described in section 3.6, the bias and precision are defined as the mean and standard deviation of the differences between the reference and estimated measurements, respectively (BARKER, 2002 apud YAN; POON; ZHANG, 2005). The way the data from the "Vols" dataset was splitted is the same as described in the previous paragraph.

In Figure 40[2], it is possible to observe that, during rest, both versions of OxiTidy had a better average performance in estimating SpO_2 than the other approaches in most splits. Likewise, the average performance of the algorithms proposed here, during the motion, had an even better average performance than in the raw, DFT and SMA approaches, especially in OxiTidy v.2.

[2] Herein, the red color was used to indicate the worst performance, i.e., the redder the cell, the worse the performance. This also applies to Figure 41.

Figure 40 – Performance of compared approaches in estimating SpO_2 using the Vols PPG Dataset.

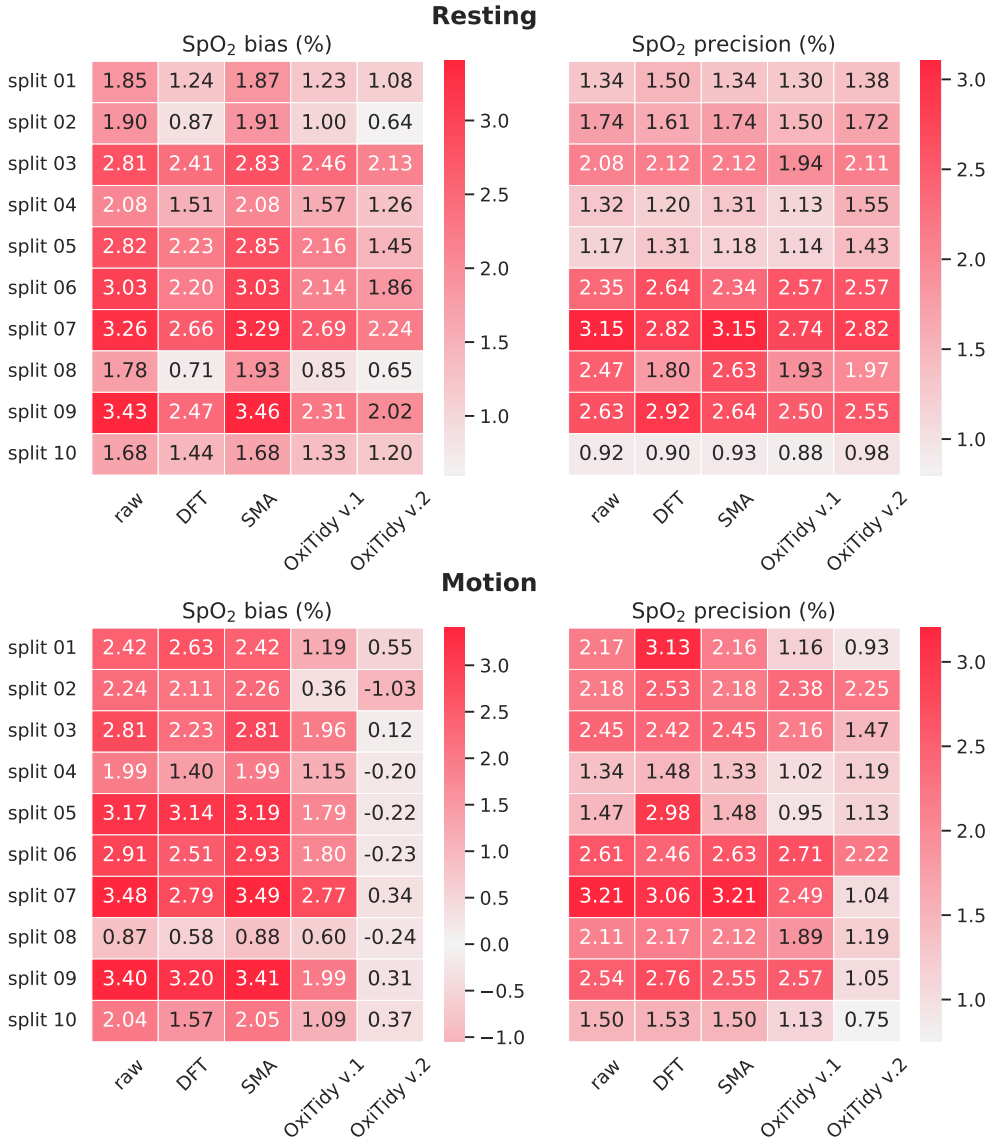

Source – Caíque Santos Lima, 2022.

Conversely, despite the fact that OxiTidy presented an HR bias close to zero in certain splits, the trend of better performance in most splits was not found in any of the states: resting and motion. The bias and precision in estimating HR, in both states, can be seen in Figure 41 below.

It is worth noting that although OxiTidy does not have a consistent performance in estimating HR as seen for SpO_2, the HR PPG differentials method used in both versions showed, in general, a better performance in relation to the HR spectral analysis method used in the DFT approach. This suggests the hypothesis that the HR PPG differentials method may be more accurate to estimate heart rate.

Figure 41 – ANN performance using the Vols PPG Dataset.

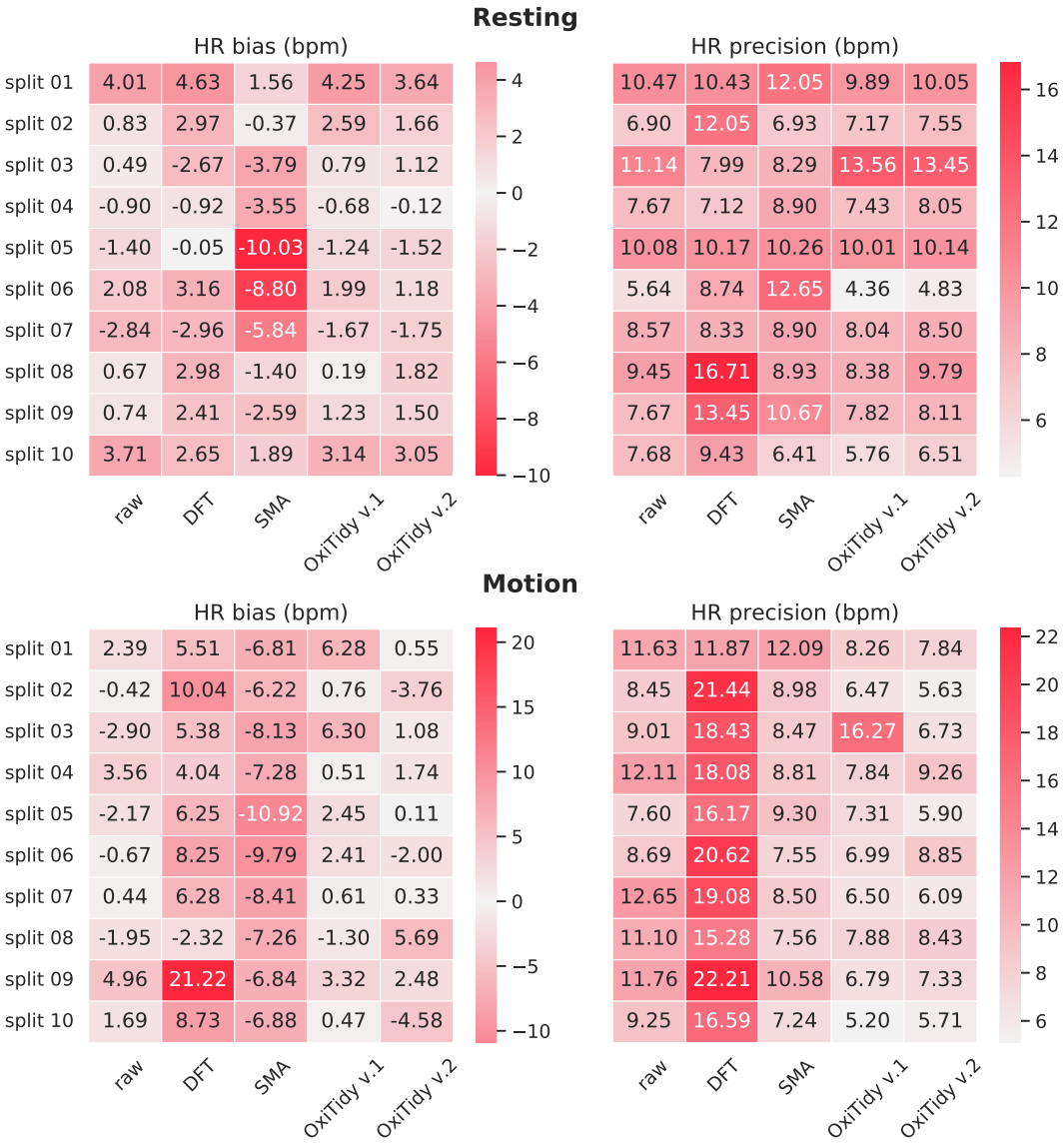

Source – Caíque Santos Lima, 2022.

8 Conclusions and recommendations

Digital transformation has impacted people's lives in several areas, especially in healthcare. Technological evolution in health has brought benefits to both professionals and patients. What became popularly known as Health 4.0 — which integrates several innovations such as IoT, Big Data and Artificial Intelligence — has revolutionized modern medicine. What was possible to do only with high-cost and unwieldy biomedical equipment, has been popularized with the emergence of wearable devices.

This technology allows clinical monitoring beyond medical offices, i.e., these devices can be incorporated into patients' day-to-day, enabling a much more efficient control of physiological signals. In this way, wearables work as another tool for the prevention and promotion of health and well-being.

Among the various features present in wearables is pulse oximetry, this non-invasive technique allows the monitoring of physiological signals in a very simplified way, making it possible to measure SpO_2 and HR. However, the way pulse oximeters are developed and used directly influences the quality of the information provided to the user. There are several issues that can impair the accuracy of the data generated by these devices, among the main problems are motion artifacts. They can cause measurement errors and false alarms.

In order to mitigate these undesirable effects, in this work, an algorithm based on ANN capable of detecting noise in the PPG signal and correct SpO_2 and HR measurements was proposed. The performance of this algorithm, named OxiTidy, was compared with three other approaches using a Wi-Fi pulse oximeter under development by the Department of Electrical Engineering, Computing Department and Medicine Department at the Federal University of São Carlos.

OxiTidy was developed in two versions, the first has a classifier based on MLP (3-3-1) capable of detecting the affected PPG samples and instead of using them to the measurements computation, a linear interpolation between two normal measurements SpO_2 or HR is performed. Conversely, OxiTidy v.2 uses a regression ANN to predict the measurements from the affected samples detected by the same classifier.

OxiTidy identified the intervals where the measurements were incorrect and then estimated new SpO_2 values with a good approximation to the readings performed by a

pulse oximeter certified by the Anvisa. However, this was not observed for HR in most splits, showing that the versions proposed in this work had a better performance for SpO_2 measurements, especially OxiTidy v.2.

It should be considered that these results are limited to a dataset of 17 subjects with normal oxygen saturation. Therefore, the next step would be to evaluate the performance of the algorithm proposed here in low saturation conditions and in a larger group of people. OxiTidy could also be compared with other techniques such as SPWVD, SSA, VFCDM, etc. Thus, it would be possible to assess the performance of this algorithm with the other techniques present in the literature. It is also recommended that OxiTidy v.2 be improved, i.e., evaluating other ANN topologies and inserting other attributes working with a data window in the inputs of the regression networks.

Indeed, OxiTidy was applied to post-processed data, i.e., the PPGs signals were collected and then the SpO_2 and HR measurements were computed. This approach aimed to demonstrate its performance and serve as a basis for future implementations. For example, embedding it in a microcontroller to run online, since in this work, OxiTidy was developed only to work with post-processed data. For this, it would be interesting to alert the user (e.g. using a buzzer or LED) the presence of MA, thus asking the user to rest so that the measurements are correctly computed.

Bibliography

AGÊNCIA DE INOVAÇÃO DA UFSCAR. *Sistema de Monitoramento UFSCar - Prova de Conceito*. 2020. Available at: ⟨http://ain.ufscar.br/oximetro_UFSCar/12u80f34/⟩. Access on: 03 Oct. 2020. Quoted on page 51.

ALIAN, A. A.; SHELLEY, K. H. Photoplethysmography. *Best Practice & Research Clinical Anaesthesiology*, v. 28, n. 4, p. 395–406, 4 2014. Quoted on page 25.

AMERICAN HEART ASSOCIATION. *Target Heart Rates Chart*. 2021. Available at: ⟨https://www.heart.org/en/healthy-living/fitness/fitness-basics/target-heart-rates⟩. Access on: 16 Mar. 2022. Quoted on page 23.

AOYAGI, T. Pulse oximetry: its invention, theory, and future. *Journal of Anesthesia*, v. 17, n. 4, p. 259–266, 8 2003. Quoted on page 24.

ASSOCIAÇÃO BRASILEIRA DE NORMAS TÉCNICAS. *ABNT NBR ISO 80601-2-61:2015*: Equipamento eletromédico parte 2-61: Requisitos particulares para a segurança básica e o desempenho essencial de equipamentos para oximetria de pulso. Rio de Janeiro, RJ, 2015. 99 p. Quoted on page 38.

AZIZ, H.; ABOCHAR, H. Telemedicine. *Clinical Laboratory Science*, v. 28, n. 4, p. 256–259, 4 2015. Quoted 2 times on pages 19 and 20.

BARKER, S. J. Motion-resistant pulse oximetry: A comparison of new and old models. *Anesthesia & Analgesia*, v. 95, n. 4, p. 967–972, 2002. Quoted 4 times on pages 41, 60, 74, and 81.

CHACON, P. J. et al. A wearable pulse oximeter with wireless communication and motion artifact tailoring for continuous use. *IEEE Transactions on Biomedical Engineering*, v. 66, n. 6, p. 1505–1513, 6 2019. Quoted 4 times on pages 20, 26, 27, and 28.

CHARLTON, P. *The PPG Diary project*. 2021. Available at: ⟨https://peterhcharlton.github.io/ppg-diary/index.html⟩. Access on: 04 Jun. 2021. Quoted 2 times on pages 44 and 46.

CHO, J. H.; KIM, J. C.; YOON, G. W. Robust design of pulse oximeter using dynamic control and motion artifact detection algorithms. *Journal of Electrical Engineering and Technology*, Korean Institute of Electrical Engineers, v. 9, n. 5, p. 1780–1787, 2014. Quoted 2 times on pages 41 and 42.

COOLEY, J. W.; TUKEY, J. W. An algorithm for the machine calculation of complex fourier series. *Mathematics of Computation*, v. 19, p. 297–301, 1965. Quoted 2 times on pages 56 and 57.

COUZIN-FRANKEL, J. The mystery of the pandemic's 'happy hypoxia'. *Science*, American Association for the Advancement of Science, v. 368, n. 6490, p. 455–456, 2020. Quoted 2 times on pages 21 and 22.

DCSTUDIO. *Homem doente hospitalizado*. 2022. Available at: ⟨https://br.freepik.com/fotos-gratis/enfermeira-medica-discutindo-tratamento-de-doencas-com-homem-doente-hospitalizado-descansando-na-cama-durante-a-terapia-de-reabilitacao-na-enfermaria-do-hospital_15853769.htm⟩. Access on: 02 apr. 2022. Quoted on page 24.

DCSTUDIO. *Oxímetro paciente idoso*. 2022. Available at: ⟨https://br.freepik.com/fotos-gratis/feche-a-mao-de-um-paciente-idoso-com-oximetro-na-cama-pessoa-senior-com-ferramenta-medica-no-dedo-para-medicao-de-saturacao-de-oxigenio-e-pressao-de-pulso-aposentado-com-doenca_20982533.htm⟩. Access on: 02 apr. 2022. Quoted on page 24.

DUMAS, C.; WAHR, J. A.; TREMPER, K. K. Clinical evaluation of a prototype motion artifact resistant pulse oximeter in the recovery room. *Anesthesia and Analgesia*, v. 83, n. 2, p. 269–272, 1996. Quoted on page 41.

ELGENDI, M. *PPG signal analysis: an introduction using MATLAB*. 1. ed. Boca Raton: CRC Press, 2021. Quoted on page 27.

FACELI, K. et al. *Inteligência artificial: uma abordagem de aprendizado de máquina*. 2. ed. Rio de Janeiro: LTC, 2021. Quoted 2 times on pages 66 and 80.

FREEPIK. *Mulher usando smartwatch*. 2022. Available at: ⟨https://br.freepik.com/fotos-gratis/feche-a-mao-usando-smartwatch_20078967.htm⟩. Access on: 02 apr. 2022. Quoted on page 24.

GALLAGHER, N. B. Savitzky-Golay smoothing and differentiation filter. *Eigenvector Research Incorporated*, 2020. Quoted on page 54.

GIULIANO, K. K.; LIU, L. M. Knowledge of pulse oximetry among critical care nurses. *Dimensions of Critical Care Nursing*, v. 25, n. 1, p. 44–49, 1 2006. Quoted on page 29.

GOLDBERGER, A. L. et al. PhysioBank, PhysioToolkit, and PhysioNet: Components of a new research resource for complex physiologic signals. *Circulation*, American Heart Association, Inc., v. 101, n. 23, p. e215–e220, 6 2000. Quoted on page 44.

HAGHI, M.; THUROW, K.; STOLL, R. Wearable devices in medical internet of things: Scientific research and commercially available devices. *Healthcare Informatics Research*, v. 23, n. 1, p. 4–15, 1 2017. Quoted on page 24.

HARVEY, J. et al. OxiMA: A Frequency-Domain approach to address motion artifacts in photoplethysmograms for improved estimation of arterial oxygen saturation and pulse rate. *IEEE Transactions on Biomedical Engineering*, v. 66, n. 2, p. 311–318, 2 2019. Quoted on page 42.

HAYES, M. J.; SMITH, P. R. A new method for pulse oximetry possessing inherent insensitivity to artifact. *IEEE Transactions on Biomedical Engineering*, v. 48, n. 4, p. 452–461, 4 2001. Quoted on page 29.

HAYKIN, S. *Neural Networks: A Comprehensive Foundation*. New Jersey: Pearson, 1998. Quoted on page 52.

HAYKIN, S. *Neural networks and learning machines - 3rd ed.* New Jersey: Pearson, 2008. Quoted on page 53.

INTERNATIONAL ORGANIZATION FOR STANDARDIZATION. *ISO 80601-2-61:2017*: Medical electrical equipment – part 2-61: Particular requirements for basic safety and essential performance of pulse oximeter equipment. Geneva, CH, 2017. 90 p. Quoted on page 38.

INVENSENSE INC. *MPU-9250 Product Specification - Revision 1.0*. 2014. Available at: ⟨https://img.filipeflop.com/files/download/Datasheet_MPU9250_REV1.0.pdf⟩. Access on: 03 Aug. 2021. Quoted on page 51.

JOHNS HOPKINS MEDICINE. *Vital Signs (Body Temperature, Pulse Rate, Respiration Rate, Blood Pressure)*. 2022. Available at: ⟨https://www.hopkinsmedicine.org/health/conditions-and-diseases/vital-signs-body-temperature-pulse-rate-respiration-rate-blood-pressure⟩. Access on: 16 Mar. 2022. Quoted on page 23.

JOHNSTON, W. S. *Development of a Signal Processing Library for Extraction of SpO2, HR, HRV, and RR from Photoplethysmographic Waveforms*. Dissertação (Mestrado) — Worcester Polytechnic Institute, 7 2006. Quoted 4 times on pages 33, 34, 35, and 36.

JUBRAN, A. Pulse oximetry. *Critical Care*, v. 19, n. 1, p. 1–7, 1 2015. Quoted 2 times on pages 20 and 29.

KINOSHITA, H. et al. Application of co-oximeter for forensic samples. In: DOGAN, K. H. (Ed.). *Post Mortem Examination and Autopsy*. Rijeka: IntechOpen, 2017. cap. 9. Quoted on page 40.

KOCHEVA, D. *What is Health 4.0?* 2021. Healthcare Digital Magazine. Available at: ⟨https://healthcare-digital.com/digital-healthcare/what-health-40⟩. Access on: 04 May 2022. Quoted on page 19.

KONG, Q.; SIAUW, T.; BAYEN, A. *Python Programming And Numerical Methods: A Guide For Engineers And Scientists*. [S.l.]: Academic Press, 2020. ⟨https://pythonnumericalmethods.berkeley.edu/notebooks/Index.html⟩. Quoted 3 times on pages 55, 56, and 58.

LEE, J.; JUNG, W.; KANG, I. Design of filter to reject motion artifact of pulse oximetry. v. 26, p. 241–249, 4 2003. Quoted 2 times on pages 29 and 40.

LONGONI, C.; MOREWEDGE, C. *AI Can Outperform Doctors. So Why Don't Patients Trust It?* 2019. Harvard Business Review. Available at: ⟨https://hbr.org/2019/10/ai-can-outperform-doctors-so-why-dont-patients-trust-it⟩. Access on: 27 Jul. 2022. Quoted on page 52.

MASIMO. *Clinical Applications of Perfusion Index*. 2007. Available at: ⟨https://www.masimo.co.uk/siteassets/uk/documents/pdf/clinical-evidence/whitepapers/lab3410f_whitepapers_perfusion_index.pdf⟩. Access on: 09 apr. 2022. Quoted on page 25.

MASIMO. *Masimo Signal Extraction Technology*. 2020. Available at: ⟨https://www.masimo.com/technology/co-oximetry/set/⟩. Access on: 05 Sep. 2020. Quoted on page 41.

MAXIM INTEGRATED. *Guidelines for SPO2 measurement using the MAXIM® MAX32664 Sensor Hub: application note 6845*. 2014. Available at: ⟨https://www.maximintegrated.com/en/design/technical-documents/app-notes/6/6845.html⟩. Access on: 10 Sep. 2020. Quoted 2 times on pages 26 and 27.

MAXIM INTEGRATED. *MAX30102: High-Sensitivity Pulse Oximeter and Heart-Rate Sensor for Wearable Health*. 2018. Available at: ⟨https://datasheets.maximintegrated.com/en/ds/MAX30102.pdf⟩. Access on: 17 Mar. 2022. Quoted 2 times on pages 32 and 50.

MAXIM INTEGRATED. *Recommended Configurations and Operating Profiles For MAX30101/MAX30102 EV Kits*. 2018. Available at: ⟨https://www.maximintegrated.com/en/design/technical-documents/userguides-and-manuals/6/6409.html⟩. Access on: 24 Jul. 2021. Quoted 2 times on pages 31 and 32.

MEDICAL SYSTEM BRASIL. *Oxímetro de Pulso*. 2021. Available at: ⟨https://medicalsystembrasil.com.br/produto/oximetro-de-pulso/⟩. Access on: 02 Aug. 2021. Quoted on page 119.

MENDELSON, Y. Pulse oximetry: theory and applications for noninvasive monitoring. *Clinical Chemistry*, v. 38, n. 9, p. 1601–1607, 9 1992. Quoted on page 33.

MISHRA, S. Does modern medicine increase life-expectancy: Quest for the moon rabbit? *Indian Heart Journal*, v. 68, n. 1, p. 19–27, 1 2016. Quoted on page 19.

MOYLE, J. T. B. *Pulse oximetry*. 2. ed. London: BMJ Books, 2002. Quoted 4 times on pages 22, 37, 39, and 40.

OPPENHEIM, A. V.; SCHAFER, R. W. *Discrete-Time Signal Processing*. 3. ed. Harlow: Pearson, 2014. Quoted on page 54.

PALIWAL, M.; KUMAR, U. A. Neural networks and statistical techniques: A review of applications. *Expert Systems with Applications*, v. 36, n. 1, p. 2–17, 2009. Quoted on page 52.

PIMENTEL, M. A. F. et al. Toward a robust estimation of respiratory rate from pulse oximeters. *IEEE Transactions on Biomedical Engineering*, v. 64, n. 8, p. 1914–1923, 8 2017. Quoted on page 44.

PRESS, W. H.; TEUKOLSKY, S. A. Savitzky-Golay smoothing filters. *Comput. Phys. Commun.*, AIP Publishing, v. 4, n. 6, p. 669, 1990. Quoted on page 54.

RAM, M. R. et al. A novel approach for motion artifact reduction in ppg signals based on as-lms adaptive filter. *IEEE Transactions on Instrumentation and Measurement*, v. 61, n. 5, p. 1445–1457, 5 2012. Quoted on page 29.

REIS, B. *Introdução às Redes Neurais*. 2016. Available at: ⟨http://www2.decom.ufop.br/imobilis/redes-neurais-introcucao/⟩. Access on: 01 Aug. 2021. Quoted on page 52.

REUSS, J. L.; BAHR, D. E. Period domain analysis in fetal pulse oximetry. In: *Proceedings of the Second Joint 24th Annual Conference and the Annual Fall Meeting of the EMBS/BMES*. [S.l.: s.n.], 2002. v. 2, p. 1742–1743 vol.2. Quoted on page 36.

ROCHA, J. E. C. da et al. Redes neurais artificiais na previsão de contágio e Óbitos por covid-19: Um estudo no estado do pará, brasil. *International Journal of Development Research*, v. 10, n. 4, p. 35416–35421, 4 2020. Quoted on page 52.

RODRIGUES, E. M. et al. Experimental low cost reflective type oximeter for wearable health systems. *Biomedical Signal Processing and Control*, v. 31, n. 1, p. 419–433, 1 2017. Quoted on page 20.

ROUX, P. D. L.; ODDO, M. Parenchymal brain oxygen monitoring in the neurocritical care unit. *Neurosurgery Clinics of North America*, v. 24, n. 3, p. 427–439, 2013. Neurocritical Care in Neurosurgery. Disponível em: ⟨https://www.sciencedirect.com/science/article/pii/S1042368013000223⟩. Quoted on page 20.

SALEHIZADEH, S. M. A. et al. Photoplethysmograph signal reconstruction based on a novel motion artifact detection-reduction approach. part ii: Motion and noise artifact removal. *Annals of biomedical engineering*, v. 42, n. 11, p. 2251–2263, 11 2014. Quoted 3 times on pages 24, 40, and 42.

SAVITZKY, A.; GOLAY, M. J. E. Smoothing and differentiation of data by simplified least squares procedures. *Analytical Chemistry*, American Chemical Society, v. 36, n. 8, p. 1627–1639, 7 1964. Quoted on page 54.

SINCHAI, S. et al. A photoplethysmographic signal isolated from an additive motion artifact by frequency translation. *IEEE Transactions on Biomedical Circuits and Systems*, v. 12, n. 4, p. 904–917, 8 2018. Quoted on page 24.

SMART PROTOTYPING. *MPU6500 6DOF Sensor Breakout Board*. 2022. Available at: ⟨https://www.smart-prototyping.com/MPU6500-6DOF-Sensor-Breakout-Board⟩. Access on: 18 Mar. 2022. Quoted on page 51.

SMART PROTOTYPING. *Pulse Oximeter and Heart Rate Sensor (MAX30102)*. 2022. Available at: ⟨https://www.smart-prototyping.com/Pulse-Oximeter-and-Heart-Rate-Sensor-MAX30102⟩. Access on: 18 Mar. 2022. Quoted on page 50.

STROGONOVS, R. *Implementing pulse oximeter using MAX30100*. 2017. Available at: ⟨https://morf.lv/implementing-pulse-oximeter-using-max30100⟩. Access on: 24 Jul. 2021. Quoted on page 31.

TARVIRDIZADEH, B. et al. A novel online method for identifying motion artifact and photoplethysmography signal reconstruction using artificial neural networks and adaptive neuro-fuzzy inference system. *Neural Computing & Applications*, v. 32, n. 8, p. 3549–3566, 4 2020. Quoted 2 times on pages 41 and 42.

TOBIN, M. J.; LAGHI, F.; JUBRAN, A. Why COVID-19 silent hypoxemia is baffling to physicians. *American Journal of Respiratory and Critical Care Medicine*, v. 202, n. 3, p. 356–360, 8 2020. Quoted 3 times on pages 20, 21, and 22.

TORTORA, G. J.; DERRICKSON, B. *Principles of Anatomy and Physiology*. 14. ed. New York: John Wiley & Sons, Inc., 2014. Quoted on page 21.

UNITED NATIONS. *World Population Prospects 2019*. 2019. ed. [S.l.]: United Nations, Department of Economic and Social Affairs, 2019. v. 2. (1, v. 2). Quoted on page 19.

URPALAINEN, K. *Development of a fractional multi-wavelength pulse oximetry algorithm*. Dissertação (Mestrado) — Aalto University, 10 2011. Quoted 6 times on pages 22, 25, 26, 27, 38, and 39.

VANDERPLAS, J. *Understanding the FFT Algorithm*. 2013. Available at: ⟨https://jakevdp.github.io/blog/2013/08/28/understanding-the-fft/⟩. Access on: 23 Mar. 2022. Quoted 2 times on pages 56 and 57.

VIRTANEN, P. et al. SciPy 1.0: Fundamental Algorithms for Scientific Computing in Python. *Nature Methods*, v. 17, p. 261–272, 2020. Quoted on page 55.

WEBSTER, J. G. *Design of Pulse Oximeters*. Bristol and Philadelphia: Institute of Physics Publishing, 1997. Quoted 6 times on pages 21, 22, 37, 38, 39, and 40.

WHITTEMORE, S. *The Respiratory System*. New York: Chelsea House, 2004. Quoted on page 20.

WILLIAMSON, J. R. et al. Motion artifact mitigation for wearable pulse oximetry. In: *2018 IEEE 15th International Conference on Wearable and Implantable Body Sensor Networks (BSN)*. [S.l.: s.n.], 2018. p. 74–77. Quoted on page 42.

WORLD HEALTH ORGANIZATION. *Pulse Oximetry Training Manual*. 2011. Available at: ⟨https://www.who.int/patientsafety/safesurgery/pulse_oximetry/who_ps_pulse_oximetry_training_manual_en.pdf⟩. Access on: 18 Jul. 2021. Quoted on page 23.

YAN, Y.-S.; POON, C. C.; ZHANG, Y.-T. Reduction of motion artifact in pulse oximetry by smoothed pseudo wigner-ville distribution. *Journal of NeuroEngineering and Rehabilitation*, v. 2, n. 1, p. 3, 3 2005. Quoted 7 times on pages 41, 42, 43, 54, 60, 74, and 81.

YOUSEFI, R. et al. A motion-tolerant adaptive algorithm for wearable photoplethysmographic biosensors. *IEEE Journal of Biomedical and Health Informatics*, v. 18, n. 2, p. 670–681, 3 2014. Quoted on page 29.

YUKI, K.; FUJIOGI, M.; KOUTSOGIANNAKI, S. Covid-19 pathophysiology: A review. *Clinical Immunology*, v. 215, p. 108427, 2020. Quoted on page 21.

ZENEWICZ, L. A. Oxygen levels and immunological studies. *Frontiers in Immunology*, v. 8, p. 324, 2017. Quoted on page 20.

APPENDIX A – Pulse oximeter kit

The pulse oximeter kit consists of a prototype developed to capture the data that make up the Personal PPG and Vols PPG Datasets. It has a PCB that connects the microcontroller to fingertip-clip. The PCB has a button that was used to start recording the data and a buzzer to signal to the volunteer the moments of beginning/end of the movement.

1 Pulse oximeter kit schematic

The schematic shown on page 93 was designed using Autodesk Fusion 3D software application and after its validation on the breadboard, the PCB was made. The electronic components used to make the pulse oximeter kit are listed in Table 13.

Table 13 – Electronic components of pulse oximeter kit.

Part	Description	Value
J1, J3	8x1 female socket header	J-08-SIP-100-40
J2	KK connector 6 pins	J-06-KK-4455-A06
R1	Resistor fixed ANSI	10,000 ohms
R2	Resistor fixed ANSI	100 ohms
S1	Momentary switch (Pushbutton)	SPST-PTH-6.0MM
SG1	Piezo buzzer	5 V
–	5-Core cable	26 AWG
–	Copper clad board, single sided	50×50 mm

Source – Caíque Santos Lima, 2022.

2 Pulse oximeter kit printed circuit board

The pulse oximeter kit PCB was manufactured in the Electronic Instrumentation Laboratory (LIEPO-USP) by Tayná Bertacine. The 3D view of the PCB and the photomask used to manufacture it are shown on page 94.

3 3D printed fingertip-clip

The 3D model of fingertip-clip that houses the sensors detailed in Tables 3 and 4, was designed by Marcos Endo. The three parts that make up the fingertip-clip (top-clip, bottom-clip and lid-clip), are shown on page 95.

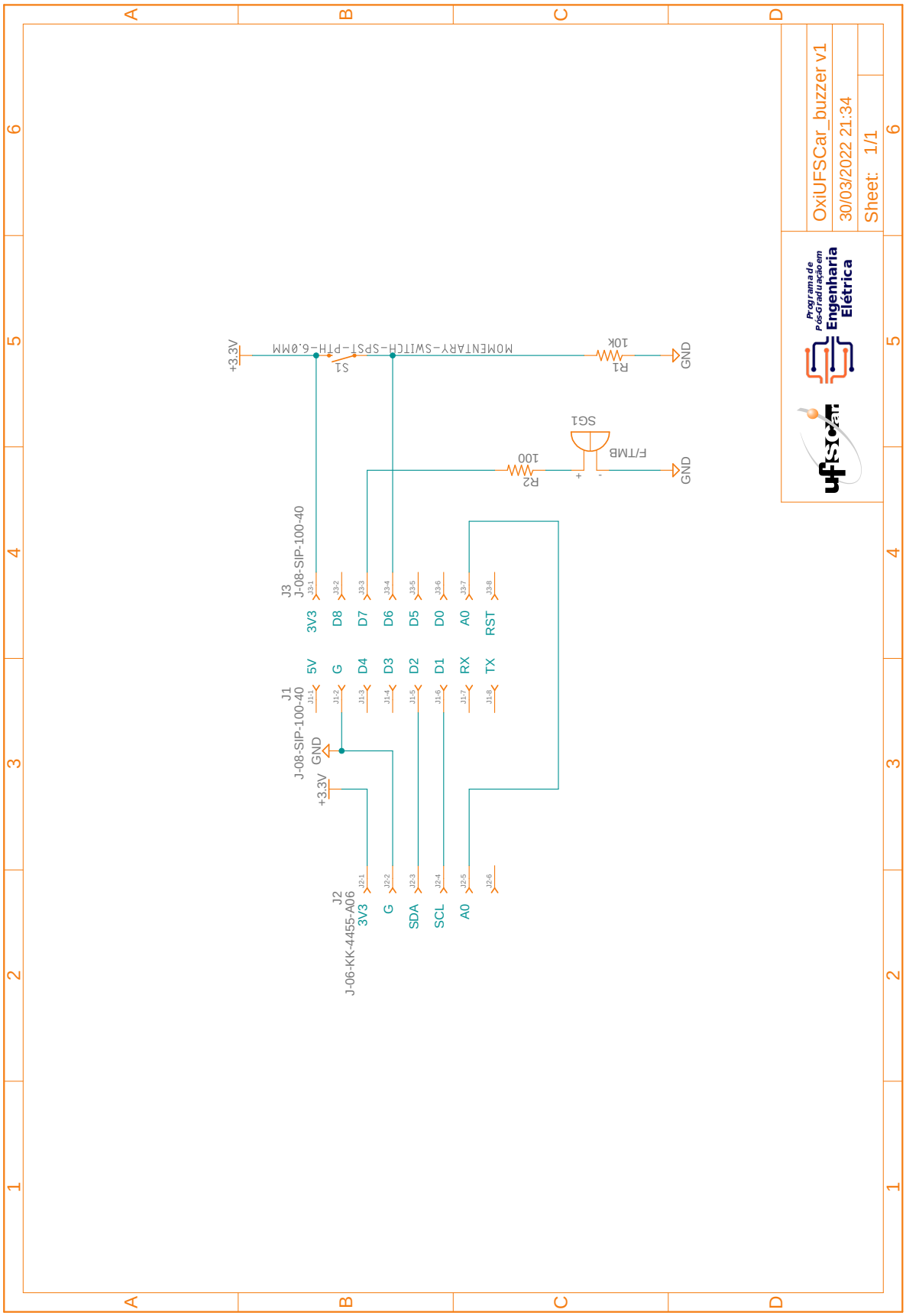
OxiUFSCar_buzzer v1
30/03/2022 21:34
Sheet: 1/1
Programa de Pós-Graduação em Engenharia Elétrica
+3.3V
S1
MOMENTARY-SWITCH-SPST-PTH-6.0MM
R1
10K
GND
SG1
F/TMB
R2
100
GND
J3
J-08-SIP-100-40
3V3
D8
D7
D6
D5
D0
A0
RST
J1
J-08-SIP-100-40
5V
G
D4
D3
D2
D1
RX
TX
GND
+3.3V
J2
J-06-KK-4455-A06
3V3
G
SDA
SCL
A0

PCB top view

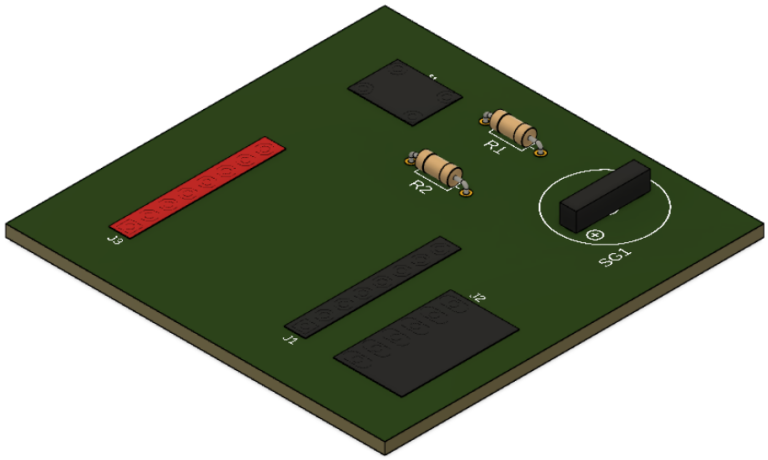

PCB bottom view

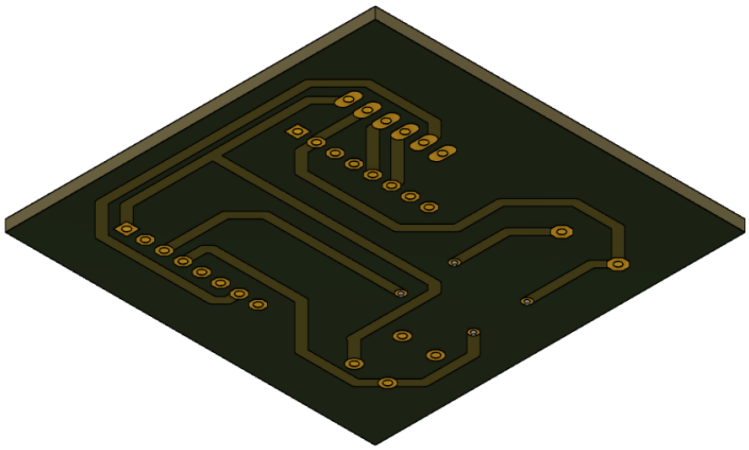

PCB photomask

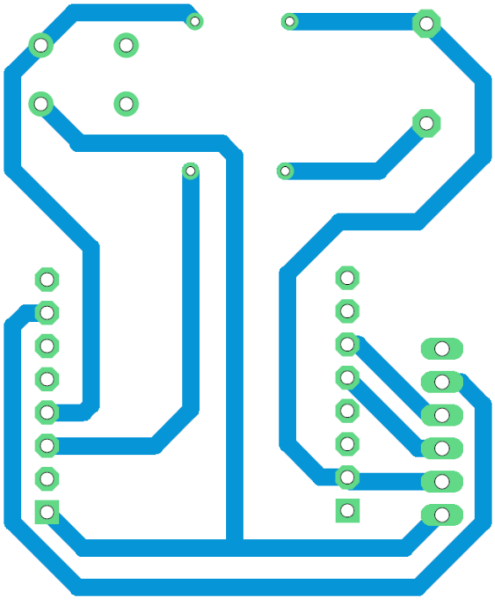

Lid-clip

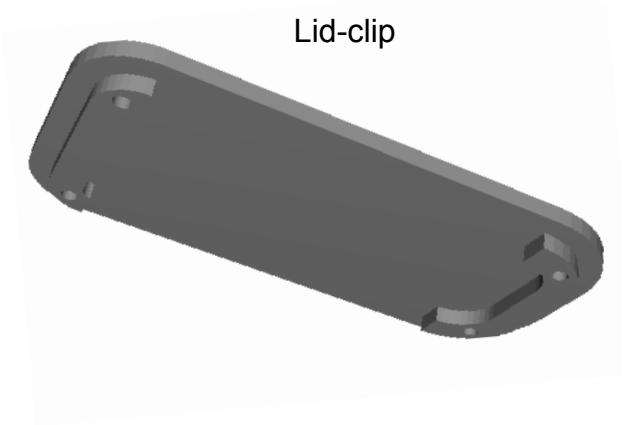

Top-clip

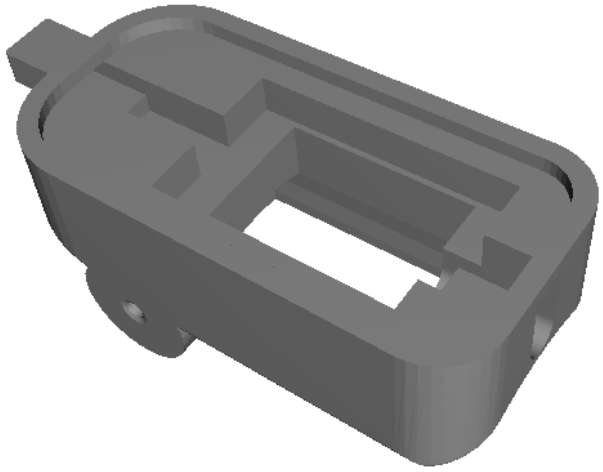

Bottom-clip

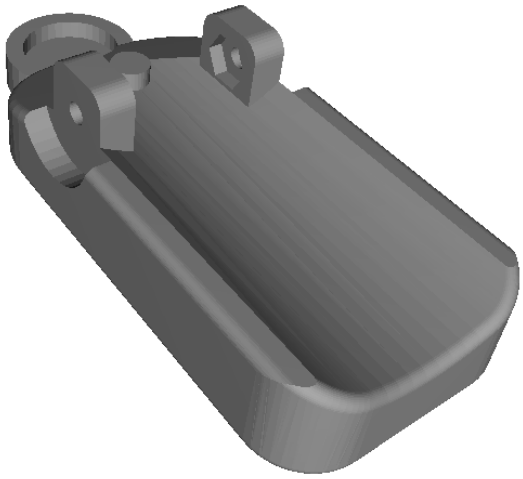

APPENDIX B – Human research project submitted to the Research Ethics Committee of UFSCar

The Dataset Vols PPG was created in compliance with the human research project (CAAE: 54173421.2.0000.5504) approved by the Research Ethics Committee (CEP) of UFSCar. Due to the COVID-19 pandemic scenario, this project was also submitted to the Executive Center for Health Surveillance (NEVS) and, by ID 37050, it was enabled in accordance with Resolution 39 and/or Official Letters 196/2021/GR and 15/2021/GR.

1 Free and Informed Consent Form

The purpose of the Free and Informed Consent Form (TCLE) is to provide research volunteers with the broadest possible explanation of the investigation to be carried out, its risks and benefits, so that their expression of will to participate (or not) is effectively free and conscious. The TCLE of this research is shown on page 97.

2 Embodied opinion of the Research Ethics Committee

This project was approved by the opinion number 5.230.864, additional details about this project approved by the CEP can be found on page 99.

3 Embodied opinion of the Research Ethics Committee – amendment

Throughout this research, some procedures were adjusted, such as: duration of each oximetry collection, acquisition of volunteers' data, changes in the TCLE and schedule of activities. These modifications were approved by the CEP through amendment number 5.307.521. This amendment can be consulted on page 106.

4 Embodied opinion of the Executive Center for Health Surveillance

In order to protect those involved in face-to-face activities related to this research and to mitigate risks related to COVID-19, a contingency plan was created and approved by NEVS. This opinion can be consulted on page 113.

Universidade Federal de São Carlos – UFSCar
Centro de Ciências Exatas e de Tecnologia – CCET
Departamento de Engenharia Elétrica – DEE

TERMO DE CONSENTIMENTO LIVRE E ESCLARECIDO

1. Convidamos a participar da realização do processo de pesquisa "Algoritmo inteligente robusto a interferências externas em oxímetros de pulso". Ao participar desse processo de pesquisa estará contribuindo para o desenvolvimento de tecnologias visando melhorar a qualidade da avaliação clínica para o profissional da saúde, bem como o desenvolvimento de um dispositivo biomédico útil para a prevenção, diagnóstico e tratamento de doenças.
2. O objetivo deste estudo é desenvolver um algoritmo baseado em inteligência artificial para atenuar os efeitos indesejáveis em um sinal de oximetria provocados pela movimentação do oxímetro. O oxímetro de pulso é um dispositivo eletrônico amplamente utilizado por profissionais da saúde para detectar e tratar os efeitos produzidos por agentes infecciosos, ou seja, microrganismos responsáveis por causar doenças infecciosas. Esse instrumento não invasivo é de grande relevância para monitoramento da oxigenação sanguínea e tem sido uma importante ferramenta para detecção de casos de hipoxemia (baixa concentração de oxigênio no sangue) em pessoas acometidas pela COVID-19, por exemplo. Com esse sistema inteligente será possível aperfeiçoar um oxímetro de pulso que está sendo desenvolvido pelo Departamento de Engenharia Elétrica (DEE), Departamento de Medicina (DMed) e Departamento de Computação (DC) da Universidade Federal de São Carlos (UFSCar).
3. A participação nesta pesquisa consistirá em coleta dos dados de oximetria (1) com um oxímetro de pulso certificado pela Agência Nacional de Vigilância Sanitária (ANVISA), denominado 'oxímetro padrão'; e (2) com o oxímetro em desenvolvimento, denominado 'protótipo'. Assim, o(a) participante terá que comparecer apenas uma vez para a realização da pesquisa. Essa participação não envolve a doação de materiais biológicos.
4. Aos(Às) participantes será solicitado que se sentem em uma cadeira e coloquem suas mãos sobre uma mesa de modo que não haja movimentação de seus dedos. O oxímetro padrão será colocado no dedo médio da mão esquerda e o protótipo será colocado no dedo médio da mão direita. Serão realizadas coletas de sinais de oximetria com duração de 72 segundos cada uma, e será solicitado ao(à) participante que movimente sua mão direita (protótipo) de modo que o sinal de oximetria seja completamente afetado pelos movimentos. Este estudo está firmado nas condições de que oferece baixo risco à saúde do(a) participante, sendo este referente a desconfortos decorrentes da movimentação da mão durante os movimentos. Vale destacar que o(a) profissional da saúde envolvido no estudo prestará todo apoio necessário.
5. Caso o(a) participante sinta algum desconforto que o impeça de realizar os testes desta pesquisa, poderá desistir de participar e retirar seu consentimento a qualquer momento, sendo que isso não trará nenhuma penalização ou prejuízo em sua relação com o pesquisador ou com a instituição.
6. O(A) participante tem direito a assistência gratuita e imediata em caso de danos decorrentes da pesquisa, bem como o direito de buscar indenização, se necessário. A assistência consistirá de atendimento fisioterápico para os desconfortos músculos-esqueléticos e primeiros socorros se necessário, serão oferecidos e poderão ser realizados pelo(a) profissional de saúde vinculado à equipe de pesquisa.
7. Todos os procedimentos deste estudo serão realizados em colaboração com a equipe de pesquisa pelo pesquisador responsável sob supervisão de seu orientador de mestrado, Professor Dr. André Carmona Hernandes.

8. Eventuais dúvidas a respeito dos procedimentos e da sua participação na pesquisa serão esclarecidas antes e durante o curso desta pesquisa, pelo próprio pesquisador responsável, identificado no fim deste termo.

9. As informações obtidas através dessa pesquisa serão confidenciais e asseguramos o sigilo sobre sua participação. Os arquivos gerados no processo de coleta dos dados serão identificados a partir de uma numeração que somente o pesquisador principal saberá a quem se refere. Os dados coletados poderão ser divulgados em eventos, revistas, repositório e/ou trabalhos científicos, sempre preservando a sua identidade.

10. Caso haja custos com transporte para deslocamento, alimentação ou outros gastos decorrentes da participação neste projeto de pesquisa, o(a) participante será ressarcido(a) pelo pesquisador deste projeto mediante a(s) comprovação(ões) de recibo(s) de pagamento(s).

11. Além do Termo de Consentimento Livre e Esclarecido o participante responderá um questionário digital de autoavaliação de suas condições de saúde denominado 'Ficha do(a) Participante'.

12. Visando a segurança de todos os envolvidos nesta pesquisa, durante os testes serão adotadas todas as medidas preconizadas pelas autoridades sanitárias para prevenção à COVID-19, como, por exemplo, o uso correto de máscaras, limpeza das mãos e distanciamento seguro.

13. Este projeto de pesquisa será realizado no endereço: Rua Capitão Luiz Rufo, nº 39 - Quintino Facci I - CEP 14.077-020 - Ribeirão Preto - SP, onde se encontra o Instituto Crescer Cidadão.

14. O Comitê de Ética em Pesquisa localiza-se no endereço Rod. Washington Luís, km 235 - São Carlos/SP, CEP 13565-905 - Prédio da Reitoria. Tel. (16) 3351-8028, e-mail: cephumanos@ufscar.br funcionamento de segunda a sexta-feira no horário das 8:00 às 12:00 (via e-mail durante a pandemia), tendo por finalidade avaliar os aspectos éticos das pesquisas envolvendo seres humanos, realizadas por pesquisador(a) da UFSCar, de acordo com as legislações vigentes, especialmente a Resolução do Conselho Nacional de Saúde nº 466 de 2012, cuja finalidade é assegurar a dignidade e a proteção dos(as) participantes de pesquisa.

15. Este termo deverá ser assinado em duas vias e todas as páginas de ambas as vias deverão ser rubricadas pelo pesquisador e pelo(a) participante, ficando uma via retida com o pesquisador responsável. O(A) participante receberá a outra via deste termo devidamente assinada onde consta o telefone e o endereço do pesquisador principal, podendo tirar suas dúvidas sobre o projeto e sua participação, agora ou a qualquer momento.

Pesquisador Responsável:
Caíque Santos Lima
Mestrando em Engenharia Elétrica
DEE-UFSCar
Tel.: (19) 9 9783-1796 | e-mail: ccaique.lima@gmail.com
Universidade Federal de São Carlos - Departamento de Engenharia Elétrica
Rodovia Washington Luis, km 235 - São Carlos - SP - BR - CEP: 13565-905

Declaro que entendi os objetivos, riscos e benefícios de minha participação na pesquisa e concordo em participar.

Ribeirão Preto, _____ de _____ de _____.

_____ _____
Assinatura do Participante da Pesquisa Assinatura do Pesquisador

UFSCAR - UNIVERSIDADE FEDERAL DE SÃO CARLOS

PARECER CONSUBSTANCIADO DO CEP

DADOS DO PROJETO DE PESQUISA

Título da Pesquisa: Algoritmo inteligente robusto a interferências externas em oxímetros de pulso.
Pesquisador: CAIQUE SANTOS LIMA
Área Temática:
Versão: 1
CAAE: 54173421.2.0000.5504
Instituição Proponente: Universidade Federal de São Carlos/UFSCar
Patrocinador Principal: FUND COORD DE APERFEICOAMENTO DE PESSOAL DE NIVEL SUP

DADOS DO PARECER

Número do Parecer: 5.230.864

Apresentação do Projeto:
As informações apresentadas neste campo foram extraídas do documento PB_INFORMAÇÕES_BÁSICAS_DO_PROJETO_1869337.pdf, de 15/12/2021.

Desenho:
Aos(Às) participantes será solicitado que se sentem em uma cadeira e coloquem suas mãos sobre uma mesa de modo que não haja movimentação de seus dedos. O oxímetro padrão será colocado no dedo médio da mão esquerda e o protótipo será colocado no dedo médio da mão direita. Dois testes serão realizados para cada participante: (1) devido à comparação da similaridade do desempenho dos dois oxímetros da mão direita e esquerda, dois sinais de oximetria serão coletados simultaneamente pelo período de 2,5 minutos enquanto ambas as mãos repousarão sobre a mesa; (2) dois sinais de oximetria serão coletados simultaneamente pelo período de 2,5 minutos enquanto a mão esquerda (oxímetro padrão) repousará sobre a mesa, e será solicitado ao(à) participante que movimente sua mão direita (protótipo) de modo que o sinal de oximetria seja completamente afetado pelos movimentos. Vale destacar que antes de se começar os testes, será solicitado aos(às) participantes o preenchimento da Ficha do(a) Participante, este documento tem como objetivo avaliar se a pessoa tem condições de participar do estudo e servirá também para auxiliar o processo de classificação dos dados de oximetria coletados.

Endereço: WASHINGTON LUIZ KM 235
Bairro: JARDIM GUANABARA **CEP:** 13.565-905
UF: SP **Município:** SAO CARLOS
Telefone: (16)3351-9685 **E-mail:** cephumanos@ufscar.br

UFSCAR - UNIVERSIDADE FEDERAL DE SÃO CARLOS

Continuação do Parecer: 5.230.864

Resumo:
A evolução tecnológica tem permitido o avanço em diversas áreas do conhecimento humano ao longo dos últimos anos, especialmente na medicina moderna. Além das inovações em medicamentos, tratamentos e serviços de cuidados à saúde, tem se destacado o conceito de telemedicina, que ampliou o alcance de atendimentos clínicos à população mundial. Novos dispositivos biomédicos são indispensáveis para os serviços de saúde, seja em hospitais e clínicas de grande porte, como em casa no uso doméstico para telemonitoramento. Dentre vários equipamentos eletrônicos úteis aos profissionais de saúde para prevenção, diagnóstico e tratamento de doenças, destaca-se o oxímetro de pulso. Esse dispositivo não invasivo é de grande relevância para monitoramento da oxigenação sanguínea, e tem sido uma importante ferramenta para detecção de casos de hipoxemia em pessoas acometidas pela COVID-19. Os oxímetros de pulso são suscetíveis a ruídos no sinal medido que, em grande parte, são provocados pela movimentação do paciente durante o monitoramento. Isso pode provocar erros nas leituras e causar alarmes falsos. Visando atenuar esses efeitos indesejáveis, este projeto se propõe a desenvolver um algoritmo inteligente capaz de mitigar o ruído no sinal de oximetria. Esse algoritmo será aplicado em um oxímetro de pulso desenvolvido pelo Departamento de Engenharia Elétrica (DEE), Departamento de Computação (DC) e Departamento de Medicina (DMed) da Universidade Federal de São Carlos (UFSCar). A partir deste algoritmo, espera-se reduzir os erros de leitura no oxímetro de pulso em desenvolvimento.

Hipótese:
A coleta de dados de saturação de oxigênio com um oxímetro de pulso padrão (certificado pela ANVISA) e, simultaneamente, com o oxímetro em desenvolvimento a fim de correlacionar estes dados.

Metodologia Proposta:
Serão analisados sujeitos com idade entre 18 e 60 anos, homens e mulheres. Os dados pessoais, como: nome, contato, idade e histórico de saúde serão coletados através da 'Ficha do(a) Participante' que será requerida antes do início da coleta da oximetria. Este documento tem como objetivo avaliar se a pessoa tem condições de participar do estudo e servirá também para auxiliar o processo de classificação dos dados de oximetria coletados. A coleta da saturação de oxigênio será realizada em duas etapas para cada sujeito. (1) devido à comparação da similaridade do desempenho dos dois oxímetros da mão direita e esquerda, dois sinais de oximetria serão

Endereço: WASHINGTON LUIZ KM 235
Bairro: JARDIM GUANABARA **CEP:** 13.565-905
UF: SP **Município:** SAO CARLOS
Telefone: (16)3351-9685 **E-mail:** cephumanos@ufscar.br

coletados simultaneamente pelo período de 3 minutos enquanto ambas as mãos repousarão sobre a mesa; (2) dois sinais de oximetria serão coletados simultaneamente pelo período de 3 minutos enquanto a mão esquerda (oxímetro padrão) repousará sobre a mesa, e será solicitado ao(à) participante que movimente sua mão direita (protótipo) de modo que o sinal de oximetria seja completamente afetado pelos movimentos. Os dados coletados serão armazenados em um banco de dados protegido por senha, onde somente o pesquisador responsável terá acesso. Os arquivos gerados no processo de coleta dos dados serão identificados a partir de uma numeração que somente o pesquisador principal saberá a quem se refere. Os dados coletados poderão ser divulgados em eventos, revistas, repositórios e/ou trabalhos científicos, sempre preservando a identidade do(a) participante. Visando a segurança de todos os envolvidos nesta pesquisa, vale destacar que durante os testes serão adotadas todas as medidas preconizadas pelas autoridades sanitárias para prevenção à COVID-19, como o uso correto de máscaras, limpeza das mãos e distanciamento seguro. E este projeto obteve a habilitação de seu plano de contingência pelo NEVS-UFSCar através do processo ID 37050.

Critério de Inclusão:
Sujeitos homens e mulheres saudáveis com idade entre 18 e 60 anos.

Critério de Exclusão:
Sujeitos homens e mulheres com idade entre 18 e 60 anos, que apresentam algum quadro álgico e incapacidade física e cognitiva.

Metodologia de Análise de Dados:
Os dados de saturação de oxigênio serão analisados através da fotopletismografia, onde propriedades ópticas do tecido corporal e do sangue podem ser caracterizadas utilizando fontes de luz (vermelha e infravermelha) e um fotodetector. Os dados de oximetria serão analisados através de ferramentas computacionais, baseadas em linguagem C++ e Python, com bibliotecas de código aberto, técnicas de aprendizado de máquina (machine learning) e inteligência artificial.

Desfecho Primário:
Obtenção de dados de saturação de oxigênio capilar com um oxímetro de pulso padrão (certificado pela ANVISA) e com o oxímetro em desenvolvimento a fim de correlacionar estes dados visando à implementação de um algoritmo inteligente capaz de mitigar os efeitos indesejáveis

causados pelo movimento no oxímetro.

Objetivo da Pesquisa:

As informações apresentadas neste campo foram extraídas do documento PB_INFORMAÇÕES_BÁSICAS_DO_PROJETO_1869337.pdf, de 15/12/2021.

Objetivo Primário:

O objetivo é coletar os dados de oximetria de voluntários utilizando um oxímetro de pulso certificado pela ANVISA e um oxímetro em desenvolvimento. A partir destes dados será possível analisar como os movimentos da mão do sujeito afetam o sinal de oximetria e desenvolver um algoritmo inteligente capaz de mitigar os efeitos indesejáveis causados pelos movimentos.

Avaliação dos Riscos e Benefícios:

As informações apresentadas neste campo foram extraídas do documento PB_INFORMAÇÕES_BÁSICAS_DO_PROJETO_1869337.pdf, de 15/12/2021.

Riscos:

O participante poderá, eventualmente, apresentar algum grau de ansiedade durante a realização da coleta, mas conforme descrito no TCLE, o participante poderá retirar o seu consentimento e o procedimento será interrompido. Também existe a remota possibilidade do surgimento de algum desconforto tátil durante o uso do oxímetro no dedo. A fim de evitar esses problemas mencionados, todos os procedimentos a serem realizados serão explicados ao(à) participante de forma clara e de modo que ele(a) se sinta a vontade. E em casos de desconforto, vale destacar que o(a) profissional da saúde envolvido no estudo prestará todo apoio necessário.

Benefícios:

O(A) voluntário(a) ao participar desse processo de pesquisa estará contribuindo para o desenvolvimento de tecnologias visando melhorar a qualidade da avaliação clínica para o profissional da saúde, bem como o desenvolvimento de um dispositivo biomédico útil para a prevenção, diagnóstico e tratamento de doenças. O(A) participante terá acesso aos resultados obtidos imediatamente durante a realização do experimento (oximetria, frequência cardíaca, temperatura corpórea).

Comentários e Considerações sobre a Pesquisa:

Projeto de mestrado em desenvolvimento no Programa de Pós-Graduação em Engenharia Elétrica

UFSCAR - UNIVERSIDADE FEDERAL DE SÃO CARLOS

do Centro de Ciências Exatas e de Tecnologia da Universidade Federal de São Carlos.

Considerações sobre os Termos de apresentação obrigatória:

Vide campo "Conclusões ou Pendências e Lista de Inadequações".

Recomendações:

Vide campo "Conclusões ou Pendências e Lista de Inadequações".

Conclusões ou Pendências e Lista de Inadequações:

O projeto foi apresentado adequadamente, atendendo aos preceitos éticos estabelecidos pela Resolução CNS nº 466/2012 e suas complementares.

Considerações Finais a critério do CEP:

Diante do exposto, o Comitê de ética em pesquisa - CEP, de acordo com as atribuições definidas na Resolução CNS nº 466 de 2012 e 510 de 2016, manifesta-se por considerar "Aprovado" o projeto. A responsabilidade do pesquisador é indelegável e indeclinável e compreende os aspectos éticos e legais, cabendo-lhe, após aprovação deste Comitê de Ética em Pesquisa: II - conduzir o processo de Consentimento e de Assentimento Livre e Esclarecido; III - apresentar dados solicitados pelo CEP ou pela CONEP a qualquer momento; IV - manter os dados da pesquisa em arquivo, físico ou digital, sob sua guarda e responsabilidade, por um período mínimo de 5 (cinco) anos após o término da pesquisa; V - apresentar no relatório final que o projeto foi desenvolvido conforme delineado, justificando, quando ocorridas, a sua mudança ou interrupção. Este relatório final deverá ser protocolado via notificação na Plataforma Brasil. OBSERVAÇÃO: Nos documentos encaminhados por Notificação NÃO DEVE constar alteração no conteúdo do projeto. Caso o projeto tenha sofrido alterações, o pesquisador deverá submeter uma "EMENDA".

Considerando a situação sócio sanitária, bem como os planos de contingenciamento da pandemia da COVID-19 municipais e Estaduais; considerando que as Portarias/Resoluções de Instituições Proponentes de pesquisa são constantemente atualizadas; considerando o papel do sistema CEP/CONEP em garantir a segurança e proteção do participante da pesquisa por meio dos Protocolos submetidos na Plataforma Brasil; considerando a corresponsabilidade do pesquisador pela integridade e bem-estar dos participantes da pesquisa; este CEP orienta aos pesquisadores o acompanhamento da situação sócio sanitária da região em que ocorrerá a pesquisa, bem como as determinações legais dos planos de contingenciamento do COVID-19 para determinação do início,

Endereço: WASHINGTON LUIZ KM 235
Bairro: JARDIM GUANABARA **CEP:** 13.565-905
UF: SP **Município:** SAO CARLOS
Telefone: (16)3351-9685 **E-mail:** cephumanos@ufscar.br

UFSCAR - UNIVERSIDADE FEDERAL DE SÃO CARLOS

suspensão ou continuidade de atividades de pesquisas presenciais, mesmo que o Protocolo já se encontre aprovado pelo CEP.

Este parecer foi elaborado baseado nos documentos abaixo relacionados:

Tipo Documento	Arquivo	Postagem	Autor	Situação
Informações Básicas do Projeto	PB_INFORMAÇÕES_BÁSICAS_DO_PROJETO_1846104.pdf	24/11/2021 21:57:43		Aceito
Projeto Detalhado / Brochura Investigador	projeto_detalhado.pdf	24/11/2021 21:54:07	CAIQUE SANTOS LIMA	Aceito
TCLE / Termos de Assentimento / Justificativa de Ausência	TCLE.pdf	24/11/2021 21:52:25	CAIQUE SANTOS LIMA	Aceito
Outros	plano_contingencia_NEVS.pdf	24/11/2021 21:51:39	CAIQUE SANTOS LIMA	Aceito
Parecer Anterior	parecer_NEVS_habilitado_37050.pdf	24/11/2021 21:50:58	CAIQUE SANTOS LIMA	Aceito
Declaração do Patrocinador	termo_compromisso_CAPES.pdf	24/11/2021 21:50:30	CAIQUE SANTOS LIMA	Aceito
Declaração de Instituição e Infraestrutura	carta_autorizacao_ICC.pdf	24/11/2021 21:50:05	CAIQUE SANTOS LIMA	Aceito
Outros	ficha_participante.pdf	24/11/2021 21:49:42	CAIQUE SANTOS LIMA	Aceito
Cronograma	cronograma_projeto.pdf	24/11/2021 21:48:36	CAIQUE SANTOS LIMA	Aceito
Folha de Rosto	folha_rosto.pdf	24/11/2021 21:47:51	CAIQUE SANTOS LIMA	Aceito

Situação do Parecer:
Aprovado

Necessita Apreciação da CONEP:
Não

Endereço: WASHINGTON LUIZ KM 235
Bairro: JARDIM GUANABARA **CEP:** 13.565-905
UF: SP **Município:** SAO CARLOS
Telefone: (16)3351-9685 **E-mail:** cephumanos@ufscar.br

UFSCAR - UNIVERSIDADE FEDERAL DE SÃO CARLOS

Continuação do Parecer: 5.230.864

SAO CARLOS, 08 de Fevereiro de 2022

Assinado por:
Adriana Sanches Garcia de Araújo
(Coordenador(a))

Endereço: WASHINGTON LUIZ KM 235
Bairro: JARDIM GUANABARA **CEP:** 13.565-905
UF: SP **Município:** SAO CARLOS
Telefone: (16)3351-9685 **E-mail:** cephumanos@ufscar.br

UFSCAR - UNIVERSIDADE FEDERAL DE SÃO CARLOS

PARECER CONSUBSTANCIADO DO CEP

DADOS DA EMENDA

Título da Pesquisa: Algoritmo inteligente robusto a interferências externas em oxímetros de pulso.
Pesquisador: CAIQUE SANTOS LIMA
Área Temática:
Versão: 3
CAAE: 54173421.2.0000.5504
Instituição Proponente: Universidade Federal de São Carlos/UFSCar
Patrocinador Principal: FUND COORD DE APERFEICOAMENTO DE PESSOAL DE NIVEL SUP

DADOS DO PARECER

Número do Parecer: 5.307.521

Apresentação do Projeto:
As informações apresentadas neste campo foram extraídas do documento PB_INFORMAÇÕES_BÁSICAS_DO_PROJETO_1869337.pdf, de 15/12/2021.

Desenho
Aos(Às) participantes será solicitado que se sentem em uma cadeira e coloquem suas mãos sobre uma mesa de modo que não haja movimentação de seus dedos. O oxímetro padrão será colocado no dedo médio da mão esquerda e o protótipo será colocado no dedo médio da mão direita. Dois testes serão realizados para cada participante: (1) devido à comparação da similaridade do desempenho dos dois oxímetros da mão direita e esquerda, dois sinais de oximetria serão coletados simultaneamente pelo período de 2,5 minutos enquanto ambas as mãos repousarão sobre a mesa; (2) dois sinais de oximetria serão coletados simultaneamente pelo período de 2,5 minutos enquanto a mão esquerda (oxímetro padrão) repousará sobre a mesa, e será solicitado ao(à) participante que movimente sua mão direita (protótipo) de modo que o sinal de oximetria seja completamente afetado pelos movimentos. Vale destacar que antes de se começar os testes, será solicitado aos(às) participantes o preenchimento da Ficha do(a) Participante, este documento tem como objetivo avaliar se a pessoa tem condições de participar do estudo e servirá também para auxiliar o processo de classificação dos dados de oximetria coletados.

Endereço: WASHINGTON LUIZ KM 235
Bairro: JARDIM GUANABARA **CEP:** 13.565-905
UF: SP **Município:** SAO CARLOS
Telefone: (16)3351-9685 **E-mail:** cephumanos@ufscar.br

UFSCAR - UNIVERSIDADE FEDERAL DE SÃO CARLOS

Continuação do Parecer: 5.307.521

Resumo:
A evolução tecnológica tem permitido o avanço em diversas áreas do conhecimento humano ao longo dos últimos anos, especialmente na medicina moderna. Além das inovações em medicamentos, tratamentos e serviços de cuidados à saúde, tem se destacado o conceito de telemedicina, que ampliou o alcance de atendimentos clínicos à população mundial. Novos dispositivos biomédicos são indispensáveis para os serviços de saúde, seja em hospitais e clínicas de grande porte, como em casa no uso doméstico para telemonitoramento. Dentre vários equipamentos eletrônicos úteis aos profissionais de saúde para prevenção, diagnóstico e tratamento de doenças, destaca-se o oxímetro de pulso. Esse dispositivo não invasivo é de grande relevância para monitoramento da oxigenação sanguínea, e tem sido uma importante ferramenta para detecção de casos de hipoxemia em pessoas acometidas pela COVID-19. Os oxímetros de pulso são suscetíveis a ruídos no sinal medido que, em grande parte, são provocados pela movimentação do paciente durante o monitoramento. Isso pode provocar erros nas leituras e causar alarmes falsos. Visando atenuar esses efeitos indesejáveis, este projeto se propõe a desenvolver um algoritmo inteligente capaz de mitigar o ruído no sinal de oximetria. Esse algoritmo será aplicado em um oxímetro de pulso desenvolvido pelo Departamento de Engenharia Elétrica (DEE), Departamento de Computação (DC) e Departamento de Medicina (DMed) da Universidade Federal de São Carlos (UFSCar). A partir deste algoritmo, espera-se reduzir os erros de leitura no oxímetro de pulso em desenvolvimento.

Hipótese:
A coleta de dados de saturação de oxigênio com um oxímetro de pulso padrão (certificado pela ANVISA) e, simultaneamente, com o oxímetro em desenvolvimento a fim de correlacionar estes dados.

Metodologia Proposta:
Serão analisados sujeitos com idade entre 18 e 60 anos, homens e mulheres. Os dados pessoais, como: nome, contato, idade e histórico de saúde serão coletados através da 'Ficha do(a) Participante' que será requerida antes do início da coleta da oximetria. Este documento tem como objetivo avaliar se a pessoa tem condições de participar do estudo e servirá também para auxiliar o processo de classificação dos dados de oximetria coletados. A coleta da saturação de oxigênio será realizada em duas etapas para cada sujeito. (1) devido à comparação da similaridade do desempenho dos dois oxímetros da mão direita e esquerda, dois sinais de oximetria serão

Endereço: WASHINGTON LUIZ KM 235
Bairro: JARDIM GUANABARA **CEP:** 13.565-905
UF: SP **Município:** SAO CARLOS
Telefone: (16)3351-9685 **E-mail:** cephumanos@ufscar.br

coletados simultaneamente pelo período de 3 minutos enquanto ambas as mãos repousarão sobre a mesa; (2) dois sinais de oximetria serão coletados simultaneamente pelo período de 3 minutos enquanto a mão esquerda (oxímetro padrão) repousará sobre a mesa, e será solicitado ao(à) participante que movimente sua mão direita (protótipo) de modo que o sinal de oximetria seja completamente afetado pelos movimentos. Os dados coletados serão armazenados em um banco de dados protegido por senha, onde somente o pesquisador responsável terá acesso. Os arquivos gerados no processo de coleta dos dados serão identificados a partir de uma numeração que somente o pesquisador principal saberá a quem se refere. Os dados coletados poderão ser divulgados em eventos, revistas, repositórios e/ou trabalhos científicos, sempre preservando a identidade do(a) participante. Visando a segurança de todos os envolvidos nesta pesquisa, vale destacar que durante os testes serão adotadas todas as medidas preconizadas pelas autoridades sanitárias para prevenção à COVID-19, como o uso correto de máscaras, limpeza das mãos e distanciamento seguro. E este projeto obteve a habilitação de seu plano de contingência pelo NEVS-UFSCar através do processo ID 37050.

Critério de Inclusão:
Sujeitos homens e mulheres saudáveis com idade entre 18 e 60 anos.

Critério de Exclusão:
Sujeitos homens e mulheres com idade entre 18 e 60 anos, que apresentam algum quadro álgico e incapacidade física e cognitiva.

Metodologia de Análise de Dados:
Os dados de saturação de oxigênio serão analisados através da fotopletismografia, onde propriedades ópticas do tecido corporal e do sangue podem ser caracterizadas utilizando fontes de luz (vermelha e infravermelha) e um fotodetector. Os dados de oximetria serão analisados através de ferramentas computacionais, baseadas em linguagem C++ e Python, com bibliotecas de código aberto, técnicas de aprendizado de máquina (machine learning) e inteligência artificial.

Desfecho Primário:
Obtenção de dados de saturação de oxigênio capilar com um oxímetro de pulso padrão (certificado pela ANVISA) e com o oxímetro em desenvolvimento a fim de correlacionar estes dados visando à implementação de um algoritmo inteligente capaz de mitigar os efeitos indesejáveis

causados pelo movimento no oxímetro.

Objetivo da Pesquisa:

As informações apresentadas neste campo foram extraídas do documento PB_INFORMAÇÕES_BÁSICAS_DO_PROJETO_1869337.pdf, de 15/12/2021.

Objetivo Primário:

O objetivo é coletar os dados de oximetria de voluntários utilizando um oxímetro de pulso certificado pela ANVISA e um oxímetro em desenvolvimento. A partir destes dados será possível analisar como os movimentos da mão do sujeito afetam o sinal de oximetria e desenvolver um algoritmo inteligente capaz de mitigar os efeitos indesejáveis causados pelos movimentos.

Avaliação dos Riscos e Benefícios:

As informações apresentadas neste campo foram extraídas do documento PB_INFORMAÇÕES_BÁSICAS_DO_PROJETO_1869337.pdf, de 15/12/2021.

Riscos:

O participante poderá, eventualmente, apresentar algum grau de ansiedade durante a realização da coleta, mas conforme descrito no TCLE, o participante poderá retirar o seu consentimento e o procedimento será interrompido. Também existe a remota possibilidade do surgimento de algum desconforto tátil durante o uso do oxímetro no dedo. A fim de evitar esses problemas mencionados, todos os procedimentos a serem realizados serão explicados ao(à) participante de forma clara e de modo que ele(a) se sinta a vontade. E em casos de desconforto, vale destacar que o(a) profissional da saúde envolvido no estudo prestará todo apoio necessário.

Benefícios:

O(A) voluntário(a) ao participar desse processo de pesquisa estará contribuindo para o desenvolvimento de tecnologias visando melhorar a qualidade da avaliação clínica para o profissional da saúde, bem como o desenvolvimento de um dispositivo biomédico útil para a prevenção, diagnóstico e tratamento de doenças. O(A) participante terá acesso aos resultados obtidos imediatamente durante a realização do experimento (oximetria, frequência cardíaca, temperatura corpórea).

Comentários e Considerações sobre a Pesquisa:

Projeto de mestrado em desenvolvimento no Programa de Pós-Graduação em Engenharia Elétrica do Centro de Ciências Exatas e de Tecnologia da Universidade Federal de São Carlos.

Considerações sobre os Termos de apresentação obrigatória:
Vide campo "Conclusões ou Pendências e Lista de Inadequações".

Recomendações:
Vide campo "Conclusões ou Pendências e Lista de Inadequações".Vide campo "Conclusões ou Pendências e Lista de Inadequações".

Conclusões ou Pendências e Lista de Inadequações:
Este parecer tem como objetivo analisar emenda com as seguintes solicitações alteração neste projeto:
1. no tempo de duração de cada coleta de oximetria (nova duração: 72 segundos). No decorrer da pesquisa teórica, notou-se a necessidade de se ajustar o tempo de cada coleta, que era de 3 minutos, para se adequar ao processo de aquisição e processamento dos dados;
2. mudar a forma como serão registrados os dados da 'Ficha do(a) Participante',em vez de preenchimento no papel, será feito em um formulário digital protegido por senha - isso visa tornar o processo mais adequado, rápido e seguro. Este formulário será preenchido pelo pesquisador principal (responsável pela confidencialidade dos dados) na presença de cada voluntário. As informações coletadas permanecem sendo as mesmas da 'Ficha do(a) Participante';
3. adequar o TCLE com as alterações mencionadas acima. Os trechos modificados no novo TCLE encontram-se grifados;
4. para que a execução do experimento seja possível, também foram ajustados os prazos das atividades no cronograma do projeto.

Análise: As alterações solicitadas estão claramente indicadas nos documentos PB_INFORMAÇÕES_BÁSICAS_1899428_E1.pdf de 10/03, TCLE_v2.pdf e cronograma_projeto_v2.pdf. No que tange à apreciação ética do projeto, as alterações solicitadas estão alinhadas com as determinações da Resolução No. 466/2012 e 510 de 2016.

Considerações Finais a critério do CEP:
Diante do exposto, o Comitê de ética em pesquisa - CEP, de acordo com as atribuições definidas na Resolução CNS nº 466 de 2012 e 510 de 2016, manifesta-se por considerar "Aprovada" a emenda. A responsabilidade do pesquisador é indelegável e indeclinável e compreende os aspectos éticos e legais, cabendo-lhe, após aprovação deste Comitê de Ética em Pesquisa: II - conduzir o processo de Consentimento e de Assentimento Livre e Esclarecido; III - apresentar

UFSCAR - UNIVERSIDADE FEDERAL DE SÃO CARLOS

dados solicitados pelo CEP ou pela CONEP a qualquer momento; IV - manter os dados da pesquisa em arquivo, físico ou digital, sob sua guarda e responsabilidade, por um período mínimo de 5 (cinco) anos após o término da pesquisa; V - apresentar no relatório final que o projeto foi desenvolvido conforme delineado, justificando, quando ocorridas, a sua mudança ou interrupção. Este relatório final deverá ser protocolado via notificação na Plataforma Brasil. OBSERVAÇÃO: Nos documentos encaminhados por Notificação NÃO DEVE constar alteração no conteúdo do projeto. Caso o projeto tenha sofrido alterações, o pesquisador deverá submeter uma "EMENDA". Considerando a situação sócio sanitária, bem como os planos de contingenciamento da pandemia da COVID-19 municipais e Estaduais; Considerando que as Portarias/Resoluções de Instituições Proponentes de pesquisa são constantemente atualizadas; Considerando o papel do sistema CEP/CONEP em garantir a segurança e proteção do participante da pesquisa por meio dos Protocolos submetidos na Plataforma Brasil; Considerando a corresponsabilidade do pesquisador pela integridade e bem-estar dos participantes da pesquisa;

Este CEP orienta aos pesquisadores o acompanhamento da situação sócio sanitária da região em que ocorrerá a pesquisa, bem como as determinações legais dos planos de contingenciamento do COVID-19 para determinação do início, suspensão ou continuidade de atividades de pesquisas presenciais, mesmo que o Protocolo já se encontre aprovado pelo CEP.

Este parecer foi elaborado baseado nos documentos abaixo relacionados:

Tipo Documento	Arquivo	Postagem	Autor	Situação
Informações Básicas do Projeto	PB_INFORMAÇÕES_BÁSICAS_1899428_E1.pdf	10/03/2022 15:18:32		Aceito
Cronograma	cronograma_projeto_v2.pdf	10/03/2022 15:11:36	CAIQUE SANTOS LIMA	Aceito
TCLE / Termos de Assentimento / Justificativa de Ausência	TCLE_v2.pdf	10/03/2022 15:10:40	CAIQUE SANTOS LIMA	Aceito
Outros	carta_apresentacao_emenda.pdf	10/03/2022 15:09:44	CAIQUE SANTOS LIMA	Aceito
Projeto Detalhado / Brochura Investigador	projeto_detalhado.pdf	24/11/2021 21:54:07	CAIQUE SANTOS LIMA	Aceito
Outros	plano_contingencia_NEVS.pdf	24/11/2021 21:51:39	CAIQUE SANTOS LIMA	Aceito
Parecer Anterior	parecer_NEVS_habilitado_37050.pdf	24/11/2021 21:50:58	CAIQUE SANTOS LIMA	Aceito

Endereço: WASHINGTON LUIZ KM 235
Bairro: JARDIM GUANABARA **CEP:** 13.565-905
UF: SP **Município:** SAO CARLOS
Telefone: (16)3351-9685 **E-mail:** cephumanos@ufscar.br

UFSCAR - UNIVERSIDADE FEDERAL DE SÃO CARLOS

Continuação do Parecer: 5.307.521

Declaração do Patrocinador	termo_compromisso_CAPES.pdf	24/11/2021 21:50:30	CAIQUE SANTOS LIMA	Aceito
Declaração de Instituição e Infraestrutura	carta_autorizacao_ICC.pdf	24/11/2021 21:50:05	CAIQUE SANTOS LIMA	Aceito
Folha de Rosto	folha_rosto.pdf	24/11/2021 21:47:51	CAIQUE SANTOS LIMA	Aceito

Situação do Parecer:
Aprovado

Necessita Apreciação da CONEP:
Não

SAO CARLOS, 23 de Março de 2022

Assinado por:
Adriana Sanches Garcia de Araújo
(Coordenador(a))

Endereço: WASHINGTON LUIZ KM 235
Bairro: JARDIM GUANABARA **CEP:** 13.565-905
UF: SP **Município:** SAO CARLOS
Telefone: (16)3351-9685 **E-mail:** cephumanos@ufscar.br

UNIVERSIDADE FEDERAL DE SÃO CARLOS
NÚCLEO EXECUTIVO DE VIGILÂNCIA EM SAÚDE

PARECER

São Carlos, 23 de novembro de 2021

Caro proponente,

Obrigada por submeter seu plano de contingência ao NEVS.

O plano referente à atividade Coleta de dados de Oximetria, processo ID 37050, atende à Resolução 39 e/ou aos Ofícios 196/2021/GR e 15/2021/GR (prazo de defesa em 2022).

Parecer: Habilitado

A equipe do NEVS reforça que:

1. Todos os participantes de atividades habilitadas são convidados a se cadastrarem no aplicativo Guardiões da Saúde para efetivo monitoramento de suas condições de saúde. Veja em https://www.vencendoacovid19.ufscar.br/gtve/estrategia-guardioes-da-saude .
2. quando houver casos suspeitos e/ou confirmados, estes devem ser comunicados imediatamente pelo e-mail: vigilanciaepidemiologica@ufscar.br

Atenciosamente,

Profa. Dra. Carla Andreucci Polido
Coordenadora em exercício do Núcleo Executivo de Vigilância em Saúde

APPENDIX C – Main stages of the OxiTidy algorithm

Figure 42 below helps to illustrate the stages of the OxiTidy algorithm (versions 1 and 2) presented in Tables 10 and 11, respectively.

Figure 42 – OxiTidy stages.

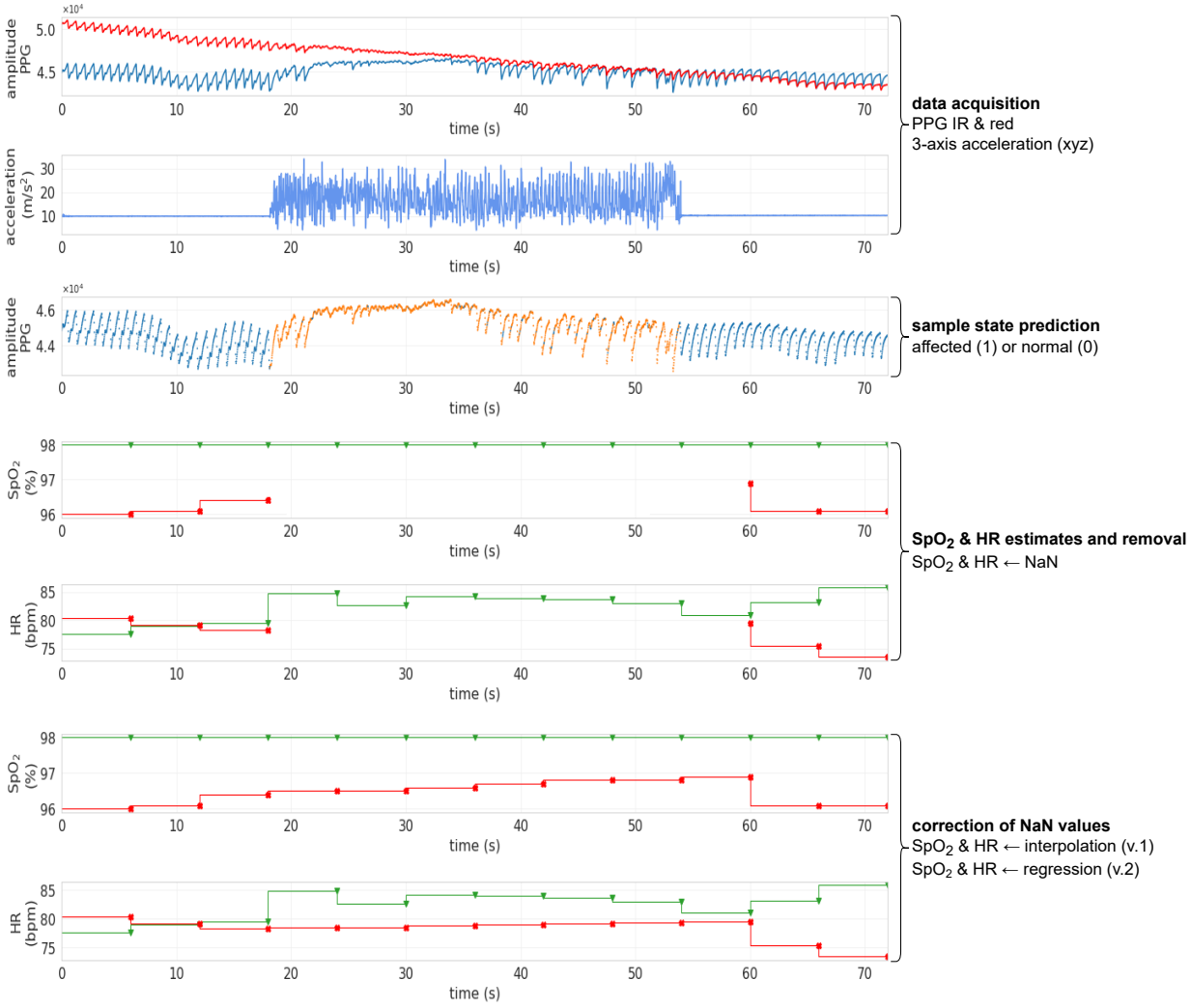

Source – Caíque Santos Lima, 2022.

APPENDIX D – Subdivisions of the Vols PPG Dataset

The data from the "Vols" dataset were arranged into subdivisions in order to facilitate the understanding of how they were used. Basically, these subdivisions are: *OxiCam failure*, *low perfusion* and *splits*. Each of these are explained in detail below and each record is arranged in a table on page 116.

OxiCam failure

Part of the records (25%) could not be synchronized with the measurements performed by the standard oximeter using OxiCam (see section 4.3), which should be investigated in due course. Thus, these 25 records were not used in this work. They were arranged into the *OxiCam failure* subdivision and can be consulted in the second column of the Table 14.

Low perfusion

Six records were arranged in the *low perfusion* subdivision because their PPG signals did not have the characteristic shape of the PPG wave. Therefore, it was not possible to obtain SpO_2 or HR precisely. Therefore, these records were not used in this work either. They can be seen in the third column of the Table 14.

Splits

The data not included in the subdivisions described above were used in the algorithms proposed in this work as well as in the other methods compared. Each "split" is subdivided into two sets: *training* (T) and *validation* (V). Data from sets T and V were used in the training and validation process of the ANNs, respectively. On the other hand, in the other methods compared in this work (raw, DFT and SMA), only data from category V were used in each split. The records that make up each training and validation set of each split can be consulted in Table 14 below.

Table 14 – Subdivisions of the "Vols" dataset.

Signal	OxiCam failure	low perfusion	split 01		split 02		split 03		split 04		split 05		split 06		split 07		split 08		split 09		split 10	
			T	V	T	V	T	V	T	V	T	V	T	V	T	V	T	V	T	V	T	V
PPG_01_01			•		•		•		•		•		•		•			•	•		•	
PPG_01_02			•		•		•		•		•		•			•	•		•		•	
PPG_01_03			•		•			•	•		•		•		•		•		•		•	
PPG_01_04			•		•		•		•		•			•	•		•		•		•	
PPG_01_05			•			•	•		•		•		•		•		•		•		•	
PPG_02_01			•		•		•		•			•	•		•		•		•		•	
PPG_02_02			•			•	•		•		•		•		•		•		•		•	
PPG_02_03			•		•		•		•			•	•		•		•		•		•	
PPG_02_04			•		•		•		•		•		•		•		•		•			•
PPG_02_05			•			•	•		•		•		•		•		•		•		•	
PPG_03_01	•																					
PPG_03_02			•		•		•		•			•	•		•		•		•		•	
PPG_03_03				•	•		•		•		•		•		•		•		•		•	
PPG_03_04			•			•	•		•		•		•		•		•		•		•	
PPG_03_05	•																					
PPG_04_01			•		•		•		•		•		•			•	•		•		•	
PPG_04_02			•		•		•		•		•		•		•			•	•		•	
PPG_04_03			•		•		•		•		•		•		•			•	•		•	
PPG_04_04			•		•		•		•		•		•		•		•		•			•
PPG_04_05			•		•		•		•		•		•		•		•			•	•	
PPG_05_01			•			•	•		•		•		•		•		•		•		•	
PPG_05_02			•		•		•		•		•		•		•		•			•	•	
PPG_05_03			•		•		•		•		•			•	•		•		•		•	
PPG_05_04	•																					
PPG_05_05			•		•		•		•		•		•		•		•			•	•	
PPG_06_01			•		•		•			•	•		•		•		•		•		•	
PPG_06_02			•		•		•		•		•		•		•		•		•			•
PPG_06_03			•		•			•	•		•		•		•		•		•		•	
PPG_06_04			•		•		•		•		•		•			•	•		•		•	
PPG_06_05			•		•		•		•		•		•		•			•	•		•	
PPG_07_01	•																					
PPG_07_02				•	•		•		•		•		•		•		•		•		•	

Continued on next page

Table 14 – continued from previous page

Signal	OxiCam failure	low perfusion	split 01		split 02		split 03		split 04		split 05		split 06		split 07		split 08		split 09		split 10	
			T	V	T	V	T	V	T	V	T	V	T	V	T	V	T	V	T	V	T	V
PPG_07_03			●		●		●		●		●		●		●			●	●		●	
PPG_07_04				●	●		●		●		●		●		●		●		●		●	
PPG_07_05	●																					
PPG_08_01		●																				
PPG_08_02		●																				
PPG_08_03		●																				
PPG_08_04			●		●		●		●		●		●		●			●	●		●	
PPG_08_05		●																				
PPG_09_01			●		●		●		●		●		●		●			●	●		●	
PPG_09_02	●																					
PPG_09_03	●																					
PPG_09_04		●																				
PPG_09_05		●																				
PPG_10_01			●		●		●		●		●		●		●		●			●	●	
PPG_10_02			●		●			●	●		●		●		●		●		●		●	
PPG_10_03			●		●		●		●		●		●			●	●		●		●	
PPG_10_04			●		●			●	●		●		●		●		●		●		●	
PPG_10_05			●		●		●		●			●	●		●		●		●		●	
PPG_11_01			●		●		●		●		●		●			●	●		●		●	
PPG_11_02	●																					
PPG_11_03			●		●		●		●		●		●		●		●			●	●	
PPG_11_04	●																					
PPG_11_05			●		●		●		●		●			●	●		●		●		●	
PPG_12_01			●		●		●		●		●			●	●		●		●		●	
PPG_12_02			●		●		●			●	●		●		●		●		●		●	
PPG_12_03			●		●			●	●		●		●		●		●		●		●	
PPG_12_04			●		●		●			●	●		●		●		●		●		●	
PPG_12_05			●		●		●			●	●		●		●		●		●		●	
PPG_13_01			●		●		●		●			●	●		●		●		●		●	
PPG_13_02				●	●		●		●		●		●		●		●		●		●	
PPG_13_03			●		●		●		●		●		●		●		●		●			●
PPG_13_04			●			●	●		●		●		●		●		●		●		●	
PPG_13_05			●		●		●		●		●		●		●		●		●			●
PPG_14_01			●		●		●		●		●		●		●		●			●	●	

Continued on next page

Table 14 – continued from previous page

Signal	OxiCam failure	low perfusion	split 01		split 02		split 03		split 04		split 05		split 06		split 07		split 08		split 09		split 10	
			T	V	T	V	T	V	T	V	T	V	T	V	T	V	T	V	T	V	T	V
PPG_14_02			•		•		•		•		•			•	•		•		•		•	
PPG_14_03				•	•		•		•		•		•		•		•		•		•	
PPG_14_04			•		•		•		•		•			•	•		•		•		•	
PPG_14_05			•		•		•		•		•		•			•	•		•		•	
PPG_15_01	•																					
PPG_15_02	•																					
PPG_15_03	•																					
PPG_15_04	•																					
PPG_15_05	•																					
PPG_16_01			•		•		•		•		•			•	•		•		•		•	
PPG_16_02			•			•	•		•		•		•		•		•		•		•	
PPG_16_03			•		•		•			•	•		•		•		•		•		•	
PPG_16_04				•	•		•		•		•		•		•		•		•		•	
PPG_16_05				•	•		•		•		•		•		•		•		•		•	
PPG_17_01	•																					
PPG_17_02	•																					
PPG_17_03	•																					
PPG_17_04	•																					
PPG_17_05	•																					
PPG_18_01	•																					
PPG_18_02	•																					
PPG_18_03	•																					
PPG_18_04	•																					
PPG_18_05	•																					
PPG_19_01			•		•		•		•			•	•		•		•		•		•	
PPG_19_02			•		•		•			•	•		•		•		•		•		•	
PPG_19_03			•		•		•		•			•	•		•		•		•		•	
PPG_19_04	•																					
PPG_19_05			•		•			•	•		•		•		•		•		•		•	
PPG_20_01			•		•		•			•	•		•		•		•		•		•	
PPG_20_02			•		•			•	•		•		•		•		•		•		•	
PPG_20_03			•		•		•		•		•		•		•		•			•	•	
PPG_20_04			•		•		•		•		•		•			•	•		•		•	
PPG_20_05			•		•		•		•		•		•		•		•		•			•

ANNEX A – Pulse oximeter Model L5 user manual

Pulse oximeter Model L5 manufactured by Heyuan Leyuan Intelligent Technology Co., Ltd. is distributed in Brazil by BRA Medical under Anvisa registration number 81334699002. Figure 43 below shows a picture of the Model L5 oximeter.

Figure 43 – Pulse oximeter Model L5 certified by Anvisa.

Source – Medical System Brasil (2021).

The following Model L5 manual user describes, in accordance with the pulse oximeter's features and requirements, main structure, functions, specifications, correct methods for transportation, installation, usage, operation, repair, maintenance and storage, etc. As well as the safety procedures to protect both the user and equipment.

MedicalSystem

ANVISA
Registro ANVISA:
81334699002

Oxímetro de pulso

Manual do usuário

Instruções aos usuários

Caros usuários, muito obrigado por adquirir nosso produto.

Este manual foi escrito e compilado de acordo com a diretiva do conselho MDD93 / 42 / EEC para dispositivos médicos e padrões harmonizados. O manual foi escrito para o oxímetro de pulso atual. No caso de modificações e atualizações de software, as informações contidas neste documento estão sujeitas a alterações sem aviso prévio. O Manual descreve, de acordo com os recursos e requisitos do Oxímetro de Pulso, estrutura principal, funções, especificações, métodos corretos de transporte, instalação, uso, operação, reparo e armazenamento etc., bem como os procedimentos de segurança para proteger usuário e equipamento. Consulte os respectivos capítulos para obter detalhes.

Por favor, leia o manual com muito cuidado antes de usar este equipamento. Estas instruções descrevem os procedimentos operacionais a serem seguidos estritamente; o não cumprimento dessas instruções pode causar anormalidades na medição, danos ao equipamento e ferimentos pessoais. O fabricante NÃO é responsável pelos problemas de segurança, confiabilidade e desempenho e qualquer anormalidade no monitoramento, ferimentos pessoais ou danos ao equipamento devido à negligência do usuário das instruções de operação. O serviço de garantia do fabricante não cobre essas falhas.

Devido à futura renovação, os produtos específicos que você recebeu podem não estar totalmente de acordo com a descrição deste Manual do Usuário. Lamentamos sinceramente por isso.

Este produto é um dispositivo médico e pode ser usado repetidamente. Seu tempo de uso é de 3 anos.

AVISO:

* **A sensação desconfortável ou dolorosa pode aparecer se o dispositivo for utilizado incessantemente, especialmente nos pacientes com barreira à microcirculação. Recomenda-se que o sensor não seja aplicado no mesmo dedo por mais de 2 horas.**
* **Para cada paciente, deve haver uma inspeção mais prudente no processo de colocação. O dispositivo não pode ser conectado ao edema e tecido sensível.**
* **A luz (o infravermelho é invisível) emitida pelo dispositivo é prejudicial aos olhos; portanto, o usuário e o técnico de manutenção não podem olhar para a luz.**
* **O testador não pode usar esmalte ou outra maquiagem.**
* **A unha do testador não pode ser muito longa.**
* **Leia o conteúdo relativo sobre as restrições clínicas e os cuidados.**
* **Este dispositivo não está destinado ao tratamento.**

1. Segurança

1.1 Instruções **para operações seguras**

* Verifique a unidade principal e todos os acessórios periodicamente para garantir que não haja danos visíveis que possam afetar a segurança do paciente e monitorar o desempenho de cabos e transdutores. Recomenda-se que o dispositivo seja inspecionado pelo menos uma vez por semana. Quando houver danos óbvios, pare de usar o monitor.
* A manutenção necessária deve ser realizada apenas por engenheiros de serviço qualificados. Os usuários não têm permissão para fazer a manutenção sozinhos.
* O oxímetro não pode ser usado junto com dispositivos não especificados no Manual do Usuário. Somente o acessório indicado ou recomendado pelo fabricante pode ser usado com este dispositivo.
* Este produto é calibrado antes de sair da fábrica.

1.2 Avisos

* Risco de explosão - NÃO use o oxímetro em ambiente com gás inflamável, como alguns agentes anestésicos inflamáveis..
* NÃO use o oxímetro enquanto a pessoa é medida por ressonância magnética e tomografia computadorizada.
* A pessoa alérgica à borracha não pode usar este dispositivo.
* O descarte do instrumento antigo e de seus acessórios e embalagens (incluindo bateria, sacolas plásticas, espumas e caixas de papel) deve seguir as leis e regulamentos locais.
* Verifique a embalagem antes de usar para garantir que o dispositivo e os acessórios estejam totalmente de acordo com a lista de embalagens, caso contrário, o dispositivo poderá ter a possibilidade de funcionar de maneira anormal..
* Por favor, não meça este dispositivo com papel de teste de função para obter informações relacionadas ao dispositivo.

1.3 Atenções

* Mantenha o oxímetro longe de poeira, vibração, substâncias corrosivas, materiais explosivos, alta temperatura e umidade.
* Se o oxímetro se molhar, pare de operá-lo.
* Quando transportado de ambiente frio para ambiente quente ou úmido, não o utilize imediatamente.
* NÃO opere as teclas no painel frontal com materiais pontiagudos.
* Não é permitida a desinfecção a vapor a alta temperatura ou a alta pressão do oxímetro. Consulte o Manual do Usuário no capítulo relativo para obter instruções sobre limpeza e desinfecção.
* Não deixe o oxímetro imerso em líquido. Quando precisar de limpeza, limpe a superfície com álcool medicinal e material macio. Não pulverize qualquer líquido diretamente no dispositivo.
* Ao limpar o dispositivo com água, a temperatura deve ser inferior a 60º C.
* Quanto aos dedos muito finos ou muito frios, provavelmente afetaria a medida normal da SpO^2 e da taxa de pulso dos pacientes, prenda o dedo grosso, como o polegar e o dedo médio, profundamente o suficiente na sonda.
* Não use o dispositivo em bebês ou pacientes neonatais.
* O produto é adequado para crianças acima de quatro anos e adultos (o peso deve estar entre 15 e 110 kg).
* O dispositivo pode não funcionar para todos os pacientes. Se você não conseguir obter leituras estáveis, interrompa o uso.
* O período de atualização dos dados é inferior a 5 segundos, que pode ser alterado de acordo com a taxa de pulso individual diferente.
* A forma de onda é normalizada. Por favor, leia o valor medido quando a forma de onda na tela for igual e constante. Aqui, este valor medido é o valor ideal. E a forma de onda no momento é a padrão.
* Se algumas condições anormais aparecerem na tela durante o processo de teste, puxe o dedo e reinsira para restaurar o uso normal.
* O dispositivo tem vida útil normal por três anos desde o primeiro uso eletrificado.
* O cabo de suspensão anexado ao produto é fabricado com material anti-alérgico, se um grupo em particular for sensível ao cabo de suspensão, pare de usá-lo. Além disso, preste atenção ao uso da corda pendurada, não use ao redor do pescoço, evitando causar danos ao paciente.
* O instrumento não possui a função de alarme de baixa voltagem, apenas mostra a baixa voltagem. Troque a bateria quando a energia da bateria estiver esgotada.
* Quando o parâmetro é particular. O instrumento não possui função de alarme. Não use o dispositivo em situações em que são necessários alarmes.
* As baterias devem ser removidas se o dispositivo for armazenado por mais de um mês, caso contrário as baterias poderão vazar.

* Um circuito flexível conecta as duas partes do dispositivo. Não torça nem puxe a conexão.

2. Visão Geral

A saturação de oxigênio no pulso é a porcentagem de HbO2 no total de Hb no sangue, a chamada concentração de O2 no sangue. É um importante parâmetro biológico para a respiração. Com o objetivo de medir a SpO2 com mais facilidade e precisão, nossa empresa desenvolveu o Oxímetro de Pulso. Ao mesmo tempo, o dispositivo pode medir a taxa de pulso simultaneamente.

O oxímetro de pulso apresenta em pequeno volume, baixo consumo de energia, operação conveniente e portátil. É necessário apenas que o paciente coloque um dos dedos em um sensor fotoelétrico na ponta dos dedos para diagnóstico, e uma tela mostrará diretamente o valor medido da saturação da hemoglobina.

2.1 Classificação:

Classe II b, (MDD93/42/EEC IX Regra 10)

2.2 Características

* A operação do produto é simples e conveniente.
* O produto é pequeno em volume, leve (peso total é de cerca de 50g, incluindo baterias) e fácil de transportar.
* O consumo de energia do produto é baixo e as duas pilhas AAA originalmente equipadas podem ser operadas continuamente por 20 horas.
* O produto será desligado automaticamente quando não houver sinal no produto em 5 segundos.

2.3 Principais aplicações e escopo de aplicação

O oxímetro de pulso pode ser usado para medir a saturação da hemoglobina humana e a taxa de pulso através do dedo e indicar a intensidade do pulso pela barra. O produto é adequado para uso em família, hospital (enfermaria comum), barra de oxigênio, organizações médicas sociais e também para medir a saturação de oxigênio e a taxa de pulso..

* **O produto não é adequado para uso em supervisão contínua para pacientes.**
* **O problema de classificação excessiva surgiria quando o paciente estivesse sofrendo de toxicose causada por monóxido de carbono; não é recomendável que o dispositivo seja usado nessas circunstâncias.**

2.4 Requisitos ambientais

Ambiente de armazenamento

a) Temperatura: -40º C - +60º C
b) Umidade relativa ≤ 95 %
c) Pressão atmosférica: 500hPa – 1060hPa

Ambiente operacional

a) Temperatura: 10º C – 40º C
b) Umidade relativa ≤ 75 %
c) Pressão atmosférica: 700hPa – 1060hPa

3. Princípio e Cuidado

3.1 Princípio da medição

O princípio do oxímetro é o seguinte: Uma fórmula de experiência do processo de dados é estabelecida utilizando a Lei Lambert Beer de acordo com as Características de Absorção do Espectro da Hemoglobina Redutiva (Hb) e Oxihemoglobina (HbO2) nas zonas de brilho e infravermelho próximo. O princípio de operação do instrumento é: é: Fotoelétrico. A tecnologia de inspeção de oxihemoglobina é adotada de acordo com a Tecnologia de digitalização e gravação por pulso de capacidade, de modo que dois feixes de diferentes comprimentos de onda das luzes possam ser focados na ponta da unha humana através do sensor do tipo dedo da pinça em perspectiva. Em seguida, o sinal medido pode ser obtido por um elemento fotossensível, informações adquiridas através das quais serão mostradas na tela através do tratamento em circuitos eletrônicos e microprocessadores.

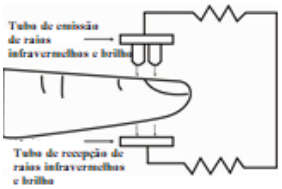

Figura 1 Princípio de funcionamento

3.2 Cuidado

1. O dedo deve ser colocado corretamente (veja a ilustração em anexo deste manual, Figura 5), ou pode causar medições imprecisas.
2. O sensor de SpO2 e o tubo receptor fotoelétrico devem ser dispostos de maneira que a arteríola do paciente esteja na posição entre eles.
3. O sensor de SpO2 não deve ser usado em um local ou membro amarrado com canal arterial ou manguito de pressão arterial ou recebendo injeção intravenosa.
4. Verifique se o caminho óptico está livre de obstáculos ópticos, como tecido emborrachado.
5. A luz ambiente excessiva pode afetar o resultado da medição. Inclui lâmpada fluorescente, luz rubi dupla, aquecedor infravermelho, luz solar direta e etc.
6. Ação extenuante do sujeito ou interferência eletrocirúrgica extrema também podem afetar a precisão.
7. O testado não pode usar esmalte ou outra maquiagem.

3.3 Clinical Restrictions

1. Como a medida é tomada com base no pulso das arteríolas, é necessário um fluxo sanguíneo pulsante substancial do indivíduo. Para um sujeito com pulso fraco devido a choque, baixa temperatura ambiente / corpo, sangramento grave ou uso de medicamento para contração vascular, a forma de onda da SpO2 (PLETH) diminuirá. Nesse caso, a medição será mais sensível à interferência.
2. Para aqueles com uma quantidade substancial de drogas de diluição para coloração (como azul de metileno, verde indigo e ácido azul indigo) ou hemoglobina monóxido de carbono (COHb) ou metionina (Me + Hb) ou hemoglobina tiosalicílica e algumas com problemas de icterícia, a determinação de SpO2 por este monitor pode ser imprecisa.
3. Drogas como dopamina, procaína, prilocaína, lidocaína e butacaína também podem ser os principais fatores responsáveis pelo erro grave da medida de SpO2.
4. Como o valor de SpO2 serve como um valor de referência para o julgamento de anóxia anêmica e anóxia tóxica, alguns pacientes com anemia grave também podem relatar boas medições de SpO2.

4. Especificações técnicas

1) **Formato de exibição**: Display OLED;
Faixa de medição de SpO2: 0% - 100%;
Faixa de medição da taxa de pulso: 30 bpm - 250 bpm;
Exibição de onda de pulso: exibição de colunização e exibição em forma de onda.

2) **Requisitos de energia**: 2 pilhas alcalinas AAA de 1,5 V (ou usando a bateria recarregável), faixa adaptável: 2.6V-3.6V.
3) **Consumo de energia**: Menor que 30mA.
4) **Resolução**: 1% para SpO2 e 1 bpm para taxa de pulso..
5) **Precisão da medição**: ± 2% no estágio de SpO2 de 70% a 100% e sem sentido quando o estágio é menor que 70%. ± 2 bpm ou ± 2% (selecione maior) para a taxa de pulso.
6) **Desempenho da medição em condições de preenchimento fraco**: SpO2 e taxa de pulso podem ser mostrados corretamente quando a taxa de preenchimento de pulso é de 0,4%. O erro de SpO2 é de + 4%, o erro de taxa de pulso é de ± 2 bpm ou ± 2% (selecione maior).
7) **Resistência à luz circundante:** o desvio entre o valor medido na condição de luz artificial ou luz natural interna e a de câmara escura é inferior a ± 1%.
8) Está equipado com um interruptor de função. O oxímetro pode ser desligado caso nenhum dedo esteja no oxímetro dentro de 5 segundos.
9) **Sensor Óptico**
Luz vermelha (comprimento de onda é 660nm, 6,65mW)
Infravermelho (comprimento de onda é 880nm, 6,75mW)

5. Acessórios

* Uma corda para pendurar
* Duas baterias (opcional)
* Um manual do usuário

6. Instalação

6.1 Vista do Painel Frontal

Figura 2 Visão Frontal

6.2 Bateria

Passo l. Veja firgura 3 e insira as duas pilhas tamanho AAA corretamente na direção certa.

Passo 2. Volte a colocar a tampa.

Tenha cuidado ao inserir as baterias, pois a inserção incorreta pode danificar o dispositivo.

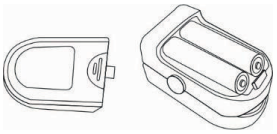

Figura 3 Instalação das baterias

6.3 Montagem da corda pendurada

Passo 1. Coloque a ponta da corda no orifício.

Passo 2. Coloque outra extremidade da corda na primeira e depois aperte-a.

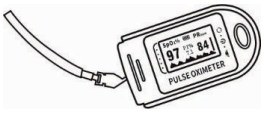

Figura 4 Montagem da corda para pendurar

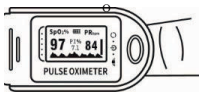

Figura 5 Coloque o dedo na posição

7. Guia de Operação

1) Insira as duas baterias corretamente na direção e, em seguida, recoloque a tampa.
2) Abra o clipe, como mostra a Figura 5.
3) Coloque o dedo do paciente nas almofadas de borracha do clipe (verifique se o dedo está na posição correta) e, em seguida, prenda o dedo.
4) Pressione o botão do interruptor uma vez no painel frontal.
5) Não sacuda o dedo e mantenha o paciente à vontade durante o processo. Enquanto isso, o corpo humano não é recomendado no status de movimento.
6) Obtenha as informações diretamente da tela.
7) O botão ⏻ – ☼ possui três funções. Quando o dispositivo está desligado, pressionar o botão pode abri-lo; Quando o dispositivo está ligado, pressionar o botão rapidamente pode mudar a direção da tela; Quando o dispositivo está ligado, pressionar o botão por muito tempo pode alterar o brilho da tela

* **As unhas e o tubo luminescente devem estar do mesmo lado.**

8. Reparação e Manutenção

* Por favor, troque as pilhas quando a baixa voltagem for exibida na tela.
* Limpe a superfície do dispositivo antes de usar. Limpe o dispositivo com álcool medicinal primeiro e depois deixe secar ao ar ou limpe-o com um pano limpo e seco.
* Usando o álcool medicinal para desinfetar o produto após o uso, evite a infecção cruzada para o próximo uso.
* Retire as pilhas se o oxímetro não estiver em uso por um longo período de tempo.
* O melhor ambiente de armazenamento do dispositivo é - temperatura ambiente de 40 ° C a 60 ° C e não superior a 95% de umidade relativa.
* Os usuários são aconselhados a calibrar o dispositivo periodicamente (ou de acordo com o programa de calibração do hospital). Também pode ser realizado no agente indicado pelo estado ou apenas entre em contato conosco para a calibração.

A esterilização a alta pressão não pode ser usada no dispositivo.

Não mergulhe o dispositivo em líquidos.

Recomenda-se que o dispositivo seja mantido em um ambiente seco. A umidade pode reduzir a vida útil do dispositivo ou até danificá-lo.

9. Solução de problemas

Problema	Possivel razão	Solução
A SpO2 e a taxa de pulso não podem ser exibidas normalmente	1. O dedo não está posicionado corretamente. 2. A SpO2 do paciente está muito baixa para ser detectada.	1. Coloque o dedo corretamente e novamente. 2. Tente novamente; Vá a um hospital para um diagnóstico se tiver certeza de que o dispositivo está funcionando bem.
A SpO2 e a taxa de pulso não são exibidas de forma estável	1. O dedo não está colocado suficientemente fundo. 2. O dedo está tremendo ou o paciente está se movendo.	1. Coloque o dedo corretamente e tente novamente. 2. Deixe o paciente manter a calma.
O dispositivo não pode ser ligado	1. As baterias estão gastas ou quase esgotadas. 2. As pilhas não estão inseridas corretamente. 3. O mau funcionamento do dispositivo.	1. Troque as pilhas. 2. Reinstale as baterias. 3. Entre em contato com o centro de serviço local.
O visor desliga repentinamente	1. O dispositivo será desligado automaticamente quando não houver sinal dentro de 5 segundos. 2. As pilhas estão quase gastas.	1. Normal. 2. Troque as pilhas.

10. Símbolos

	Descrição
	Tipo BF
	Aviso Consulte o Manual do Usuário
%SpO2	A saturação de oxigênio no pulso (%)
PRbpm	Taxa de pulso (bpm)
	A indicação de voltagem da bateria está deficiente (troque a bateria com o tempo evitando a medida inexata)
- -	1. Nenhum dedo inserido 2. Um indicador de inadequação do sinal
+	Eletrodo positivo da bateria
-	Cátodo de bateria
⏻ – ☼	1. Interruptor de alimentação 2. Mude a direção da tela 3. Altere o brilho da tela
SN	Número de série
	Inibição de alarme
	WEEE (2002/96/EC)
IP22	Proteção Internacional

11. Especificação de Função

Exibir informações	**Modo de exibição**
A saturação de oxigênio no pulso (SpO2)	OLED
Taxa de Pulso (PR)	OLED
Instensidade do Pulso (gráfico de barras)	OLED exibição de gráfico de barras
Onda de pulso	OLED
Especificação de parâmetro de SpO2	
Faixa de medição	0% - 100% (a resolução é 1%).
Precisão	70% - 100%: ± 2% Abaixo de 70% não especificado.
Sensor óptico	Luz vermelha (comprimento de onda é 660nm) Infravermelho (comprimento de onda é 880nm)
Especificação de parâmetros de pulso	
Faixa de medição	30bpm—250bpm (a resolução é 1 bpm)
Precisão	±2bpm or ±2% selecione o maior
Intensidade de pulso	
Alcance	Exibição contínua de gráfico de barras, a exibição superior indica o pulso mais forte.
Exigência da bateria	
1 pilha alcalina de 5V (tamanho AAA) x 2 ou pilha recarregável	
Vida útil da bateria	
Duas baterias podem funcionar continuamente por 20 horas	
Dimensões e Peso	
Dimensões	57(C) x 31(L) x 32(A) mm
Peso	Cerca de 50g (com as baterias)

Medical System Brasil
Avenida Londres, 40 - Arujá/SP
www.medicalsystembrasil.com.br

Medical System

Pulse Oximeter User Manual

Instructions to User

Dear Users, thank you very much for purchasing our product.

This Manual is written and compiled in accordance with the council directive MDD93/42/EEC for medical devices and harmonized standards. The Manual is written for the current Pulse Oximeter. In case of modifications and software upgrades, the information contained in this document is subject to change without notice.

The Manual describes, in accordance with the Pulse Oximeter's features and requirements, main structure, functions, specifications, correct methods for transportation, installation, usage, operation, repair, maintenance and storage, etc. as well as the safety procedures to protect both the user and equipment. Refer to the respective chapters for details.

Please read the Manual very carefully before using this equipment. These instructions describe the operating procedures to be followed strictly, failure to follow these instructions can cause measuring abnormality, equipment damage and personal injury. The manufacturer is NOT responsible for the safety, reliability and performance issues and any monitoring abnormality, personal injury and equipment damage due to user's negligence of the operation instructions. The manufacturer's warranty service does not cover such faults.

Owing to the forthcoming renovation, the specific products you received may not be totally in accordance with the description of this User Manual. We would sincerely regret for that.

This product is medical device, and can be used repeatedly. Its using life is 3 years.

WARNING:

- **The uncomfortable or painful feeling may appear if using the device ceaselessly, especially for the microcirculation barrier patients. It is recommended that the sensor should not be applied to the same finger for over 2 hours.**
- **For the individual patients, there should be a more prudent inspecting in the placing process. The device can not be clipped on the edema and tender tissue.**
- **The light (the infrared is invisible) emitted from the device is harmful to the eyes, so the user and the maintenance man, can not stare at the light.**
- **Testee can not use enamel or other makeup.**
- **Testee's fingernail can not be too long.**
- **Please peruse the relative content about the clinical restrictions and caution.**
- **This device is not intended for treatment.**

1 Safety

1.1 Instructions for Safe Operations

- Check the main unit and all accessories periodically to make sure that there is no visible damage that may affect patient's safety and monitoring performance about cables and transducers. It is recommended that the device should be inspected once a week at least. When there is obvious damage, stop using the monitor.
- Necessary maintenance must be performed by qualified service engineers ONLY. Users are not permitted to maintain it by themselves.
- The oximeter cannot be used together with devices not specified in User's Manual.Only the accessory that appointed or recommendatory by manufacture can be used with this device.
- This product is calibrated before leaving factory.

1.2 Warnings

- Explosive hazard—DO NOT use the oximeter in environment with inflammable gas such as some ignitable anesthetic agents.
- DO NOT use the oximeter while the testee measured by MRI and CT.
- The person who is allergic to rubber can not use this device.
- The disposal of scrap instrument and its accessories and packings (including battery, plastic bags, foams and paper boxes) should follow the local laws and regulations.
- Please check the packing before use to make sure the device and accessories are totally in accordance with the packing list, or else the device may have the possibility of working abnormally.
- Please don't measure this device with function test paper for the device's related information.

1.3 Attentions

- Keep the oximeter away from dust, vibration, corrosive substances, explosive materials, high temperature and moisture.
- If the oximeter gets wet, please stop operating it.
- When it is carried from cold environment to warm or humid environment, please do not use it immediately.
- DO NOT operate keys on front panel with sharp materials.
- High temperature or high pressure steam disinfection of the oximeter is not permitted. Refer to User Manual in the relative chapter for instructions of cleaning and disinfection.
- Do not have the oximeter immerged in liquid. When it needs cleaning, please wipe its surface with medical alcohol by soft material. Do not spray any liquid on the device directly.
- When cleaning the device with water, the temperature should be lower than 60℃.
- As to the fingers which are too thin or too cold, it would probably affect the normal measure of the patients' SpO_2 and pulse rate, please clip the thick finger such as thumb and middle finger deeply enough into the probe.
- Do not use the device on infant or neonatal patients.
- The product is suitable for children above four years old and adults (Weight should be between 15kg to 110kg).
- The device may not work for all patients. If you are unable to achieve stable readings, discontinue use.
- The update period of data is less than 5 seconds, which is changeable according to different individual pulse rate.
- The waveform is normalized.Please read the measured value when the waveform on screen is equably and steady-going, Here this measured value is optimal value. And the waveform at the moment is the standard one.
- If some abnormal conditions appear on the screen during test process, pull out the finger and reinsert to restore normal use.
- The device has normal useful life for three years since the first electrified use.
- The hanging rope attached the product is made from Non- allergy material, if particular group are sensitive to the hanging rope, stop using it. In addition, pay attention to the use of the hanging rope , do not wear around the neck avoiding cause harm to the patient.
- The instrument dose not have low-voltage alarm function, it only shows the low-voltage,please change the it battery when the battery energy is used out.
- When the parameter is particularly, The instrument dose not have alarm function.Do not use the device in situations where alarms are required.
- Batteries must be removed if the device is going to be stored for more than one month, or else batteries may leak.
- A flexible circuit connects the two parts of the device. Do not twist or pull on the connection.

2 Overview

The pulse oxygen saturation is the percentage of HbO_2 in the total Hb in the blood, so-called the O_2 concentration in the blood. It is an important bio-parameter for the respiration. For the purpose of measuring the SpO_2 more easily and accurately, our company developed the Pulse Oximeter. At the same time, the device can measure the pulse rate simultaneously.

The Pulse Oximeter features in small volume, low power consumption, convenient operation and being portable. It is only necessary for patient to put one of his fingers into a fingertip photoelectric sensor for diagnosis, and a display screen will directly show measured value of Hemoglobin Saturation.

2.1 Classification:

Class II b, (MDD93/42/EEC IX Rule 10)

2.2 Features

- Operation of the product is simple and convenient.
- The product is small in volume, light in weight (total weight is about 50g including batteries) and convenient in carrying.
- Power consumption of the product is low and the two originally equipped AAA batteries can be operated continuously for 20 hours.
- The product will automatically be powered off when no signal is in the product within 5 seconds.

2.3 Major Applications and Scope of Application

The Pulse Oximeter can be used to measure human Hemoglobin Saturation and pulse rate through finger, and indicate the pulse intensity by the bar-display. The product is suitable for use in family, hospital (Ordinary sickroom), Oxygen Bar, social medical organizations and also the measure of saturation oxygen and pulse rate.

⚠ **The product is not suitable for use in continuous supervision for patients.**

⚠ **The problem of overrating would emerge when the patient is suffering from toxicosis which caused by carbon monoxide, the device is not recommended to be used under this circumstance.**

2.4 Environment Requirements

Storage Environment

a) Temperature :-40℃~+60℃

b) Relative humidity :≤95%

c) Atmospheric pressure :500hPa~1060hPa

Operating Environment

a) Temperature :10℃~40℃

b) Relative Humidity :≤75%

c) Atmospheric pressure :700hPa~1060hPa

3 Principle and Caution

3.1 Principle of Measurement

Principle of the Oximeter is as follows: An experience formula of data process is established taking use of Lambert Beer Law according to Spectrum Absorption Characteristics of Reductive Hemoglobin (Hb) and Oxyhemoglobin (HbO_2) in glow & near-infrared zones. Operation principle of the instrument is: Photoelectric Oxyhemoglobin Inspection Technology is adopted in accordance with Capacity Pulse Scanning & Recording Technology, so that two beams of different wavelength of lights can be focused onto human nail tip through perspective clamp finger-type sensor. Then measured signal can be obtained by a photosensitive element, information acquired through which will be shown on screen through treatment in electronic circuits and microprocessor.

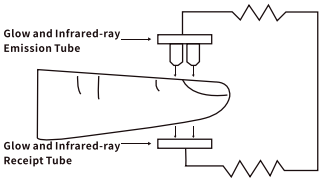

Figure 1 Operating principle

3.2 Caution

1. The finger should be placed properly (see the attached illustration of this manual ,Figure 5), or else it may cause inaccurate measurement.
2. The SpO_2 sensor and photoelectric receiving tube should be arranged in a way with the subject's arteriole in a position there between.
3. The SpO_2 sensor should not be used at a location or limb tied with arterial canal or blood pressure cuff or receiving intravenous injection.
4. Make sure the optical path is free from any optical obstacles like rubberized fabric.
5. Excessive ambient light may affect the measuring result. It includes fluorescent lamp, dual ruby light, infrared heater, direct sunlight and etc.
6. Strenuous action of the subject or extreme electrosurgical interference may also affect the accuracy.
7. Testee can not use enamel or other makeup.

3.3 Clinical Restrictions

1. As the measure is taken on the basis of arteriole pulse, substantial pulsating blood flow of subject is required. For a subject with weak pulse due to shock, low ambient/body temperature, major bleeding, or use of vascular contracting drug, the SpO_2 waveform (PLETH) will decrease. In this case, the measurement will be more sensitive to interference.
2. For those with a substantial amount of staining dilution drug (such as methylene blue, indigo green and acid indigo blue), or carbon monoxide hemoglobin (COHb), or methionine (Me+Hb) or thiosalicylic hemoglobin, and some with icterus problem, the SpO_2 determination by this monitor may be inaccurate.
3. The drugs like dopamine, procaine, prilocaine, lidocaine and butacaine may also be a major factor blamed for serious error of SpO_2 measure.
4. As the SpO_2 value serves as a reference value for judgement of anemic anoxia and toxic anoxia, some patients with serious anemia may also report good SpO_2 measurement.

4 Technical Specifications

1) **Display Format:** OLED Display;
SpO_2 Measuring Range: 0% - 100%;
Pulse Rate Measuring Range: 30 bpm - 250 bpm;
Pulse Wave Display: columniation display and the waveform display.

2) **Power Requirements:** 2 ×1.5V AAA alkaline battery(or using the rechargeable battery instead), adaptable range: 2.6V~3.6V.
3) **Power Consumption:** Smaller than 30mA.
4) **Resolution:** 1% for SpO_2 and 1 bpm for Pulse Rate.
5) **Measurement Accuracy:** ±2% in stage of 70%-100% SpO_2, and meaningless when stage being smaller than 70%. ±2 bpm or±2% (select larger) for Pulse Rate.
6) **Measurement Performance in Weak Filling Condition:** SpO_2 and pulse rate can be shown correctly when pulse-filling ratio is 0.4%. SpO_2 error is ±4%, pulse rate error is ±2 bpm or ±2% (select larger).
7) **Resistance to surrounding light:** The deviation between the value measured in the condition of man-made light or indoor natural light and that of darkroom is less than ±1%.
8) It is equipped with a function switch. The Oximeter can be powered off in case no finger is the Oximeter within 5 seconds.
9) **Optical Sensor**
Red light (wavelength is 660nm, 6.65mW)
Infrared (wavelength is 880nm, 6.75mW)

5 Accessories

- One hanging rope;
- Two batteries (optional);
- One User Manual.

6 Installation

6.1 View of the Front Panel

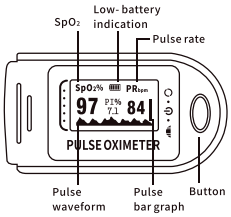

Figure 2 Front view

6.2 Battery

Step 1. Refer to Figure 3. and insert the two AAA size batteries properly in the right direction.

Step 2. Replace the cover.

⚠**Please take care when you insert the batteries for the improper insertion may damage the device.**

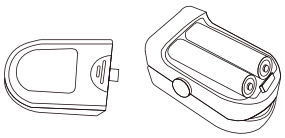

Figure 3 Batteries installation

6.3 Mounting the Hanging Rope

Step 1. Put the end of the rope through the hole.

Step 2. Put another end of the rope through the first one and then tighten it.

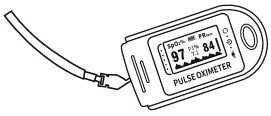

Figure 4 Mounting the hanging rope

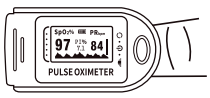

Figure 5 Put finger in position

7 Operating Guide

1) Insert the two batteries properly to the direction, and then replace the cover.
2) Open the clip as shown in Figure 5.
3) Let the patient's finger put into the rubber cushions of the clip (make sure the finger is in the right position), and then clip the finger.
4) Press the switch button once on front panel.
5) Do not shake the finger and keep the patient at ease during the process. Meanwhile, human body is not recommended in movement status.
6) Get the information directly from screen display.
7) The button ⏻ − ⚲ has three functions.When the device is power off, pressing the button can open it; When the device is power on, pressing the button shortly can change direction of the screen; When the device is power on, pressing the button long can change brightness of the screen

⚠ **Fingernails and the luminescent tube should be on the same side.**

8 Repairing and Maintenance

- Please change the batteries when the low-voltage displayed on the screen.
- Please clean the surface of the device before using. Wipe the device with medical alcohol first, and then let it dry in air or clean it by dry clean fabric.
- Using the medical alcohol to disinfect the product after use, prevent from cross infection for next time use.
- Please take out the batteries if the oximeter is not in use for a long time.
- The best storage environment of the device is - 40ºC to 60ºC ambient temperature and not higher than 95% relative humidity.
- Users are advised to calibrate the device termly (or according to the calibrating program of hospital). It also can be performed at the state-appointed agent or just contact us for calibration.

⚠ **High-pressure sterilization cannot be used on the device.**

⚠ **Do not immerse the device in liquid.**

⚠ **It is recommended that the device should be kept in a dry environment. Humidity may reduce the useful life of the device, or even damage it.**

9 Troubleshooting

Trouble	Possible Reason	Solution
The SpO_2 and Pulse Rate can not be displayed normally	1. The finger is not properly positioned. 2. The patient's SpO_2 is too low to be detected.	1. Place the finger properly and try again. 2. Try again; Go to a hospital for a diagnosis if you are sure the device works all right.
The SpO_2 and Pulse Rate are not displayed stably	1. The finger is not placed inside deep enough. 2. The finger is shaking or the patient is moving.	1. Place the finger properly and try again. 2. Let the patient keep calm
The device can not be turned on	1. The batteries are drained or almost drained. 2. The batteries are not inserted properly. 3. The malfunction of the device.	1. Change batteries. 2. Reinstall batteries. 3. Please contact the local service center.
The display is off suddenly	1. The device will power off automatically when it gets no signal within 5 seconds. 2. The batteries are almost drained.	1. Normal. 2. Change batteries.

10 Key of Symbols

	Description
	Type BF
	Warning – See User Manual
%SpO2	The pulse oxygen saturation(%)
PRbpm	Pulse rate (bpm)
	The battery voltage indication is deficient (change the battery in time avoiding the inexact measure)
	1. No finger inserted 2. An indicator of signal inadequacy
+	Battery positive electrode
−	Battery cathode
⏻ − ⚲	1.Power switch 2.Change direction of the screen 3.Change brightness of the screen
SN	Serial number
	Alarm inhibit
	WEEE (2002/96/EC)
IP22	International Protection

11 Function Specification

Display Information	Display Mode
The Pulse Oxygen Saturation(SpO_2)	OLED
Pulse Rate(PR)	OLED
Pulse Intensity (bar-graph)	OLED bar-graph display
Pulse wave	OLED
SpO_2 Parameter Specification	
Measuring range	0%~100%, (the resolution is 1%).
Accuracy	70%~100%:±2%, Below 70% unspecified.
Optical Sensor	Red light (wavelength is 660nm) Infrared (wavelength is 880nm)
Pulse Parameter Specification	
Measuring range	30bpm~250bpm (the resolution is 1 bpm)
Accuracy	±2bpm or±2% select larger
Pulse Intensity	
Range	Continuous bar-graph display, the higher display indicate the stronger pulse.
Battery Requirement	
1.5V (AAA size) alkaline batteries × 2 or rechargeable battery	
Battery Useful Life	
Two batteries can work continually for 20 hours	
Dimensions and Weight	
Dimensions	57(L) × 31(W) × 32(H) mm
Weight	About 50g (with the batteries)

Medical System USA Inc.
8600 Commodity Cir #115
Orlando, FL 32819
www.medicalsystemusa.com

Customer Service:
info@medicalsystemusa.com